Experimental Study of Hygrothermal Properties for Building Materials

Yang Wu

A Thesis

in

The Department

of

Building, Civil and Environmental Engineering

Presented in the Partial Fulfillment of the Requirements

of the Degree of Master of Applied Science (Building Engineering) at

Concordia University

Montreal, Quebec, Canada

July 2007

Your file Votre référence
ISBN: 978-0-494-34657-0
Our file Notre référence
ISBN: 978-0-494-34657-0

Abstract

Experimental Study of Hygrothermal Properties for Building Materials

Yang Wu

In this thesis, the hygrothermal properties of building materials are studied experimentally and numerically. The properties of 10 building materials which are widely used in Canada were determined using either international standard or well-documented and peer-reviewed approaches. The measured products include OSB, plywood, fiberboard and spruce, stucco, gypsum board, two insulation products, one vapor membrane, and construction paper. The properties that were determined include thermal conductivity, sorption/desorption isotherms, vapor permeability, water absorption coefficient, liquid diffusivity, and air permeability. Those data will be used as the input of advanced heat, air, and moisture movement (HAM) models.

The moisture storage and release of building materials during the indoor humidity changes were investigated in this thesis. A test facility was developed to characterize this property, which is referred to as moisture buffering value (MBV). MBVs of five products were determined. It is found that fiberboard has the greatest MBV while plywood has the least MBV. Through the curve fitting of measurement data, the relationship of mass change and time elapsed have been represented by mathematical equations.

The HAM model, hygIRC 1D, was used to simulate the MBC experiment. The measured material properties from current work were used as the input for the simulation model. For gypsum board, OSB, and fiberboard the overall agreement between the experimental and simulation results is acceptable. However, the simulated weight changes of plywood

and stucco are higher than the measured value. These differences could be the resultant of the variation in material properties of these building products. In addition, parametric analysis was performed. It shows that moisture transfer coefficient has the greatest effect in the numerical simulation of moisture transfer within fiberboard; the sorption isotherm also gives significant influence. Whereas, the liquid diffusivity has almost no effect.

Acknowledgements

The achievement of this Master thesis would not have been made possible without the support and advice of a number of people. I would like to express my sincere gratitude to my supervisor, Dr. P. Fazio, for his thorough guidance, invaluable advice, and constant support throughout this research. I would also like to gratefully thank my co-supervisor, Dr. M. K. Kumaran, for his valuable comments, encouragement suggestions with regards to my research. I have learnt a lot during the time I had the privilege to work closely with him.

This project was supported by the Natural Science and Engineering Council of Canada (NSERC) through a Special Research Opportunity grant no (305760) and the Programme de soutien aux initiatives internationales de recherche et d'innovation (PSIIRI) from the Government of Quebec and by Concordia University. The experiments were carried out at the facilities of the Institute for Research in Construction (IRC), National Research Council of Canada under the supervision of Dr. Kumaran. This financial support and the use of these first-class facilities are gratefully acknowledged.

Special thanks to Mr. J. Lackey, Ms. N. Normandin, Mr. F. Tariku, and Mr. D.V. Reenen at IRC for their technical assistance in experimental measurements and their friendship during the long experimental period. I would also like to express my thanks to all my colleagues and friends at Concordia University for the help and care.

Last but not least, I would like to express my appreciation to my parents for their love, patience, understanding, and encouragement.

Table of Contents

List of Figures

List of Tables

Nomenclature

English Symbols

A	area of the specimen surface (m^2)
A_w	water absorption coefficient ($kg/m^2s^{1/2}$)
AR	the resistance offered by still air (m·s·Pa/kg)
C_p	effective specific heat capacity (J/kg · K)
D	diffusivity of water vapor (m^2/s)
d	thickness of the specimen (m)
f_l	Liquid fraction (-)
g	flow rate (kg/m^2s)
$\vec{g}$	gravitational vector (m/s^2)
I	intensity of the transmitted gamma radiation (photon/m^2·s)
J_a	air flow rate across the area (m^3/s)
K	hydraulic conductivity (kg/Pa·m·s)
k	thermal conductivity (W/m·K)
K_a	air permeance (m/s·Pa)
L	enthalpy (J/kg)
l	the thickness of the air layer (m)
m	mass of the test specimen (kg)
MBV	moisture buffering value (kg/m^2·% RH)
P	pressure (Pa)

P_0	standard atmospheric pressure (101325 Pa)
Δp	difference in air pressure across the specimen surfaces (Pa)
q	heat transfer rate (W/m^2)
R_v	gas constant for water (461.5 J/K·kg)
S_R	resistance offered by specimen surfaces. ($Pa \cdot s \cdot m^2/kg$)
S_w	moisture source (kg/m^2s)
T	temperature (K)
t	time (s)
u	moisture content expressed by weight (kg/kg)
V	volume (m^3)
$\vec{V}_a$	air velocity vector (m/s)
w	moisture content expressed by volume (kg/m^3)
WVT	water vapor transmission rate ($kg/m^2 \cdot s$)
WVP	water vapor permeance ($kg/m^2 \cdot s \cdot Pa$)
WVR	water vapor resistance ($m^2 \cdot s \cdot Pa/kg$)
x	distance along the flow path (m)

Greek Symbols

Ψ	moisture content expressed by the ratio of moisture volume and dry material volume (m^3/m^3)
φ	relative humidity (-)

ρ	density (kg/m^3)
δ_a	water vapor permeability of the still air (kg/m·s·Pa)
δ_p	water vapor permeability of the material (kg/Pa·m·s)
μ	vapor diffusion resistance (-)
μ_w	mass attenuation coefficient of water (kg/m^3)
λ	Boltzmann variable (m/s$^{1/2}$)

Subscripts

a	air
b	boundary
c	capillary suction
cr	critical
d	dry
i	initial value
ice	freeze/thaw
l	liquid water
T	total value
v	water vapor
w	wet

Chapter 1
Introduction

The use of computer based building simulation programs is steadily increasing with the rapid change of building technologies. Heat, air and moisture response (HAM-response) in buildings can be simulated by hygrothermal computer models, which is part of the whole building simulation. Usually HAM simulation tools account for the hygrothermal behavior of the building components and microclimate near the building envelope. Besides the adequate description about the envelope configuration, the quality of the simulation results depends largely on the reliability of material property data as an input.

1.1 Background

Building envelope continuously responds to the changes of indoor and outdoor heat, air and moisture conditions. This brings on the exchange of energy and mass between outside and inside environments through the building envelope component.

Moisture in the building envelope is an important issue in building science. Unsuccessfully controlled, moisture accumulation can lead to the performance failure of building envelopes. These problems include negative health effects, damage of the building envelope, and increased energy consumption of buildings. In Figure 1.1, an example is given for problem with wood cladding by moisture in Vancouver

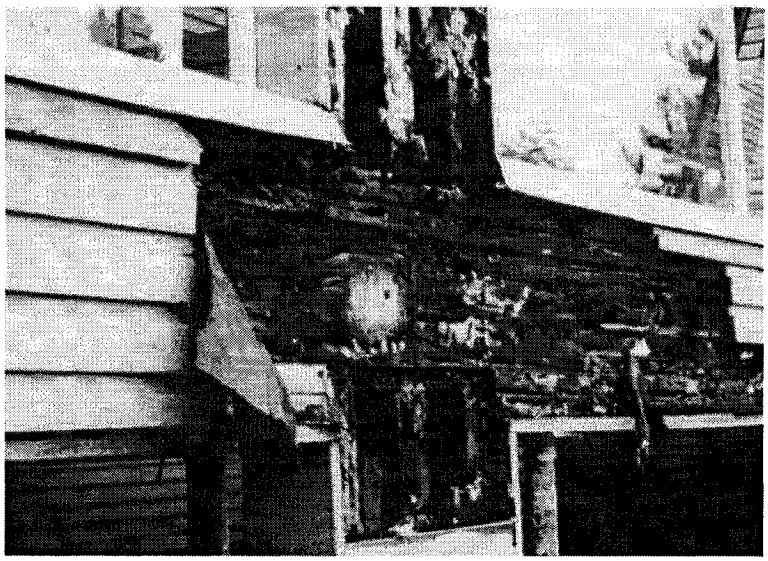

Figure 1.1 Problem with wood cladding by moisture in Vancouver

Moisture balance of a building envelope depends on the loads from external and internal environments in combination with the methods of construction, type, and properties of various building materials. Due to the heterogeneity of the building construction methods, materials, indoor and outdoor climatic conditions, it is not possible and economic to conduct those investigations only through experimental approaches. Therefore, there is an increasing interest in developing calculation models to predict the long-term hygrothermal performance of building envelopes. These attempts, along with the state-of-the-art computer technology, have resulted in a number of successful computational models, such as WUFI developed by IBP, and hygIRC developed at the Institute for Research in Construction (IRC) of National Research Council Canada, etc.

The whole building HAM models require high quality input parameters; otherwise the reliabilities of simulation outputs will be doubted. Among these inputs, the hygrothermal properties of building materials are one of the most important.

1.2 Current Issues in Building Material Study

Different material properties are documented in literature (Kumaran 1996, Kumaran et al. 2002a, Kumaran et al. 2002b, Mukhopadhyaya et al. 2003). However, the information is often found to be incomplete in various aspects. The material properties often show a wide variation depending on the information source, manufacturing process, test conditions, location of the raw materials, etc. On the other hand, the literature data usually lacks enough description for material identification. Information about manufacture, location, environmental condition, and detailed measurement data is hard to find in most of the published literature. Building material properties change continuously and significantly with the environmental and self condition. Therefore, the scattered data or calculated coefficients in the literature are far from adequate for simulation input.

Furthermore, with the development of manufacturing technologies, the composition and processing of building materials might change significantly. As a result, the building materials used nowadays could have different properties from those which were documented in the literature.

It is well known that indoor humidity is an important factor in determining the occupant perception of indoor air quality (Fang et al. 2000). There is increasing focus on the possibilities of using the building materials to control indoor humidity variations in the indoor air. Consequently, a new material property, moisture buffering value (MBV), was introduced during the NORDTEST project in Nordic countries (Rode 2003; Rode et al. 2005). Until now, there is no systemically documented MBV data on building materials

that are currently used in North America. It is necessary to add these data into the building material database, even though it is not a property for simulation input.

1.3 Research Objectives

The objectives of this research are to investigate the hygrothermal properties of materials which are widely used in Canadian construction.

Specifically, the objectives of the study are to:

- Review the knowledge about measuring hygrothermal properties of different building materials;
- Determine the material properties based on either international standard or well-documented and peer-reviewed approaches for 10 building materials;
- Develop a simple test methodology for characterization of MBV for building materials and determine the MBV of 5 building materials;
- Apply the HAM simulation tool, hygIRC 1-D, to simulate the MBC test using the measured material properties.

To achieve these objectives, all the experimental works were carried out in the Thermal Insulation Laboratory of the Institute for Research in Construction, National Research Council Canada, under the guidance of specialists.

1.4 Methodology

To investigate the hygrothermal properties of building materials included in this research, experimental research and numerical simulations are adopted. Experimental results can be used as input parameters for the simulation model; meanwhile, the test results of MBV

could be used for validating the simulation results by HAM model. Furthermore, parametric study on the MBV of building materials will be carried out using this verified model. Through this combined experimental and numerical approach, the objectives of this investigation will be achieved.

1.5 Overview of the Thesis

This thesis is divided into six chapters. Chapter 2 is the literature review regarding the experimental methods, HAM transport mechanisms and the development of related models by other researchers. In Chapter 3, experimentally determined hygrothermal properties of proposed building materials are presented. Chapter 4 focuses on the experimental methodology and results of MBV for 5 building materials. Chapter 5 introduces the HAM model hygIRC 1D, in addition, the simulation results of the MBV tests are compared with experimental results shown in Chapter 4. Chapter 5 also presents the results of a parametric study to investigate the uncertainty of the material properties or boundary conditions on the measurement of the MBV. Finally, a research summary, conclusions and recommendations for future work are presented in Chapter 6.

Chapter 2
Literature Review

In this chapter, the theory that is associated with the measurement methods for determining hygrothermal properties of building materials is reviewed. Since moisture is one of the most important issues in buildings, understanding the moisture transport in building envelopes is an essential task. Although some properties are dependent on temperature, all experiments expect the measurement of thermal conductivity are performed at a constant temperature. Therefore, only isothermal conditions will be treated in the discussion of the theory.

2.1 Moisture Transport Theory

2.1.1 Moisture Storage in Material

Many building materials have porous structures. Theoretically, a building material can adsorb/absorb moisture from surrounding when its pores are empty until all of them are filled with water. In practice, this information can not reflect the actual moisture storage capacity under natural conditions. Therefore, a connection between water content in the material and natural condition is established. Moisture content can be expressed by weight, u (kg/kg), by volume, w (kg/m^3), or the ratio of moisture volume and dry material volume ψ (m^3/m^3) (Kumaran 1996).

$$u = \frac{m_w - m_d}{m_0} \tag{2.1}$$

$$w = \frac{m_w - m_d}{V} = \rho_d \cdot u \tag{2.2}$$

$$\psi = \frac{(m_w - m_d)/\rho_w}{V} \tag{2.3}$$

m_w (kg) is the mass of the test specimen, m_d (kg) is the mass of dry specimen, V (m^3) is the volume of the specimen, ρ_d (kg/m^3) is dry density of the material and ρ_w (kg/m^3) is the density of water.

From the dry to saturated state, the moisture content in materials can vary with the surrounding relative humidity. The relation between them can be shown as a non-linear curve as shown in Figure 2.1, and this relationship is also called sorption curve. Previous investigations found that the moisture absorption process can be separated into three stages (Kumaran 1996, Krus 1995, and Künzel 1995). In the lower humidity range, the material is in an adsorptive state, which is hygroscopic range. It ranges from 0% to 98% RH. At the higher end of the hygroscopic range, the water from the surroundings begins to condense in the pores, and this process will continue until capillary moisture content is reached. Moreover, the capillary moisture content can be considered as the initial point of the liquid transport. From 98% RH to capillary content, capillary suction dominates in this region, therefore, it is also called capillary water region. Above the capillary moisture content, there is a saturated region. The moisture content that corresponds to this situation is called the maximum moisture content. This level is possibly achieved only under the vacuum condition and hence is often referred to as the vacuum saturation moisture content. These three regions characterize the moisture storage functions of most building materials. The sorption isotherm is enough to characterize the moisture storage in the hygroscopic range for a building material. It shows the relation between equilibrium

moisture content and relative humidity at which moisture equilibrium was measured. The measurement methods will be given in detail in Section 2.2.2.

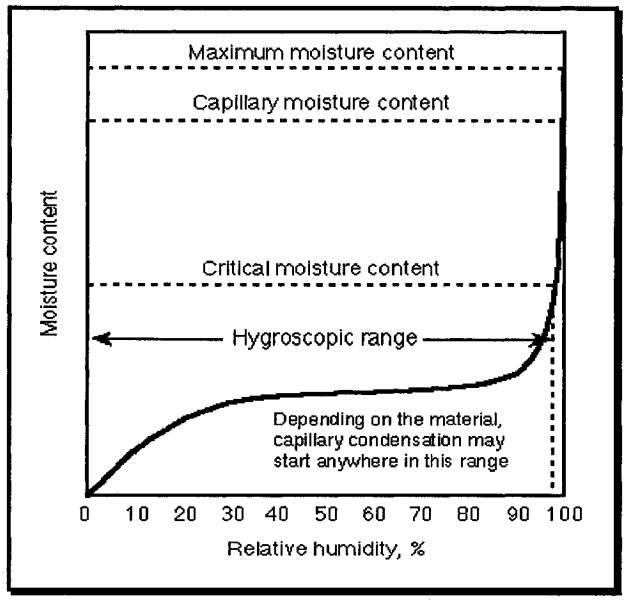

Figure 2.1 Schematic diagram of the moisture storage function of a porous building material (Kumaran 1996)

2.1.2 Moisture Transport Mechanisms

Moisture can be transported in a building material through different mechanisms. The transport can either be diffusive or convective depending on its driving forces. Moreover, moisture can be transported either in vapor phase or liquid phase. The solid phase of moisture is not regarded as movable (Pedersen 1990). Types of moisture transport commonly mentioned in the literature are listed in Table 2.1. The detailed description can be found in this section.

Table 2.1 List of major moisture transport mechanisms and their driving potential

Phase	Transport mechanisms	Driving potentials
Vapor	Water vapor diffusion	Vapor pressure (temperature and total pressure)
	Molecular transport (effusion)	Vapor pressure
	Solution diffusion	Vapor pressure
	Convection	Total pressure gradient
Liquid	Capillary suction	Suction pressure
	Surface diffusion	Relative humidity or moisture content
	Hydraulic flow	Total pressure differentials
	Electrokinesis	Electrical fields

Water Vapor Transport

The theory of moisture transport is based on Fick's law of diffusion of ions in water (Fick 1855). It is generally written as

$$g_a = -D_a \frac{\partial \rho_v}{\partial x} \tag{2.4}$$

Where g_a is the density of vapor transport in air (kg/m^{2}s), D_a the diffusivity of water vapor in stagnant air (m^2/s), ρ_v the concentration of water vapor (kg/m^3), and x represents distance along the flow path (m).

According to Equation 2.4, the driving potential of pure water vapor diffusion is ρ_v. This law is adopted to describe the diffusion of water vapor in porous materials. The total pressure P [Pa], and especially temperature T also play roles in transport, Equation 2.5 shows this influence (Schirmer 1938),

$$D_a = \frac{2.306\times10^{-5}\cdot P_0}{R_v T P_a}\left(\frac{T}{273.13}\right)^{1.81} \tag{2.5}$$

Where P_0 is standard atmospheric pressure (101325 Pa), P_a is the ambient air pressure (Pa), T the temperature (K), and R_v gas constant for water (461.5 J/K·kg).

When considering water vapor transport in porous material, the water vapor flux density in material g_v (kg/m^{2}s) can be given as

$$g_v = -\frac{D_a}{\mu}\frac{\partial \rho_v}{\partial x} \tag{2.6}$$

where the vapor diffusion resistance μ (-) is defined as

$$\mu = \frac{D_a}{\delta_v} \tag{2.7}$$

where δ_v (kg/Pa·m·s) is water vapor permeability of porous material. By applying the ideal gas law, Equation 2.6 becomes, under isothermal conditions

$$g_v = -\delta_p \frac{\partial p_v}{\partial x} \tag{2.8}$$

where p_v is the water vapor pressure (Pa), δ_p (kg/Pa·m·s) is water vapor permeability of the material, and it can be determined as

$$\delta_p = \frac{\delta_v}{R_v T} \tag{2.9}$$

Research has found that temperature does have an influence on the permeability for some building materials, especially at the high relative humidity range (Galbraith et al 2000). However, in this work, this effect is neglected.

Liquid transport

When the moisture content of the material exceeds the critical moisture content, w_{cr}, moisture will begin to transport in the liquid phase. Liquid moisture transport can usually be expressed using Darcy's law:

$$g_l = -K\frac{\partial P_c}{\partial x} \tag{2.10}$$

where g_l is the density of liquid flow (kg/m^2·s), K (kg/Pa·m·s) the hydraulic conductivity and P_c (Pa) is the suction pressure. To easily determine the liquid moisture transport experimentally, Equation 2.11 is used, where the driving potential is replaced by moisture content w (kg/m^3):

$$g_l = -D_{w,l}\frac{\partial w}{\partial x} \tag{2.11}$$

where $D_{w,l}$ (m^2/s) is the coefficient for moisture content driven liquid diffusion. This coefficient $D_{w,l}$ (m^2/s) strongly depends on relative humidity (Künzel 1995), therefore, the following relation is used:

$$g_l = -D_{\varphi,l}\frac{\partial \varphi}{\partial x} \tag{2.12}$$

where $D_{\varphi,l}$ (kg/ms) is the coefficient for relative humidity driven liquid diffusion, and φ is the relative humidity (-). In contrast to Equation 2.10, Equation 2.11 contains a material-independent moisture transport potential. The relation of $D_{\varphi,l}$ and $D_{w,l}$ can be given as:

$$D_{\varphi,l} = D_{w,l} \frac{\partial w}{\partial \varphi} \tag{2.13}$$

In the capillary region (RH > 98%), it is difficult to measure the RH experimentally. From Equation 2.13, $D_{\varphi,l}$ can be derived from $D_{w,l}$ and the moisture storage function.

2.1.3 Dynamic Moisture Transport

The dynamic moisture transport usually describes the transient moisture profile as a function of time and location. It is a significant factor of HAM modeling. The dynamic moisture transport can be expressed with the moisture balance equation, which is analogous to the heat balance equation as follows (Künzel 1995):

$$\frac{\partial w}{\partial t} = -\nabla(g_l + g_v) + S_w \tag{2.14}$$

where S_w is the moisture source (kg/m^{2}s) and t time (s). Because it is very rare that moisture sources are shown in building components, they are neglected in this study. After combining Equation 2.14 with Equation 2.8 and 2.12, the following relation is given for dynamic moisture transfer in one dimensional case:

$$\frac{\partial w}{\partial t} = -\frac{\partial}{\partial x}(D_{\varphi,l} \frac{\partial \varphi}{\partial x} + \delta_v \frac{\partial \rho_v}{\partial x}) \tag{2.15}$$

Equation 2.15 describes the vapor and liquid transport. In this equation, the driving force can be expressed as moisture content. Then, the following equation can be obtained:

$$\frac{\partial w}{\partial t} = -\frac{\partial}{\partial x}(D_w \frac{\partial w}{\partial x}) \tag{2.16}$$

where D_w (m^2/s) is the liquid diffusivity. It contains information about the liquid and vapor transports; also it reflects the moisture retention with the change of ambient condition at any time.

2.2 Measurement of Material Properties

In this section the measurement methods of hygrothermal properties of building materials are reviewed. The different methods are compared.

2.2.1 Measurement of Thermal Conductivity

The most commonly used methods for testing the thermal conductivity for the building materials are ASTM standard C177-04, Standard Test Method for Steady-State Heat Flux Measurements and Thermal Transmission Properties by Means of the Guarded-Hot-Plate Apparatus (ASTM 2004), and ASTM standard C518-04, Standard Test Method for Steady-State Thermal Transmission Properties by Means of the Heat Flow Meter Apparatus (ASTM 2004). The guarded hot plate and heat flow meter apparatus are used in these two methods separately. Both methods are based on allowing a certain amount of heat flux along the thickness of the material tested, and then the temperatures at each side of the specimen can be measured. Therefore, the thermal conductivity can be calculated through Fourier's law:

$$q_x = -k\frac{dT}{dx} \tag{2.17}$$

The heat flux q_x (W/m^2) is the heat transfer rate in the x direction per unit area perpendicular to the direction of transfer, and it is proportional to the temperature gradient, *dT/dx*, in this direction. The proportionality constant k (W/m·K) is a transport property known as the thermal conductivity.

2.2.2 Measurement of Moisture Storage Characteristics

Generally, the moisture storage characteristics are presented in a different way in the hygroscopic range and in the capillary range. In the hygroscopic range, the relation between moisture content of the material and relative humidity is given by the sorption isotherms; in the capillary range, the moisture storage capacity is represented by a relation between suction pressure and moisture content of the material (Hens 1996, Janz and Johannesson 2001).

Sorption Isotherms

Sorption isotherm characterizes the hygroscopic equilibrium moisture values of building materials (Künzel 1995). As far as building physics is concerned, the temperature effect is usually neglected (Richards et al. 1992). Among the methods to determine the sorption isotherms, the classical method uses the different saturated salt solutions. The specific humidity level will be created above the saturated salt solution in the closed environment. An alternative way to create various humidity levels is using the environmental chamber. By measuring the specimen gravimetrically when the equilibrium state is reached, the equilibrium moisture content can be determined. ASTM standard C1498-01 (ASTM 2001)

describes this method in detail. This method is reliable and simple, even though it is time consuming. Depending on the sizes and types of specimens, the whole process can last a month to a year.

However, other researchers developed faster methods to determine sorption isotherms. A review of methods to measure sorption isotherms can be found in (Wadsö 1997). In one approach, the use of a twin microcalorimeter was applied for this purpose (Wadsö and Wadsö 1996, Wadsö and Wadsö 1997). In another approach the sorption balance apparatus was used, which is given in detail in (Janz and Johannesson 2001).

Water Retention

There are several methods of measuring moisture retention in the over-hygroscopic range. The most common technique is the pressure plate technique. This method was first used for determination of soil retention curves by Richards (1948). There have been several studies of this technique recently (Krus 1995, Hansen 1997, Brocken 1998 and Hensen et al. 1999), also a European test standard called the Nordtest Standard NT building 481 (Nordtest 1997). When the pressure plate technique is applied to a fully saturated material, the main drainage or drying capillary pressure curve is obtained. The duration of the tests can extend over several weeks before equilibrium conditions are obtained. Johannesson and Janz (2002) compared the pressure plate method with three other methods to measure the sorption isotherms of sandstone and porous glass. Satisfactory agreement was found. It was also found that, of two different presaturating methods for test specimen, capillary and vacuum, the latter is generally preferred (Janz 2001). The sketch of the pressure plate apparatus can be found in Figure 2.2.

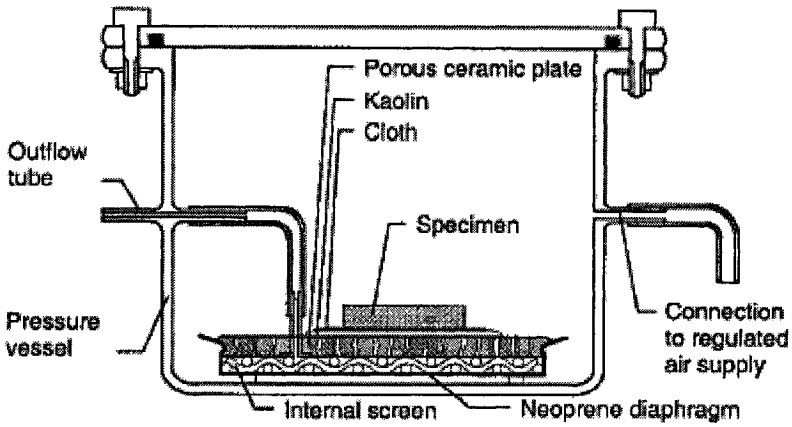

Figure 2.2 Sketch of ceramic pressure plate and specimen mounted in pressure vessel (Janz 2001)

The water retention curve can also be calculated from the measured pore size distributions. For this purpose, the mercury intrusion porosimetry method is frequently used (Abell et al. 1999, Krus and Kießel 1998). The principal difference between the pressure plate and the mercury intrusion methods is that mercury is almost non-wetting, which means that it has to be forced into pores. The advantage of using mercury intrusion method is that the measurement can be carried out more quickly than the pressure plate method. However, the use of greater pressure may fracture the pore walls (Janz 2001). Moreover mercury has negative environmental effects and thus it should be avoided.

Some less commonly used methods are also available such as the centrifuge method, determination from the liquid penetration rate, the displacement method. Detailed descriptions of those methods can be found in the literature (Fagerlund 1973a, Fagerlund 1973b).

2.2.3 Measurement of Water Vapor Permeability

The dry cup and wet cup methods are used widely to determine the water vapor permeability of building materials (Joy and Wilson 1963, Galbraith and Mclean 1986, Hansen 1990, Burch 1992, Mclean et al. 1992, Kumaran 1998a). ASTM standard E96-00 (ASTM 2000) describes these test procedures in detail in which the specimen is sealed to the mouth of an impermeable test cup containing desiccant or water and placed in a controlled environment thus creating water vapor pressure across the test specimen. When desiccant is put in the cup, it is called dry cup; in the wet cup method the RH inside the cup is maintained at 100% by the presence of water (Kumaran et al. 1994). Then, the weight change of the cups is measured until a steady state is reached. Equation 2.8 can be used for calculating the water vapor permeability of building materials.

Kumaran (1998b) suggested an extension of the cup methods described by ASTM standard E96. In the standard, the dry cup method gives the result as an average value of the property at a mean relative humidity of 25% and the wet cup at 75%. This information is not enough for detailed hygrothermal analysis of building components. The complete dependence of water vapor permeability data on relative humidity is required by most computer models for hygrothermal simulation.

Investigations found that temperature has influence on water vapor permeability. However, experimental results indicated that the influence is not only related to relative humidity but also depends upon the properties of the materials themselves and the proportion of liquid to vapor flow (Galbraith et al. 2000). There also exists some modified cup methods, an example can be seen in (Bomberg et al. 2002).

2.2.4 Measurement of Moisture Content Profile

The major objective of measuring the moisture profile of building materials is to calculate liquid diffusivity. The water uptake test or moisture redistribution test is carried out for this purpose. The transient moisture profile is obtained at various times after start of water uptake. Two of the most common methods used are Boltzmann transformation method and the Profile method (Freitas et al. 1995). With the Boltzmann transformation method the liquid diffusivity can be calculated only from the absorption process for a semi-infinite volume, the details of which will be given in Chapter 3. This method is widely used in several studies (Pel 1995, Janz 1997), while the Profile method can be used for profiles measured from the absorption and redistribution test (Krus 1995). There are several methods and apparatuses that can be used for the measurement of transient moisture content profiles. They can be destructive or non-destructive methods. Although there are some limitations for some of the techniques, a good overall agreement is obtained in the comprehensive study by Roels et al. (2004)

Slice-Dry-Weigh-Method

This is a traditional destructive method to obtain the moisture profile. Whenever the moisture profile is to be measured, the specimen is quickly sliced into thin pieces that are weighed, dried, and then weighed again. By this way, the moisture content of each slice of the specimen can be determined, but the specimen is destroyed. For each measurement, a new specimen is used. As a result a large number of specimens are needed to obtain the transient moisture content profile. Moreover, since the drying time of specimens is dependent on materials, the whole process can be rather slow.

This is the most accurate because the amount of water in the material is precisely measured. Therefore, it can be used for calibration of the other methods listed below.

Gamma-Ray Attenuation

The gamma ray attenuation technique has been used to determine the transient moisture distribution in soil from the 1960s (Ferguson and Gardner 1962). Later, Gamma ray equipment began to be used to measure the moisture profile in building materials (Nielsen 1972, Kumaran and Bomberg 1985, Kumaran et al. 1989, Marchand and Kumaran 1994). It has been one of the most commonly used methods to determine the moisture content profile of building materials.

In a gamma-ray test, a test specimen is placed between the source and detector of the equipment. The source can consist of Am^{241}, Cs^{137} or Co^{60}. The detector is usually a scintillation crystal, e.g. a NaI crystal. A grid of vertical and horizontal co-ordinates defines the area that faces the gamma-ray source. At each segment of the specimen, the gamma-rays are emitted from the source and captured by the detector on the other side. The test is first done on a dry material then for the wet state. By scanning each segment in the wet state and comparing with the scan in the dry state, an average value for moisture content at a given interval can be obtained. When they are all put together it results in the moisture distribution in the specimen as a function of time, during a moisture transport process. The disadvantages of this technology are the high cost of the equipment and its radioactivity for which special safety arrangements must be made.

NMR technology

NMR (nuclear magnetic resonance) method is another well-known technology applied in building material measurements; examples can be found in the literature (Gummerson et al. 1979, Krus 1995, Pel 1995). In an NMR measurement the number of hydrogen nuclei can be counted, therefore the water content in the material can be determined. In addition to water, NMR is suitable for all fluids containing hydrogen atoms. A comparison found that there is no significant difference in accuracy between gamma-ray and NMR methods (Freitas et al. 1995). An advantage of the NMR method compared with gamma-ray is that no radioactivity is involved during the experiment. However, the cost of the equipment is still a drawback.

X-Ray Projection Methods

The X-ray technology allows the visualization of the interior of non-transparent objects in a non-destructive way when an object is illuminated with X-rays and the change in transmitted X-ray intensity is measured. For a water uptake experiment, an oven dried specimen is placed in the X-ray apparatus. First, the X-ray image of dry specimen is taken; then, the specimen is placed in contact with water; and the images are taken at regular time steps. This technique was successfully used for several recent investigations (Roels et al. 2003, Carmeliet et al. 2003).

Other Methods to Determine Moisture Content Profile

Several other methods exist, such as the capacitance method (Wormald and Britch 1969), the neutron radiography (Pel et al. 1993, Prazak et al. 1990), and the newly developed TDR technique (Plagge et al. 1995).

2.2.5 Determination of Water Absorption Coefficient

The water absorption coefficient of a material represents the rate of liquid moisture movement into it. It quantifies the water entry into a building material due to absorption when its surface is just in contact with liquid water. It is defined as the ratio between the change of the amount of water entry across unit area of the surface and the corresponding change in the time expressed as the square root. In the early part of an absorption process this ratio remains constant and that constant value is designated as the water absorption coefficient. The water absorption coefficient A_w (kg/m^{2}s$^{1/2}$) can be written as:

$$A_w = \left(\frac{m_t - m_i}{A\sqrt{t}} \right) \tag{2.18}$$

Where m_t (kg) is weight of the specimen after time t (s), m_i (kg) initial mass of the specimen, and A (m^2) liquid contact area of the specimen.

The water absorption by partial immersion is determined by measuring the change in the mass of the test specimen, the bottom of which is in contact with water. The water adhered to the surface and not absorbed by the product is completely removed with a damp sponge before the specimen is weighed. This testing method is explained in the European standard for thermal performance of building components- Determination of Water Absorption Coefficient CEN/TC 89/WG10 N95 (CEN 1994). It is intended to assess the water absorption caused by a period of continuous rain. As shown in Figure 2.3, the water absorption process can be divided into two stages. The first stage is the capillary dominated part that can be illustrated by a straight line. Second stage describes

the influence of the dispersion of the water in the material until it reaches the top of the specimen. The break point is the capillary saturation moisture content w_{cap} (kg/m^3).

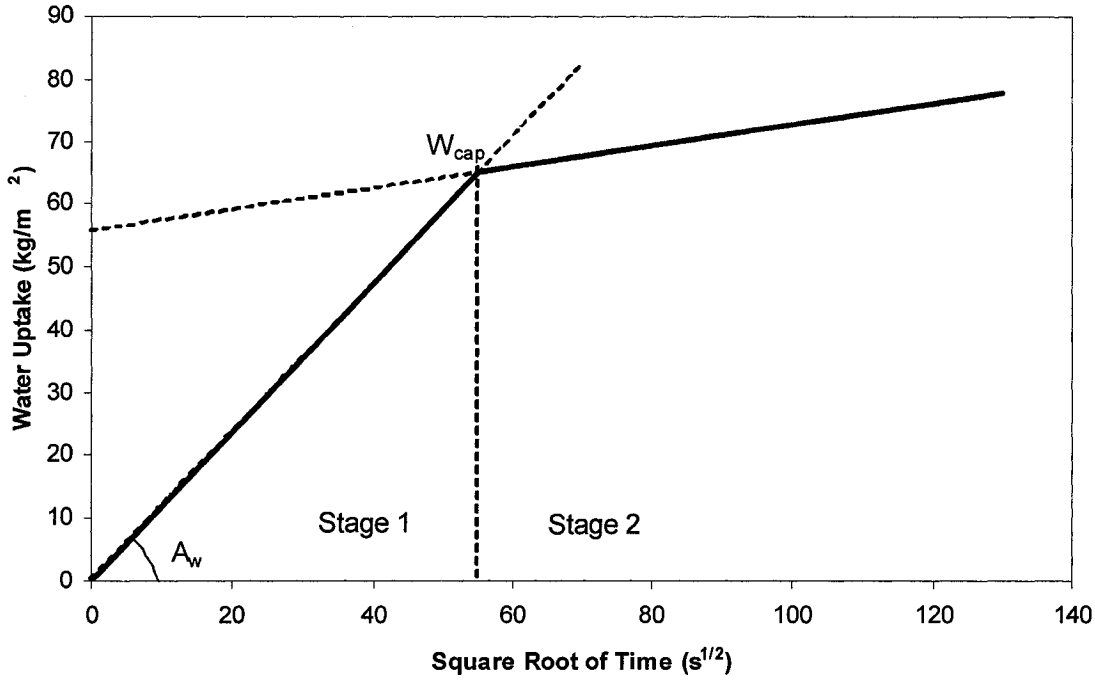

Figure 2.3 Plot of the water absorption curve versus square root of time

2.2.6 Measurement of Air Permeance

Air permeance represents the capacity of the material for resisting the air flow through it caused by the pressure difference at the two sides of the material. Air permeance K_a (m/s·Pa) can be defined as the quotient of the air pressure difference across a specimen divided by the volume velocity of airflow through the specimen, and is as follow:

$$K_a = J_a /(A \cdot \Delta p) \tag{2.19}$$

Where J_a (m^3/s) is Air flow rate across the area A, Δp (Pa) the difference in air pressure across the specimen surfaces.

For measuring air permeance of the building material, ASTM standard C 522-03, Standard Test Method for Airflow Resistance of Acoustical Materials was first used (ASTM 2003). This standard covers the measurement of airflow resistance and the related measurements of specific airflow resistance and resistivity of porous materials that can be used for absorption and attenuation of sound. The materials tested can be thick board, blankets, thin mats, fabrics, papers, and screens. This standard method was extended to apply to building materials (Bomberg and Kumaran 1986).

2.3 Review of HAM Studies

The combined HAM study for buildings began in the 1930s. In 1958, Glaser developed a diffusion based calculation method that combined steady state vapor diffusion with steady state heat conduction. In the late fifties and early sixties, the models that include vapor diffusion, capillary water transport, initial moisture, latent heat of evaporation, and transient conditions were published (Philip and de Vries 1957, Luikov 1966). Later, with the development of the personal computer, many computer codes were developed and commercialized (Kohonen 1984, Pederson 1990 and Künzel 1995). Meanwhile, efforts were undertaken to measure the material properties needed to input into the models (Burch et al. 1992, IEA-Annex 1991).

In 1990, the International Energy Agency, Executive Committee on Energy Conservation in Buildings and Community Systems, started Annex 24, HAMTIE, to enhance combined HAM modeling (Hens 1996). The annex focused on model development and comparison,

material properties, boundary conditions and the impact of combined HAM-transport on energy consumption and durability. As a result, a great number of commercial HAM models came into the market (Descamps 1997, Karagiozis 1993, Krus 1995, Künzel 1995, and Pel 1995), and the material properties collected from 14 countries were summarized (Kumaran 1996). Through these activities, more laboratories got equipped with devices to measure material properties. However, uniformity in obtained measured material property results remained a challenge. In 1999, due to the need for a systematic investigation on the properties of all current building material, ASHRAE Research Project 1018 was formulated at the Institute for Research in Construction (IRC), National Research Council Canada (NRC) (Kumaran et al. 2002a). The scope of the project was to generate a set of reliable and representative data on the hygrothermal properties of 25 common building materials, and those data are now widely used in HAM studies.

In 2001, the European Commission initiated the project HAMSTAD (Heat Air and Moisture Standards Development) that focused on the development of draft standardization procedures on the methods to determine moisture transfer properties and a draft methodology for certification of upgraded moisture modeling codes (HAMSTAD 2003). As per the materials characterization aspect, it concentrated on the evaluation of six non-destructive measuring techniques for transient moisture content profiles (Roels et al. 2004a) on the one hand and data processing and determination of moisture transfer coefficients on the other (Carmeliet et al. 2004). Furthermore, an inter-laboratory comparison of determination of basic properties of three porous materials was performed (Roels et al. 2004b). Regarding the modeling approach, the methodology was developed

on the basis of definition and calculation of 5 HAM benchmark exercises for one-dimensional cases.

These days, several HAM models are available on the market, such as MOIST (Burch et al. 1997), MATCH (Pedersen 1992), WUFI (Künzel and Kiessl 1997), its North American version WUFI ONRL/IBP (Karagiozis et al. 2001), etc. IRC at NRC Canada developed an advanced HAM model, hygIRC (Maref et al. 2002). In IRC's Consortium for Moisture Management for Exterior Wall Systems (MEWS) project, the utility and reliability of hygIRC outputs have been established through laboratory measurements and benchmarking exercises (Mukhopadhyaya et al. 2003). Moreover the hygrothermal properties of 11 building products that are currently used in North American were systematically determined, and were provided as inputs for simulation model (Kumaran et al. 2002b).

Investigations about hygrothermal properties of building materials are continuing. Recent research found that some frequently used tests, considered to be well standardized, were not as precise as initially thought (Roels et al 2004b). Moreover, efforts are being made in the development of reliable material characterization methods (Bomberg et al. 2006, Galbraith et al. 2003).

Chapter 3
Experimental Determination of Material Properties

The advanced whole building HAM model requires a set of accurate input parameters, which include the properties of different building materials. This chapter presents the measured properties of 10 building products which are widely used in Canada. Due to the different structures and compositions of building materials, for some products not all the hygrothermal properties can be measured by using current measurement methods. Table 3.1 lists the experiments which were carried out for each building product.

Table 3.1 Tests carried out for each material

	Thermal Conductivity	Sorption Isotherm	Suction Isotherm	Vapor Permeability	Liquid Diffusivity	Water Absorption Coefficient	Air Permeability
Gypsum	●	●	●	●	●	●	●
OSB	●	●	●	●	●	●	●
Plywood	●	●	●	●	●	●	●
Fiberboard	●	●	●	●	●	●	●
Spruce	●	●	●	●		●	●
Stucco	●	●	●	●		●	●
Glass Fibre Batt Insulation	●						
EPS	●	●		●		●	●
Asphalt impregnated paper				●			●
Polyethylene sheet				●			

3.1 General Description of Building Products

General information on all the products included in this investigation is given in Table 3.2. The products include: several wood-based products, such as OSB, plywood,

fiberboard, and spruce wood studs; stucco for exterior cladding; interior gypsum board; two insulation products; one building membrane; and a construction paper.

Table 3.2 Relevant information on the products investigated

Products	Information
Interior Gypsum Board	The product is available in 4' X 8' sheets with nominal thickness of 1/2". The name of manufacture is BPB, and the product name is "ProPoc Regular Gypsum Board" which conforms to CAN/CSA-A82.27. A paper layer is adhered to the surface.
Oriented Strand Board (OSB)	The product is available in 4' X 8' sheets with nominal thickness of 7/16". Louisiana Pacific manufactured the product. It is certified as conforming to CSA 0325 1R24/2F16 OSB
Plywood	The product is available 4' X 8' sheets with nominal thickness of 1/2". The product conforms to CSA O121M Douglas Fir Plywood. The Brand is Tolko.
Wood Fiber Board	The product is available in 4' X 8' sheets with nominal thickness of 7/16". It conforms to CAN/ULC-S706 Type II, Category 3. It is coated with asphalt on its both sides, and the brand is EMCO.
Spruce	This product is available in planks with dimensions of 2"X4"X8'. The 2"X4" surfaces of the planks are refereed to as the major surfaces.
Stucco	All the stucco specimens were obtained from one regular Portland stucco mix. The brand marked on the bag is Mélange à crépissage Bomix. Specimens were prepared and allowed to dry for more than 28 days as suggested by the manufacturer. Stucco slabs are embedded on metallic lath. It conforms to CAN/CSA-A5 "Portland Cement", Lime.
Glass Fibre Batt Insulation	The batt was obtained from a roll of commercial product. The brand is Owens Corning. It conforms to CAN/ULC-S702. Mark on the package says "Thermal Insulation, Mineral Fibre, for Buildings" R-20.
Extruded Polystyrene Foam Sheathing	This product is available in 4' X 8' sheets with nominal thickness of 1". The brand on the package is Owens Corning, and it conforms to CAN/ULC-S701, Type 3.
Asphalt impregnated paper	Asphalt impregnated paper #15 for walls.
Polyethylene sheet	6 mil. It conforms to CAN/CGSB-51.34-M. Mark on the package says "Vapor Barrier, Polyethylene Sheet for Use in Building Construction".

Thickness and density were measured for all the products. An electronic balance with the accuracy of ± 0.001 g, thickness-gauge (Figure 3.1) and caliper with the accuracy of 0.01 mm were used for thickness and density measurements. Depending on the size of

specimen, 4 to 19 measurement points were taken for measuring the thickness of each specimen.

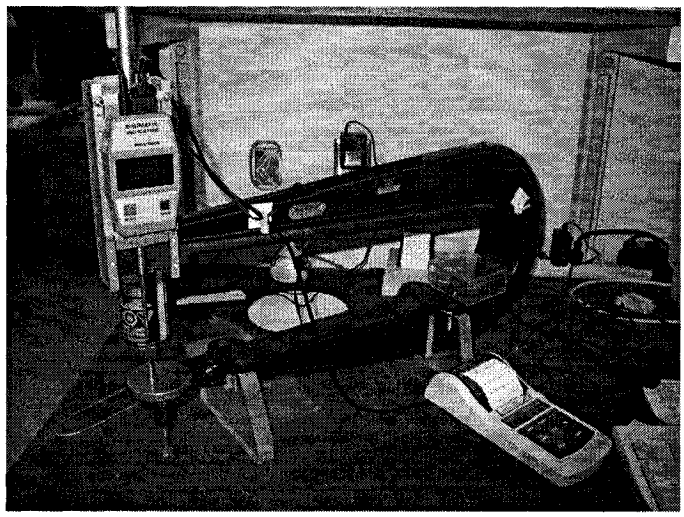

Figure 3.1 Thickness gauge with a precision of 0.01 mm

To measure the dry density, the specimens were dried in an oven at either 50°C or 70°C depending on the type of materials. The drying method and temperature have significant influence on the results of the absorption isotherm (Kumaran et al. 2006, Wilkes and Karagiozis 2004). All the test specimens were dried in an oven for at least 1 month until the weight change for each specimen was less than 0.1% in 24 hours. Some building materials change structure or dimension at high temperature and some materials experience chemical or physical change. All test specimens were grouped in two categories. Fiberboard, Gypsum Board, and EPS were dried in the oven with 50°C, other materials as another group were dried with 70°C oven. For the specimens dried in 70°C oven, after attaining of constant moisture content, they were kept at 105°C for a two hour period, then recorded the final weights as described by Kumaran et al. (2006). The densities and measured thickness of building products are listed in Table 3.3.

Table 3.3 Measured thickness and densities of the products investigated

Products	Thickness (mm)	Bulk Density (kg/m^3)	Dry Density (kg/m^3)
Interior Gypsum Board	12.60 ± 0.11	592 ± 5	569 ± 18
Oriented Strand Board	11.64 ± 0.72	664 ± 46	634 ± 63
Plywood	12.57 ± 0.37	456 ± 30	428 ± 24
Wood fibre Board	10.84 ± 0.11	279 ± 3	270 ± 3
Spruce	37.48 ± 0.32	465 ± 20	430 ± 15
Stucco	19.56 ± 0.78	1412 ± 65	1353 ± 54
Extruded Polystyrene Foam Sheathing	26.3 ± 0.7	27.2 ± 0.5	26.5 ± 0.1
Glass Fibre Batt Insulation	127.04 ± 0.7	11.5 ± 0.1	N/A
Asphalt impregnated paper	0.64 ± 0.02	1033 ± 17	N/A
Polyethylene sheet	0.153 ± 0.003	911 ± 22	N/A

3.2 Thermal Conductivity

The thermal conductivity can be calculated through Fourier's law:

$$q_x = -k\frac{dT}{dx} \tag{3.1}$$

The heat flux q_x (W/m^2) is the heat transfer rate in the x direction per unit area perpendicular to the direction of transfer, and it is proportional to the temperature gradient, dT/dx, in this direction. The proportionality constant k (W/m·K) is a transport property known as the thermal conductivity.

3.2.1 Experimental Methods and Facilities

According to ASTM standard C518-04 (ASTM 2004), the thermal conductivities of building products were determined using the heat flow meter apparatus as shown in Figure 3.2.

Figure 3.2 Heat flow meter apparatus developed by IRC-NRC

The apparatus used for the measurement of all the products was the heat flow meter with 300 mm x 300 mm plates. Each plate has a built-in heat flow sensor. The plates were maintained at different constant temperatures by a circulating thermostated fluid in a counter-flow pattern pumped by water baths. During the test three quantities were measured from each plate, they are:

- Output, E (mV), from the heat flow sensor
- Temperature, Tp (°C) from the exterior surface of the plate and
- Temperature, T (°C) from the inner surface of the plate

The schematic of the plates is shown in Figure 3.3. The metering area was 152.4 mm x 152.4 mm square, which was a thermopile with many copper-constantan junctions. The test specimen should be of the size as to cover both cold and hot plate surfaces, and the actual thickness to be applied in use or of sufficient thickness to give a true average representation of the material to be tested. For this apparatus, the maximum allowed specimen thickness was 50.8 mm. Furthermore, in order to limit the edge heat losses on

the measurement, all the surfaces exposed to the air were covered with insulation material during the test. Research also found that the thermal conductivities of building material are not much affected by relative humidity until dew point is reached at the cold side of the test specimen (Hansen et al. 2001). For this reason, the test apparatus was covered with an insulation chamber and compressed dry-air is circulated in the chamber.

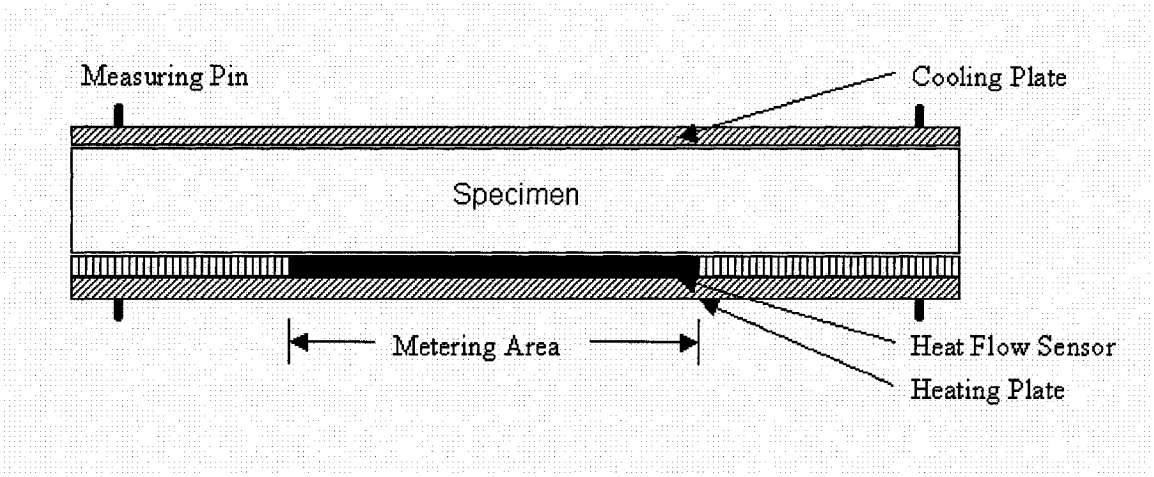

Figure 3.3 Schematic of heat flow meter apparatus

3.2.2 Specimens Preparation and Test Conditions

Two 30 cm X 30 cm specimens were used for the thermal conductivity measurement by the heat flow meter method. The specimens were exposed to different temperatures. Before the test, all the specimens were conditioned at 22 °C, and 50 % RH. For each measurement, a 12-hour period was allowed to expire for confirmation of steady state. Two tests were carried out for each specimen. One test kept the mean temperature between two plates around 24 °C, and another around 0 °C. The measurement uncertainties of the heat flow meter apparatus were within ± 2 %.

3.2.3 Thermal Conductivities of Building Products

The results show that with different plate temperature, the measured thermal conductivities for various building materials increase with the mean plate temperature. However, this difference is small, e.g. for different products, it ranges from 2 % to 11 % corresponding to the mean plate temperature from 0 °C to 24 °C. The thermal conductivities of building products are listed in Table 3.4, and the value for each product is based on the average of 2 tests under different mean temperatures on 2 specimens.

Table 3.4 Measured thermal conductivities of the products investigated

Products	Thermal Conductivities ($Wm^{-1}K^{-1}$)
Interior Gypsum Board	0.146 ± 0.002
Oriented Strand Board	0.089 ± 0.002
Plywood	0.085 ± 0.003
Wood fibre Board	0.047 ± 0.001
Spruce	0.097 ± 0.002
Stucco	0.328 ± 0.008
Extruded Polystyrene Foam Sheathing	0.027 ± 0.001
Glass Fibre Batt Insulation	0.038 ± 0.002

Comparison of measured heat conductivities for different materials is shown in Figure 3.4, and the heat conductivities are plotted logarithmically.

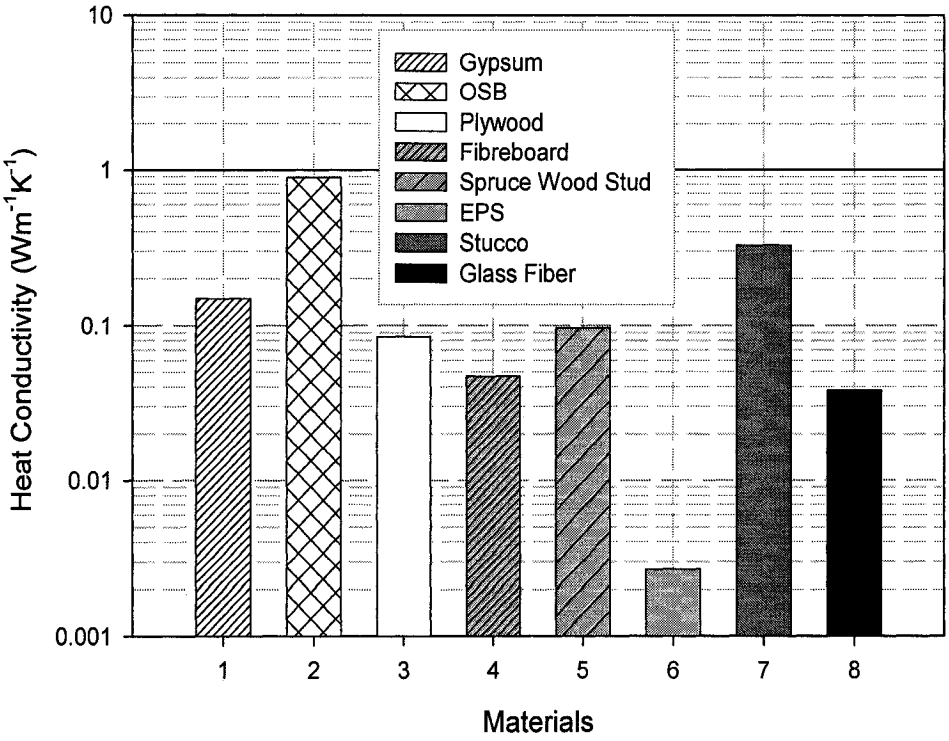

Figure 3.4 Measured heat conductivities for different building materials

Among four sheathing products, extruded polystyrene sheet has the lowest heat conductivity as expected and OSB has the highest. Comparing the measured data with ASHRAE research project 1018 (Kumaran et al. 2002a) found that for most of the building products the measured thermal conductivities have 5% to 10% differences with recorded results. Thermal conductivity of Stucco is 18% lower than the measurement made in the ASHRAE project probably due to the difference in the workmanships and manufactures.

3.3 Moisture Storage Characteristics of Building Materials

As mentioned in Chapter 2, the moisture storage characteristics are presented in a different way in hygroscopic range and capillary range. ASTM C1498 (ASTM 2001) was used for determination of sorption isotherms for building products in the hygroscopic range. The moisture retention curves were measured by the pressure plate extractor method (Nordtest 1997).

3.3.1 Experimental Methods and Facilities

Five temperature-humidity chambers were used for sorption isotherms measurements. The weights of specimens were determined by an electronic analytical balance with a resolution of 0.001g. The chambers can maintain the temperature and relative humidity of the air inside at a constant level, and they were built for exposing samples of building materials to controlled humidity and temperature levels. The conditions of these chambers are listed in Table 3.5.

Table 3.5 Temperature-humidity chambers used to determine the sorption isotherms of building products

Chamber no.	Relative humidity (%)	Temperature (°C)
1	33.7 ± 0.4	22.5 ± 0.1
2	50.0 ± 0.1	23.2 ± 0.1
3	70.4 ± 0.1	23.2 ± 0.1
4	89.4 ± 0.3	23.1 ± 0.1
5	96.1 ± 0.2	22.8 ± 0.1

Those chambers give very precise control of temperature and humidity level. They were developed by IRC-NRC, as shown in Figure 3.5.

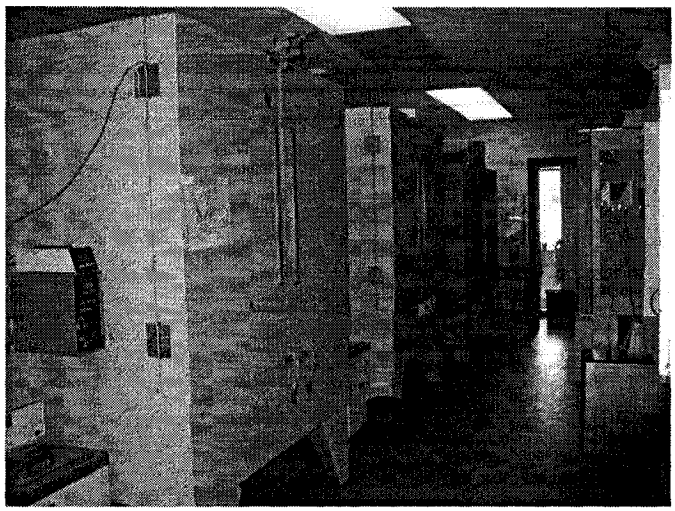

Figure 3.5 Temperature-humidity chamber developed at IRC-NRC

For water retention curve measurement, three pressure extractors were used, as shown in Figure 3.6. They were two 5 bar and one 15 bar pressure plate extractors.

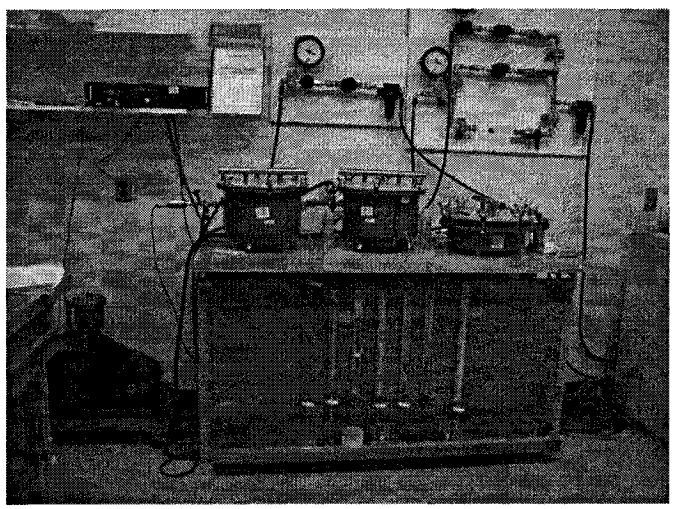

Figure 3.6 Five bar and ten bar pressure plate extractors at IRC-NRC

As shown in Figure 2.2, the pressure plate was fixed in the pressure vessel. Water in the specimen was forced out by the pressure place on the specimen through the cloth, kaolin paste, porous ceramic plate, and then out of the vessel along the outflow tube. The porous

ceramic plate on which the saturated specimens were placed was saturated with water at the beginning of the test (Figure 3.7). The saturation was obtained by soaking the plate in water for 24 hours. The side on which the specimen was placed was exposed to overpressure, while the corresponding side was under atmospheric pressure. As a result, a pressure difference was forced over the plate. Since the plates were saturated with water, they allowed only water but not air to pass through them. The maximum pressure that the plate can withstand before letting air pass through it was determined by the pore size of the plate. The kaolin paste was used to have perfect hydraulic contact between the plate and the specimens. The fabric cloth was for keeping the contaminant of kaolin paste out of the specimens.

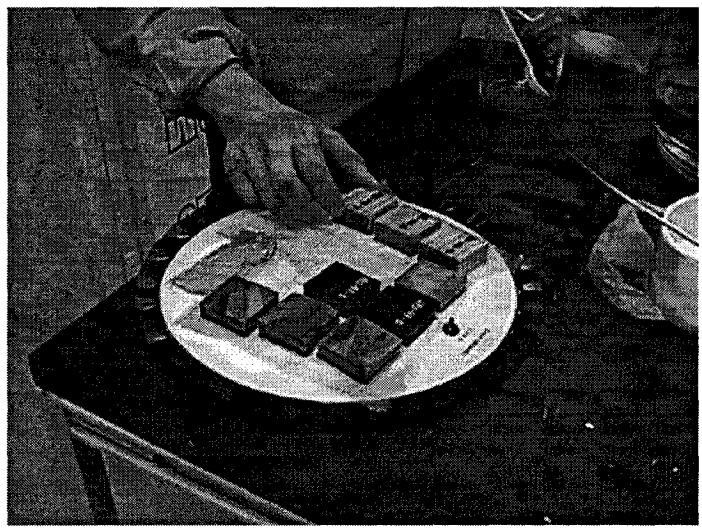

Figure 3.7 Test specimens are placed on the saturated ceramic plate

Once the ceramic plate was mounted in the pressure vessel, the lowest pressure level was applied. Excess water was forced out of the specimen, and collected in a burette. The equilibrium state was reached when water outflow was less than 0.05 cm^3 in 48 hours. At equilibrium, the mass of the specimen was determined. After that, the specimen was

remounted in the vessel, and then a higher pressure level was applied. Since the specimens were saturated at the beginning, equilibrium was reached through the desorption process.

3.3.2 Specimens Preparation and Test Conditions

For the sorption isotherms test, totally 40 specimens, with the size of 40 mm X 40 mm, were used for each building product. Nine specimens were cut for the pressure plate test. Before the test, all the specimens were oven dried as mentioned in Section 3.1. The dried Specimens were directly used for the sorption test.

For desorption and pressure plate measurements, the test specimens were vacuum saturated with de-aerated water. After drying, the specimens were evacuated using a vacuum pump to remove all trapped air within the materials, which ensured that the specimens would be completely saturated when they were finally soaked in de-aired water. After saturating the specimens in the de-aired water for at least 4 days, the weight of the wet specimens can be used as saturated weight. Figure 3.8 shows the apparatus used for saturating the specimens, which was connected to a vacuum pump. When saturating gypsum board products, special care was taken. Gypsum board specimens were soaked into plaster solution. Since gypsum loses its rigidity easily and dissolves with water, plaster powder in the solution prevented its structural dispersal.

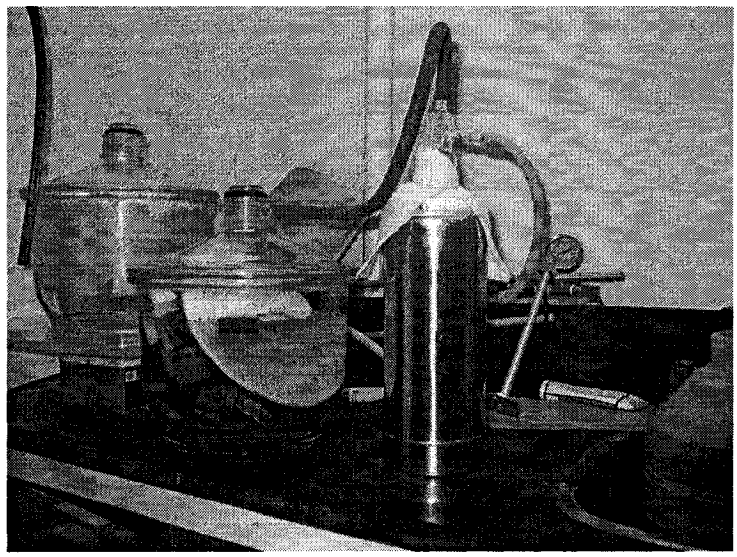

Figure 3.8 Apparatus to vacuum saturate test specimens

For the determination of the absorption and desorption isotherms, initially dried or saturated specimens were conditioned in the temperature-humidity chambers with five different relative humidity levels (33 %, 50 %, 70 %, 90 % and 96 % respectively) and the nominal temperature of 23 °C until equilibrium moisture content (EMC) was attained for test specimens. As for the pressure plate tests, 6 pressure levels were applied to the building materials.

3.3.3 Sorption Isotherms and Retention Curves of Building Materials

The sorption isotherms and retention curves of building materials were measured according to ASTM C1498 (ASTM 2001) and Nordtest standard 481 (Nordtest 1997) respectively. Glass fiber insulation and membrane products were not tested for their moisture storage characteristics. Because of the low density of the extruded polystyrene foam sheathing products, it is difficult to vacuum saturate them. Only sorption tests were carried out on EPS product. The specific measurement data are listed in Appendix A.

The comparisons of the measurements for tested materials are shown in Figures 3.9 and 3.10, which plot the sorption and desorption processes respectively.

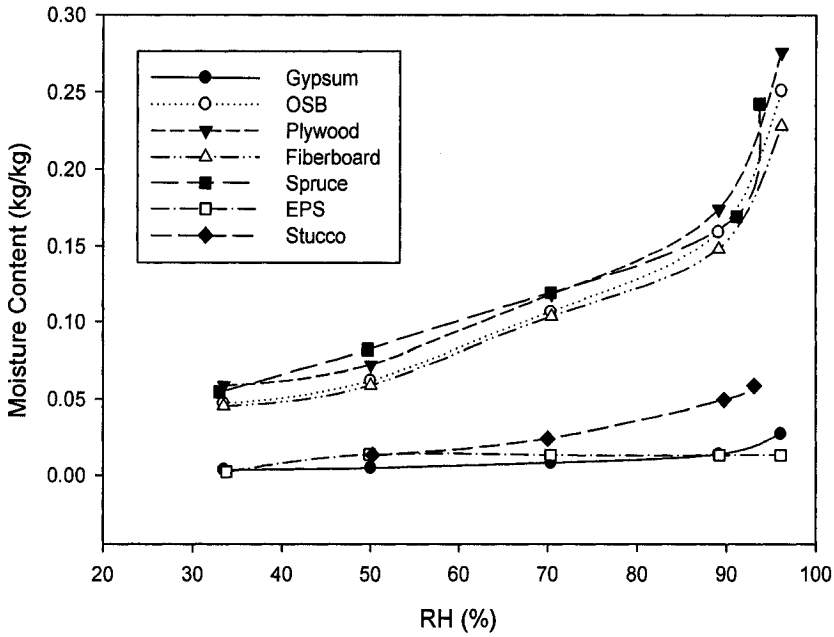

Figure 3.9 Measured sorption curves from tested building products

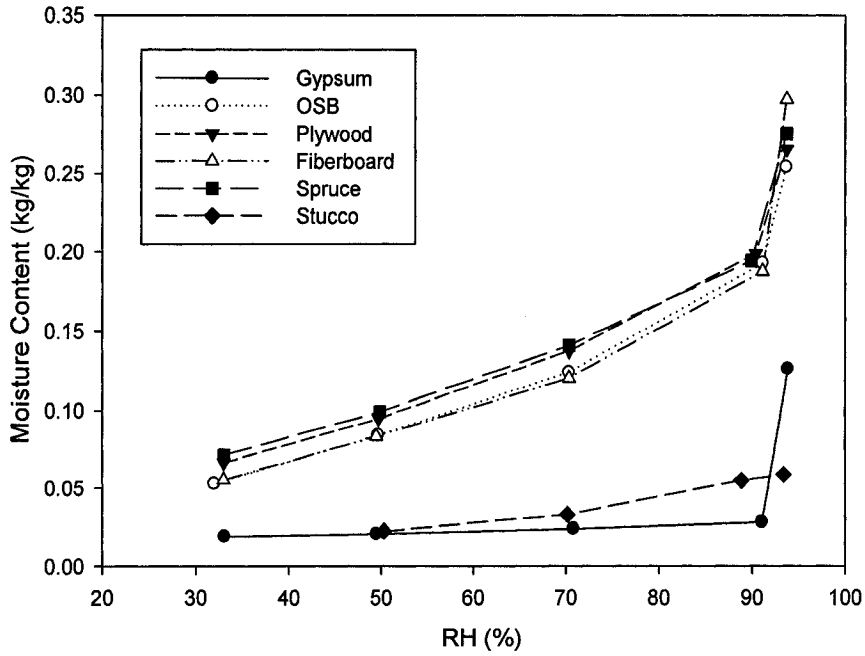

Figure 3.10 Measured desorption curves from tested building products

From the measurement data, it can be found that wood based materials have higher moisture storage capacity than others. However, the difference among wooden materials is not significant. The EPS product has low moisture content under different relative humidity conditions. Even though the gypsum board has lower moisture storage capacity than other materials, it can absorb and release moisture faster than others. It reached the equilibrium state from dry or saturation condition in a week, while the others took several months. Comparing the measured data with ASHRAE research project 1018 (Kumaran et al. 2002a) found that the measured sorption isotherms have 10% to 50% differences with recorded results. EPS and plywood have up to 10% difference, whereas, for fiberboard, spruce, and stucco products, the discrepancies with recorded data can be as high as 50%.

3.4 Water Vapor Permeabilities of Building Materials

The dry cup and wet cup methods were used for the determination of water vapor permeabilities of building materials. The experimental procedure was based on an extension (Kumaran 1998b) of the cup methods described by ASTM standard E96 (ASTM 2000).

3.4.1 Experimental Method and Facilities

The controlled temperature-humidity chambers developed for ASTM E96 test procedure were used, which are the same as those used to determine the sorption isotherms of building products. The mechanical balance, shown in Figure 3.11, used for weighing the specimens and test assemblies, satisfied the criteria specified in the ASTM E96 standard. This balance has the capacity of 5 kg, and the resolution is ± 0.001 g.

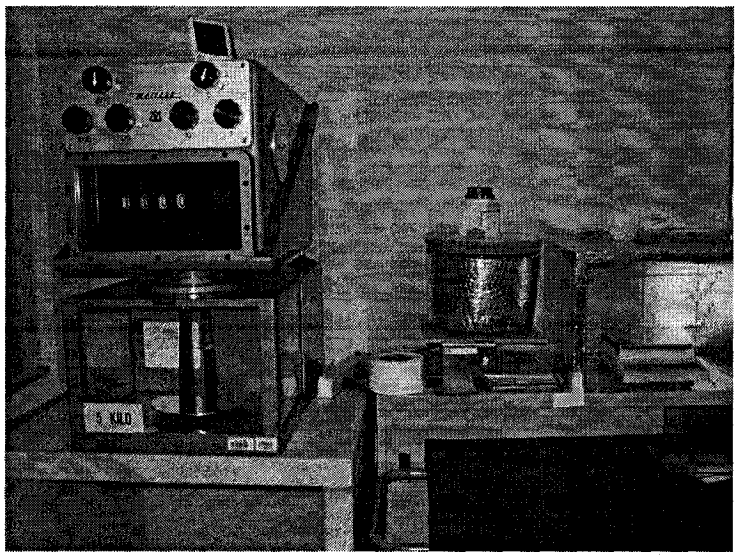

Figure 3.11 Mechanical balance used to determine water vapor permeability

The measurement results were analyzed with the same principles used in ASTM Standard E96. The change of the cup weight was plotted against the time elapsed. A straight line observation, involving at least six properly spaced points, indicated the establishment of the steady state water vapor transmission process. The slope of this straight line is the water vapor transmission rate (*WVT*). The test results obtained in this study, when plotted and curve fitted, showed a very clear straight line with an 'R-square' value 0.998 or higher.

The water vapor transmission rate (*WVT*) is calculated using the following equation.

$$WVT = \frac{G}{tA} = \frac{(G/t)}{A} \tag{3.2}$$

where G (kg) is weight change of desiccant or water, t (s) time, G/t (kg/s) slope of the straight line, and A (m^2) test area, i.e., cup mouth area.

Water Vapor Permeance

$$WVP = \frac{WVT}{S(\varphi_1 - \varphi_2)} \tag{3.3}$$

where S (Pa) is saturation vapor pressure at test temperature, φ_1 is relative humidity at the moisture source expressed as a fraction (test chamber for desiccant method; in the dish for water method), φ_2 relative humidity at the vapor sink expressed as a fraction, and WVP (kg/m^2·s·Pa) water vapor permeance.

Water Vapor Resistance

The water vapor resistance, WVR (m^2·s·Pa/kg), of a building component is expressed as the reciprocal of the WVP of the same.

$$WVR = \frac{1}{WVP} \tag{3.4}$$

In addition the following corrections are applied to the test results.

1. Corrections for resistance due to the still air layers, and

2. Corrections due to resistance offered by the specimen surface.

Resistance Due to Still Air Layer

If the thickness of the still air layer present between the desiccant and specimen or adjacent layers of specimen is known, then the corresponding water vapor resistance can be calculated using the following equation of permeability, proposed by Schirmer (1938).

$$\delta_a = \frac{2.306\times10^{-5}\cdot P_0}{R_v T P_a}\left(\frac{T}{273.13}\right)^{1.81} \tag{3.5}$$

Where δ_a (kg/m·s·Pa) is water vapor permeability of the still air, P_0 (101325 Pa) standard atmospheric pressure, P_a (Pa) is ambient air pressure, T (K) the temperature, and R_v (461.5 J/K·kg) gas constant for water.

AR is the resistance offered by still air (m·s·Pa/kg),

$$AR = \frac{l}{\delta_a} \tag{3.6}$$

where, l (m) is the thickness of the air layer.

Resistance Due to Specimen Surface

The surface resistances, i.e. inside and outside surfaces of the specimen, have been approximated using Lewis' relation (Pedersen, 1990). For the cup method, the total surface resistance offered by two surfaces is judged to be approximately 4 x 10^7 Pa·s·m^2/kg.

Water Vapor Permeability of the Materials

Corrected WVR of the specimen = (WVR from Equation 3.4) – (resistance offered by still air (Equation 3.6) for a known thickness in the cup and specimen surfaces (i.e., 4 x 10^7 Pa·s·m^2/kg)), i.e.

$$WVR_{corrected} = \frac{1}{WVP} - \frac{l}{\delta_a} - S_R \tag{3.7}$$

where S_R (Pa·s·m^2/kg) is the resistance offered by specimen surfaces.

Corrected WVP of the specimen = 1/(Corrected WVR of the specimen), i.e.,

$$WVP_{corrected} = \frac{1}{WVR_{corrected}} \tag{3.8}$$

Corrected water vapor permeability δ (kg/m·s·Pa) of the material = Corrected WVR of the specimen ×thickness of the specimen, d (m), i.e.

$$\delta_{corrected} = WVP_{corrected} \times d \tag{3.9}$$

3.4.2 Specimens Preparation and Test Conditions

For each material three dry cups and three wet cups were used. The specimens were cut into the shape of a cylinder with the diameter of 143mm. Prior to the measurement, the mass and dimensions of the specimen were recorded. Figure 3.12 shows the measuring cup assembly used at IRC. The cup was made by PVC, the specimen was sealed at the cup ring by molten wax. The molten wax was made of 60% beeswax and 40% paraffin wax warmed to 180°C. The dry cup was filled with desiccant (Calcium Chloride), and with distilled water for the wet cup. Cups were placed into the climate-controlled chamber, and the assemblies were weighed at different intervals depending on materials.

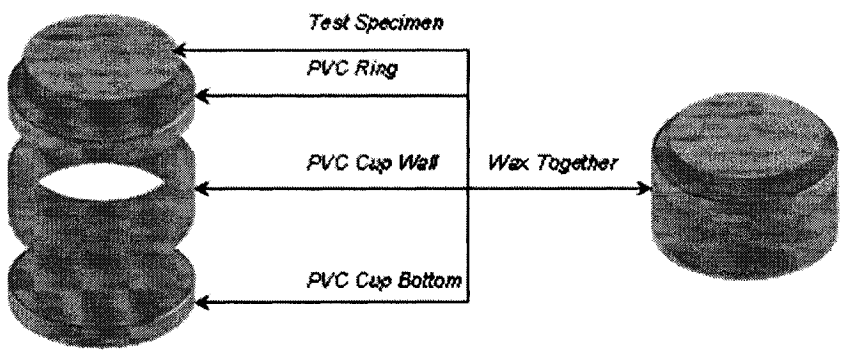

Figure 3.12 Assembly of measuring cup

The cups were filled with water or desiccant to about 15 mm below the specimen. Desiccant absorbed moisture during the test. However, it might lose its drying capacity after it has absorbed water equivalence of 10 % of its weight. The weight of desiccant was recorded so it could be easier to judge when to terminate the test at a 10 % desiccant mass gain.

Kumaran (1998b) suggested an extension of the cup methods described by ASTM standard E96. In the Standard, the dry cup method gives the results as an average value of the property at a mean relative humidity of 25 % and the wet cup at 75 %. This information is not enough for detailed hygrothermal analysis of building components. The complete dependence of water vapor permeability data on relative humidity is required by most computer models for hygrothermal simulation. Therefore, in this work a series of dry cup tests (at conditions of 50 %, 70 % and 90 % RH), and wet cups (at conditions of 50 % and 90 % RH) were used for water vapor permeability measurements.

3.4.3 Water Permeabilities of Building Materials

The water vapor permeabilities of test materials were determined according to the analysis procedure established by Kumaran (1998b). To guarantee the true steady state of each set of measurements, a linear least-squares analysis of the data of time versus mass change was used, and the linear regression coefficient should not be less than 0.998. The water vapor permeability at corresponding RH level was determined by the slope. Since it is not possible to create a relative humidity of 100 % in a chamber, the water transmission rate at 100 % RH was determined by summing the rates of water vapor transmission from both measurements of wet cups and dry cups at 70 % RH, which

theoretically would be equal to that for a dry cup measurement done at a chamber RH equal to 100 %. This sum of data combined with other dry cup data from a series of dry cup measurements defined the dependence of the water vapor transmission rate for the full range of RH. The plot of the water vapor transmission rate versus relative humidity was smoothed by curve fitting, then the obtained algebraic expression could be used to determine the derivative of the plot at any given RH. The permeance of the test assembly at a given RH could be derived by Equation 3.10 (Kumaran 1998b):

$$Permeance = \frac{Magnitude\ of\ derivative \times 100}{saturation\ water\ vapour\ pressure\ at\ 23^{O}C} \tag{3.10}$$

The measurement data of gypsum board are given below, while the data for other products are listed in Appendix A. Water vapor transmission rates at different relative humidity from dry cup and wet cup measurements of the gypsum board can be found in Tables 3.4 and 3.5 respectively. The numbers in parentheses indicate the experimental uncertainties for chamber RH and temperature and standard deviations for water vapor transmission rates, obtained from statistical analyses of the data at a steady state. The fitted curve for measured water vapor transmission rate is shown in Figure 3.13.

Table 3.6 Dry cup measurements of gypsum board

Specimen Thickness mm	Chamber RH %	Chamber Temperature °C	WVT Rate kg/s·m^2
12.62	49.97 (1)	23.22 (0.1)	3.08E-06 (2.8E-08)
12.48	49.97 (1)	23.22 (0.1)	2.94E-06 (1.8E-08)
12.63	49.97 (1)	23.22 (0.1)	2.94E-06 (2.4E-08)
12.62	70.42 (1)	23.13 (0.1)	4.71E-06 (7.1E-08)
12.48	70.42 (1)	23.13 (0.1)	4.53E-06 (5.4E-08)
12.63	70.42 (1)	23.13 (0.1)	4.50E-06 (5.9E-08)
12.62	89.80 (1)	23.06 (0.1)	5.72E-06 (5.7E-08)
12.48	89.74 (1)	23.07 (0.1)	5.57E-06 (3.9E-08)
12.63	89.75 (1)	23.06 (0.1)	5.46E-06 (1.1E-08)

Table 3.7 Wet cup measurements of gypsum board

Specimen Thickness mm	Chamber RH %	Chamber Temperature °C	WVT Rate kg/s·m^2
12.46	70.45 (1)	23.08 (0.1)	2.28E-06 (2.1E-09)
12.55	70.45 (1)	23.08 (0.1)	2.28E-06 (3.2E-09)
12.48	70.45 (1)	23.08 (0.1)	2.34E-06 (8.3E-09)
12.46	89.72 (1)	23.08 (0.1)	1.06E-06 (1.6E-08)
12.55	89.72 (1)	23.08 (0.1)	1.12E-06 (1.5E-08)
12.48	89.72 (1)	23.08 (0.1)	1.10E-06 (9.8E-09)

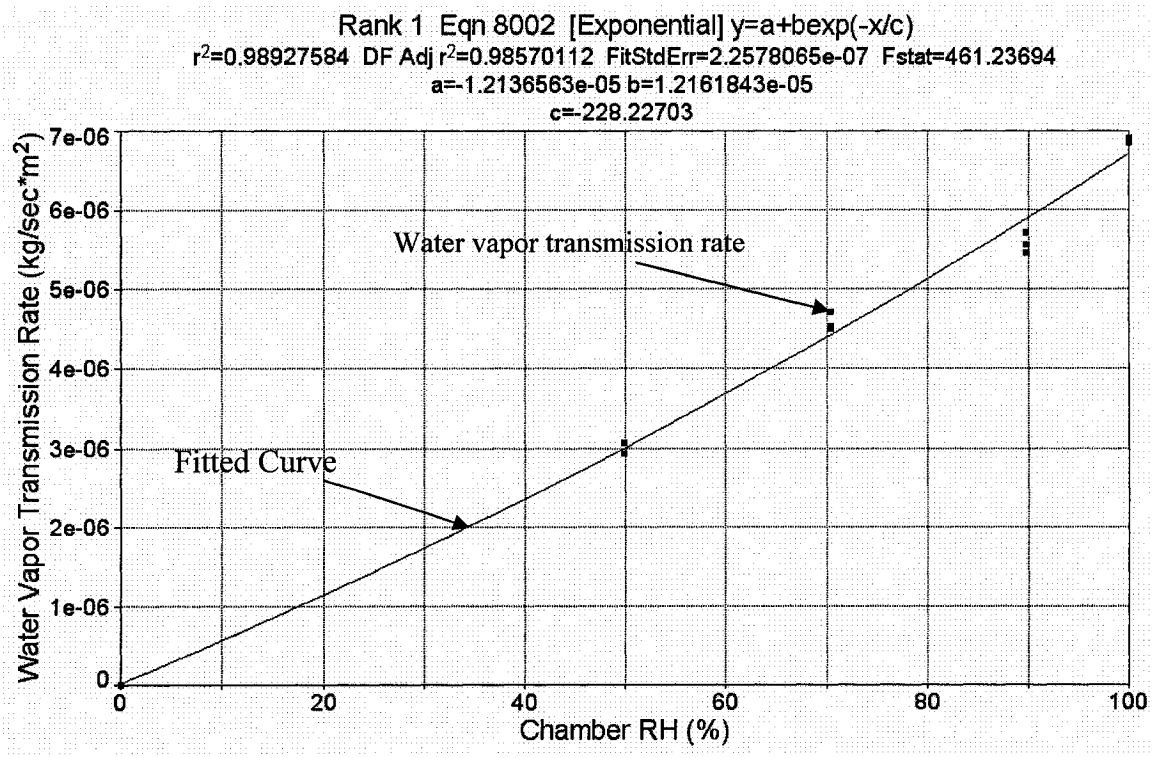

Figure 3.13 Fitted curve for measured water vapor transmission rate of gypsum board

The commercial software, TableCurve2, was used for curve fitting. The numerical summary provided by the software is listed below. The equation used for representing the relation between chamber RH and WVT is [Power] $y=ax^b$. The detailed statistics can be

seen in Table 3.8. The calculated water vapor permeabilities of gypsum board are listed in Table 3.9.

$r^2 = 0.988$
Fit Std Error = 2.2e-07
F-value = 966

Table 3.8 Statistics for curve fit of measured water vapor permeability of gypsum board

Parameter	Value	Standard Error	T-value	90% Confidence Limits
a	3.18e-08	8.49e-09	3.74	1.31e-08, 5.04e-08
b	1.16	0.06	19.34	1.03, 1.29

Table 3.9 The dependence of water vapor permeability of gypsum board on relative humidity

RH %	Permeability kg/m·s·Pa	RH %	Permeability kg/m·s·Pa
10	2.86E-11	60	4.11E-11
20	3.28E-11	70	4.24E-11
30	3.56E-11	80	4.36E-11
40	3.77E-11	90	4.47E-11
50	3.95E-11	100	4.58E-11

From the TableCurve statistics, the estimated uncertainty in the derived value of the permeability may be up to 27%. This uncertainty is calculated based on the standard error of the fitting equation and it resulted from the scatter in the measured water vapor transmission rate. Some documented uncertainties of vapor permeabilities for building materials could be as high as 50% (Kumaran et al 2002a).

Through the comparison of water vapor transmission rate for different building products tested in this work, the diverse vapor transport abilities were realized. Figure 3.14 plots this comparison logarithmically. Among those tested products, gypsum board and polyethylene membrane have the highest and lowest transmission rates respectively. Fiberboard is more permeable than other wooden sheathing products, whereas OSB has

the lowest water vapor permeability. The study also found that stucco is a permeable product. It has a transmission rate of 8 to 10 times higher than wooden materials.

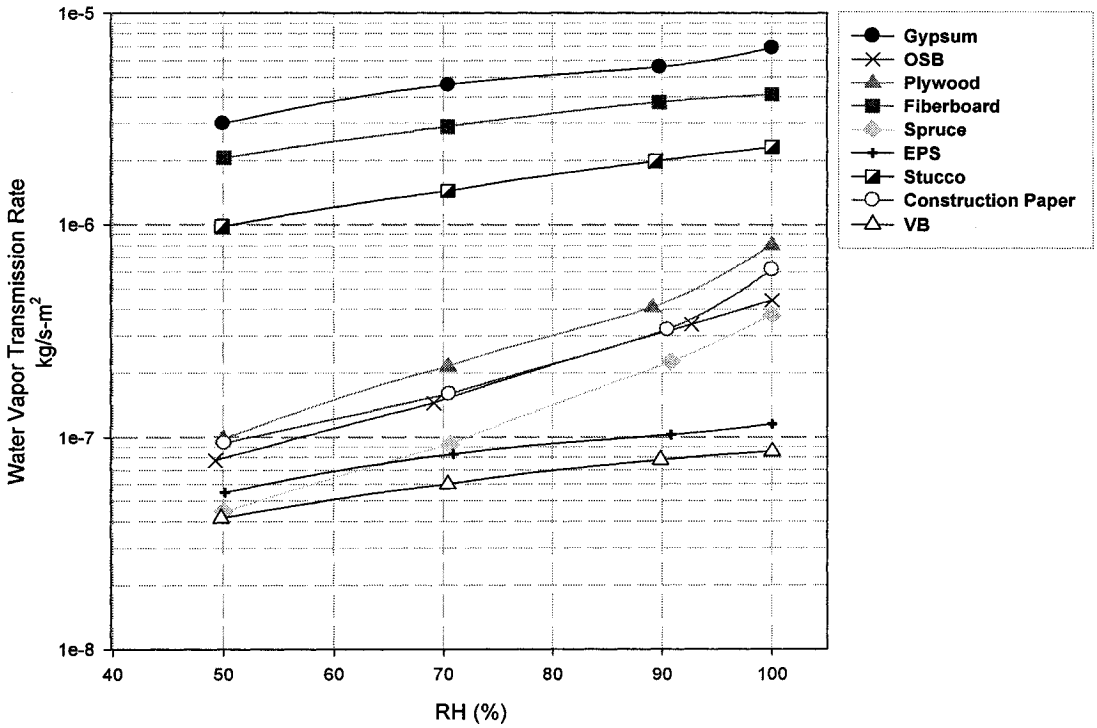

Figure 3.14 Measured water vapor transmission rates for different materials

Comparing the measured data with ASHRAE research project 1018 (Kumaran et al. 2002a) found that for most of the building products the derived water vapor permeabilities have 18% to 50% differences with recorded results. Gypsum, OSB and EPS products have up to 20% difference, whereas, for plywood and spruce, the discrepancies with recorded data can be as high as 40% and 50% respectively. A significant large discrepancy in derived vapor permeabilities is found for stucco product probably due to the difference in the workmanships and manufactures.

3.5 Transient Moisture Content Profiles of Building Materials

The main purpose of obtaining transient moisture content profiles is to derive liquid water diffusivity, D_w, of building materials. It is one of the moisture transport properties frequently used in hygrothermal analysis. The relationship between D_w and moisture content w can be seen in Equation 2.16.

3.5.1 Experimental Method and Facilities

The gamma ray spectrometer developed by IRC-NRC (Figure 3.15) was used for determining the transient moisture contents of building materials. A brief description about this method was given in Section 2.2.4.

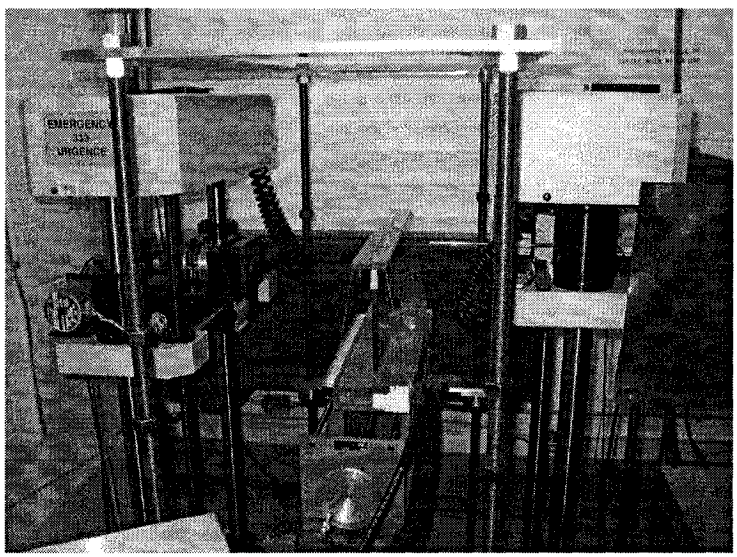

Figure 3.15 Gamma ray spectrometer used in IRC-NRC

The gamma ray equipment was made up of the source housing assembly and the detector assembly, which can be seen in Figure 3.16. The source consisted of 1) a composite of americium oxide and aluminum oxide, and 2) cesium chloride in a fused silica matrix.

Each was a line source with an active area of 2 mm x 25 mm. The external shutter, operated by electrically activated solenoids, effectively stopped all radiation from the two sources. The detector and analyzer used in gamma ray spectrometer were 51-mm thick sodium iodide (thallium) crystal with a photomultiplier tube (Harshwa model 14SHA8/3.5/x). The diameter of both of them was 89 mm. Together with the respective collimators, the source and detector were mounted on two separate platforms, each of which can be moved vertically and horizontally with the precision better than ±0.02 mm.

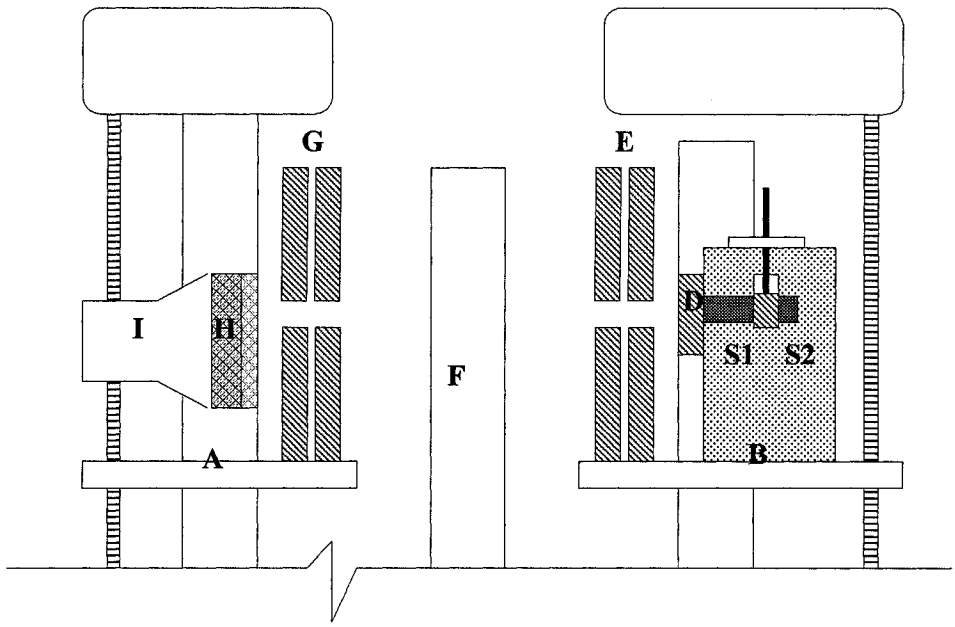

A. Platform for source assembly
B. Platform for Detector assembly
C. Internal shutter
D. External shutter
E. Lead-block collimator
F. Specimen
G. Lead-block Collimator
H. Sodium iodide (thallium) crystal
I. Photomultiplier tube
S1. Americium source
S2. Cesium source

Figure 3.16 Schematic of the gamma ray spectrometer (Kumaran and Bomberg 1985)

The movements of these two platforms were controlled by a computer system. Computer programs were used to precisely define the parameters such as starting time, vertical and horizontal coordinates, live time, etc.

An experimental procedure was developed by Kumaran and Bomberg (1985), and this procedure was followed in the present investigation. The test specimens were first dried at a certain temperature and then placed in the gamma ray equipment. The intensity of the gamma radiation transmitted through the specimen was determined. The test specimen was then subjected to a free water uptake process and during the process the transmitted gamma radiation at each location was determined at regular time intervals. This method is based on the attenuation equation.

$$\left(\frac{I}{I_0}\right) = e^{-\mu_w w d} \tag{3.11}$$

where I (photon/m^2·s) is the intensity of the transmitted gamma radiation through moist specimen, I_0 (photon/m^2·s) is the intensity of the transmitted gamma radiation through the dry specimen, μ_w (kg/m^3) is the mass attenuation coefficient of water at the selected range of the energy of the gamma radiation, and d (m) is the thickness of the test specimen. Equation 3.11 was used to calculate the moisture content of the specimen at each location and time interval. Thus the moisture distribution can be determined.

3.5.2 Specimens Preparation and Test Conditions

Three rectangular test specimens were prepared from each building material of interest. The specimens were 296 mm long and 60 mm wide. Before the test, they were dried in the oven at 50°C for 3 days to obtain constant dry conditions, and then were sealed with a

water vapor resistant epoxy resin. The fresh surfaces were opened at the ends of the specimens by cutting the epoxy coating. Sealed specimens were mounted vertically in the gamma ray spectrometer. The centerlines of the specimens were scanned from top to bottom at a consecutive 2 mm interval to determine the gamma ray attenuation due to the thicknesses of the dry materials. After scanning the dry specimens, the bottom surfaces of the test specimen were placed in contact with water in a shallow container. The water level in the water container was held at a constant level by the water circulation bath. The water temperature was kept at 21°C. Figure 3.17 illustrates the setup of the moisture intake process.

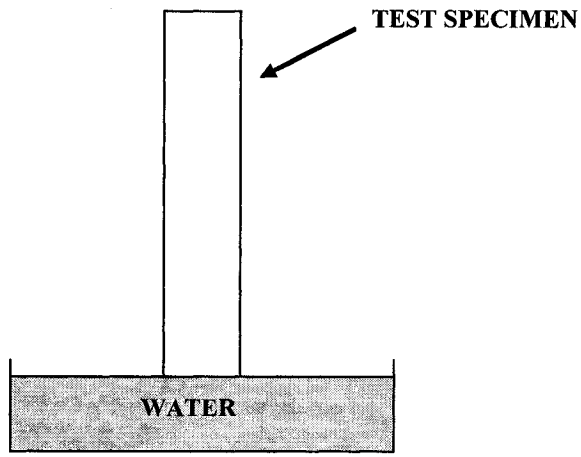

Figure 3.17 Schematic drawing of the moisture intake process

3.5.3 Moisture Diffusivities of Building Materials

Moisture diffusivities of building materials were determined using the Boltzmann transformation method. Under the initial conditions ($w = w_0$ at $x > 0$ and $t = 0$) and boundary conditions ($w = w_b$ at $x = 0$, $w = w_0$ for $x \rightarrow \infty$, $t > 0$.), the non-linear partial

differential equation, Equation 2.16, can be reduced to an ordinary differential equation (Crank, 1989)

$$-\frac{\lambda}{2}\cdot\frac{dw}{d\lambda}=\frac{d}{d\lambda}\left(D_w\frac{dw}{d\lambda}\right) \tag{3.12}$$

with the initial boundary conditions

$$\begin{aligned}\lambda = 0 &: w = w_0\\ \lambda \to \infty &: w = w_b\end{aligned} \tag{3.13}$$

The Boltzmann variable λ (m/s$^{1/2}$) is defined as

$$\lambda = x\cdot t^{-\frac{1}{2}} \tag{3.14}$$

By integrating Equation 3.12 with respect to λ using the boundary condition in Equation 3.13, the liquid diffusivity can be obtained by

$$D_w=-\frac{1}{2}\frac{\int_{w_0}^{w}\lambda dw}{\left(\frac{dw}{d\lambda}\right)_w} \tag{3.15}$$

The w- λ profile was obtained through the gamma-ray test during the free water intake process. The measurement data on the fiberboard product are given below. The moisture contents as the function of Boltzmann transformation variables are shown in Figure 3.18, and they were smoothed by curve fitting. Through the equation of the fitted curve, the first derivative of the curve at any given moisture content was obtained together with the area enclosed by the curve from zero to any given moisture content point. Therefore, the moisture diffusivities could be calculated using Equation 3.15. The moisture diffusivities

of fiberboard at a number of moisture contents are listed in Table 3.10, and plotted in Figure 3.19.

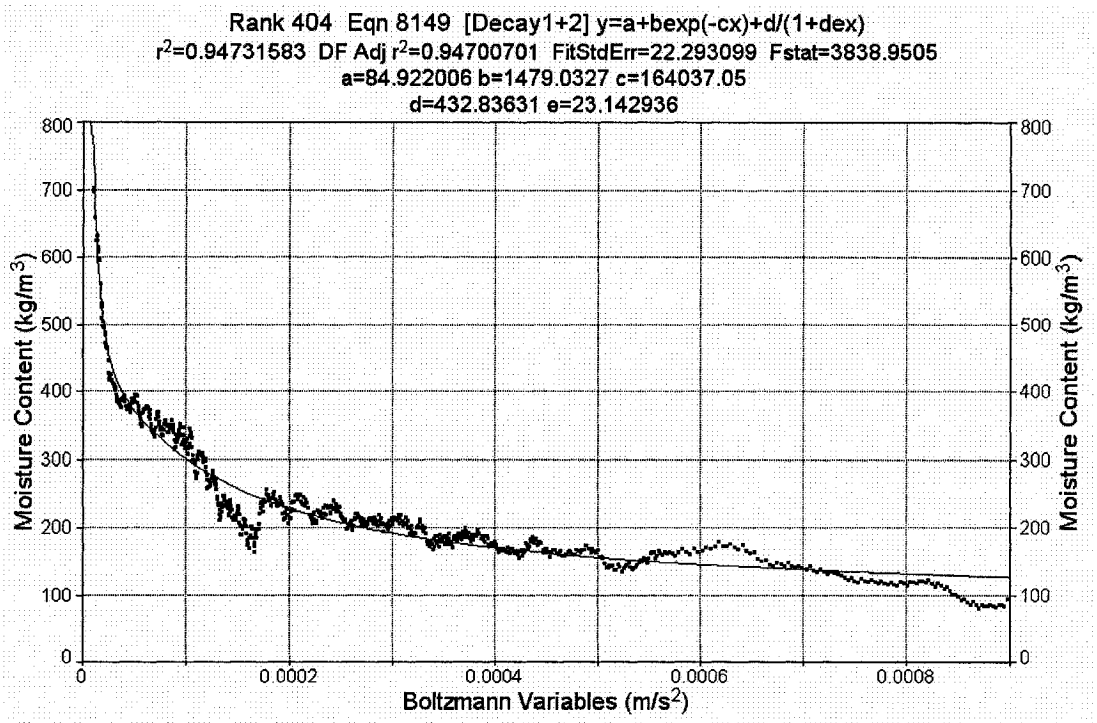

Figure 3.18 Moisture contents versus Boltzmann variables of fiberboard

Table 3.10 Moisture diffusivities of fiberboard product

Moisture Content (kg/m^3)	Diffusivities (m^2/s)	Moisture Content (kg/m^3)	Diffusivities (m^2/s)
84.9	1.06E-07	249.1	7.21E-08
101.0	1.27E-07	270.2	6.89E-08
116.7	1.52E-07	290.8	7.64E-08
131.4	1.88E-07	309.8	8.15E-08
145.7	2.92E-07	319.2	7.99E-08
161.0	4.73E-07	329.0	7.48E-08
176.9	3.09E-07	339.9	6.70E-08
191.7	3.17E-07	352.3	5.71E-08
205.2	4.09E-07	386.7	3.52E-08
221.5	1.96E-07	413.2	2.49E-08
239.7	8.25E-08	452.9	1.58E-08

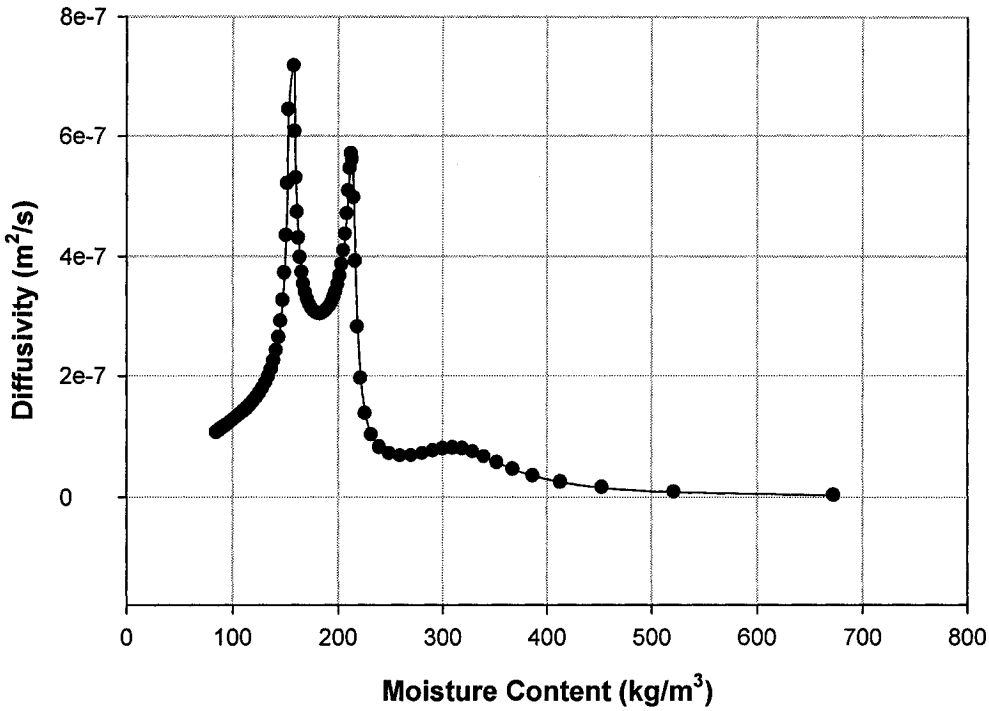

Figure 3.19 Moisture diffusivities of fiberboard product

In Table 3.10 and Figure 3.19, the liquid diffusivity calculated from Gamma-ray test clearly established the order of magnitude. The shape of the curve that shows the dependence of liquid diffusivity on moisture content is very sensitive with the first derivation of the fitted curve shown in Figure 3.18, and it significantly varies by using different measurement or analysis methods. A rather large variation was also found in the result of the round-robin test (Kumaran 1999). The unusual change of derived diffusivity of fiberboard at low moisture content can be found in Figure 3.19. Gamma ray equipment scanned the specimens point wise, and the time interval used in this test was 2 minutes. When the specimen began to absorb water at its low moisture content condition, the uptake in specimen is so fast that only some limited points can be measured leading to less reliable results and unusual change at low moisture content condition.

3.6 Water Absorption Coefficients of Building Materials

Water absorption coefficient is defined as the ratio between the change of the amount of water entry across unit area of the surface and the corresponding change in the time expressed as the square root. It can be expressed as Equation 2.18 as mentioned in Chapter 2.

3.6.1 Experimental Method and Facilities

Mukhopadhyaya et al. (2002) described the water absorption test method based on European Standard, Thermal performance of buildings and building components – Determination of water absorption coefficient (CEN TC89 1994). The partial immersion method was used in this test. One surface of the specimen was immersed in the water tank. Water flowed through a circulation bath to keep the constant water level. The specimen was weighed periodically. The schematic diagram of the water tank and circulation bath is shown in Figure 3.20. The specimen was hung by a fixable device and allowed it to move up and down to adjust the position to be just touching the surface of water.

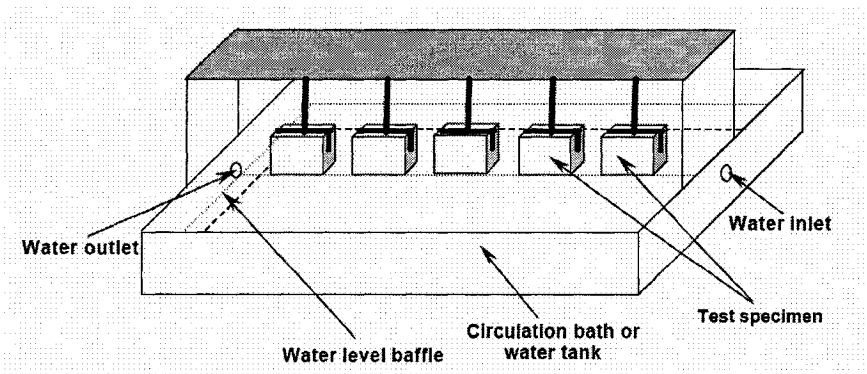

Figure 3.20 Schematic diagram of the circulation bath and water tank (Mukhopadhyaya et al. 2002)

3.6.2 Specimens Preparation and Test Conditions

Four cubic specimens of each product with the touching surface area around 25 cm^2 were tested. Before the test, all the specimens were stored at room temperature 23 °C and 40 ± 5 % relative humidity until the weight of each specimen reached a steady state. Later, the side surfaces of the specimens were sealed with molten wax to guard the one dimensional water transportation. Research found that the surface temperature of the material does have an effect on the water absorption coefficient of some building materials (Mukhopadhyaya et al. 2002). Therefore, it is important to keep the surface temperature at a constant level. The tests were carried out under the environmental temperature 23 ± 1 °C and 40 ± 5 % relative humidity. The liquid water in contact with the specimen surface was maintained at 22 °C.

3.6.3 Water Absorption Coefficient of Building Materials

The calculated absorption coefficients from the partial immersion test for tested building products are listed in Table 3.11 and plotted in Figure 3.21. The y axis is logarithmically scaled to better show the differences between them. The water absorption test data are listed in Appendix A.

Table 3.11 Water absorption coefficient of building materials

Products	Water Absorption Coefficient ($Kg/m^2 \cdot s^{1/2}$)
Interior Gypsum Board	1.6E-01 ± 4.2E-02
Oriented Strand Board	1.8E-04 ± 2.2E-04
Plywood	2.0E-03 ± 1.3E-03
Wood fiber Board	1.2E-03 ± 9.2E-04
Spruce	1.2E-02 ± 8.2E-05
Stucco	8.8E-02 ± 2.2E-02

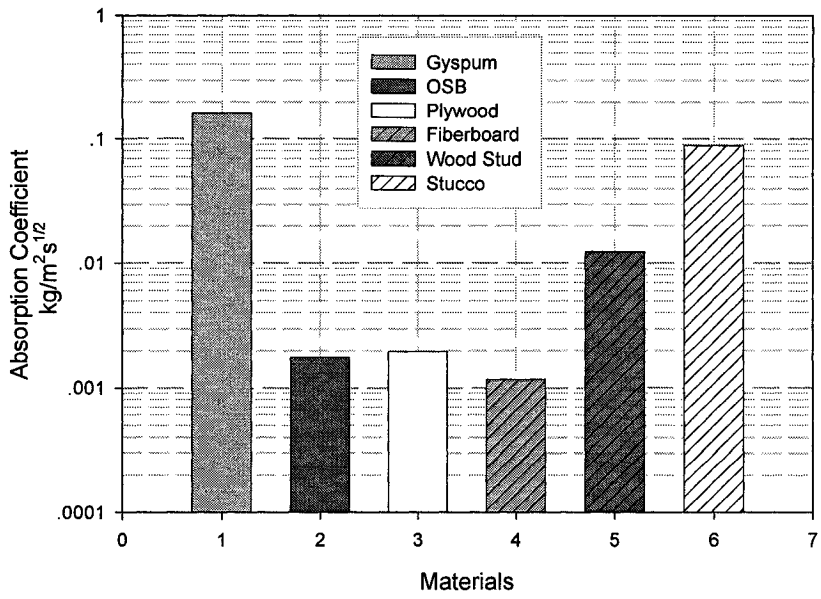

Figure 3.21 Water absorption coefficients for different building materials

From the comparison, it can be noticed that wood based products have a lower water absorption coefficients than other tested products, such as gypsum board and stucco. However, the differences of those three sheathing products are small.

Comparing the measured data with ASHRAE research project 1018 (Kumaran et al. 2002a) found that for most of the building products the water absorption coefficients have 11% to 50% difference with recorded results. OSB, fiberboard and plywood products have difference of 11%, 25% and 30% respectively. For spruce and gypsum products, the discrepancies with recorded data can be as high as 50%. A significant large discrepancy in derived water absorption coefficient is found for stucco product probably due to the difference in the workmanships and manufactures.

3.7 Air Permeabilities of Building Materials

The applicable theory of air flow through a porous membrane was described in the paper (Bomberg and Kumaran 1986). Air permeance K_a (m/s·Pa) can be defined as the quotient of the air pressure difference across a specimen divided by the volume velocity of airflow through the specimen (Equation 2.19). Measurements of air pressure difference and volumetric flow rate of air were used to calculate the air permeance.

3.7.1 Experimental Method and Facilities

Figure 3.22 shows a schematic diagram of the air permeability experiment setup at IRC-NRC. The test specimen was mounted on the top of an aluminum test chamber. It was sealed with molten wax, and one surface was exposed to the atmosphere. The compressed dry air flowed into the test chamber and passed through the test specimen into the atmosphere. Because the chamber was sealed, there was no air flowing to the outside through the test chamber. The total air flow through the specimen could be established; the pressure difference over the test specimen was measured using a pressure transducer.

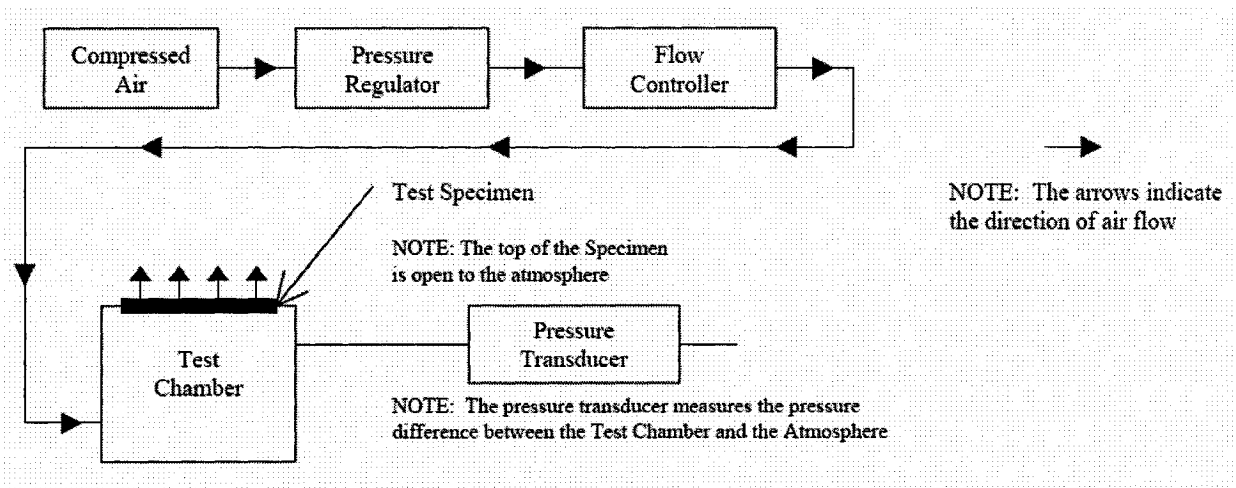

Figure 3.22 Schematic diagram of air permeability experiment setup at IRC-NRC

Two flow controllers and two pressure transducers were available at IRC-NRC for the air permeability experiment. The maximum inputs were 1000 sccm and 100 torr respectively. To measure the air permeability, the first step was to install the flow meter and pressure transducer that were best suited for the materials being tested. The ideal pressure range for the test is from zero to 200 Pa because it is the approximate value that occurs under field conditions. If the material is highly impermeable, higher pressures may be required. Based on one or more initial readings of flow and pressure, the right flow meter and pressure transducer could be determined.

The air permeability was defined from a linear regression of the readings of air flow rate and pressure difference. For each specimen, 10 sets of readings were recorded twice for a total of twenty data points. The whole procedure was controlled by a data acquisition system. A linear regression of the data points was then performed to obtain the permeability of the sample. Figure 3.23 shows the photo of the air permeability test apparatus at IRC-NRC.

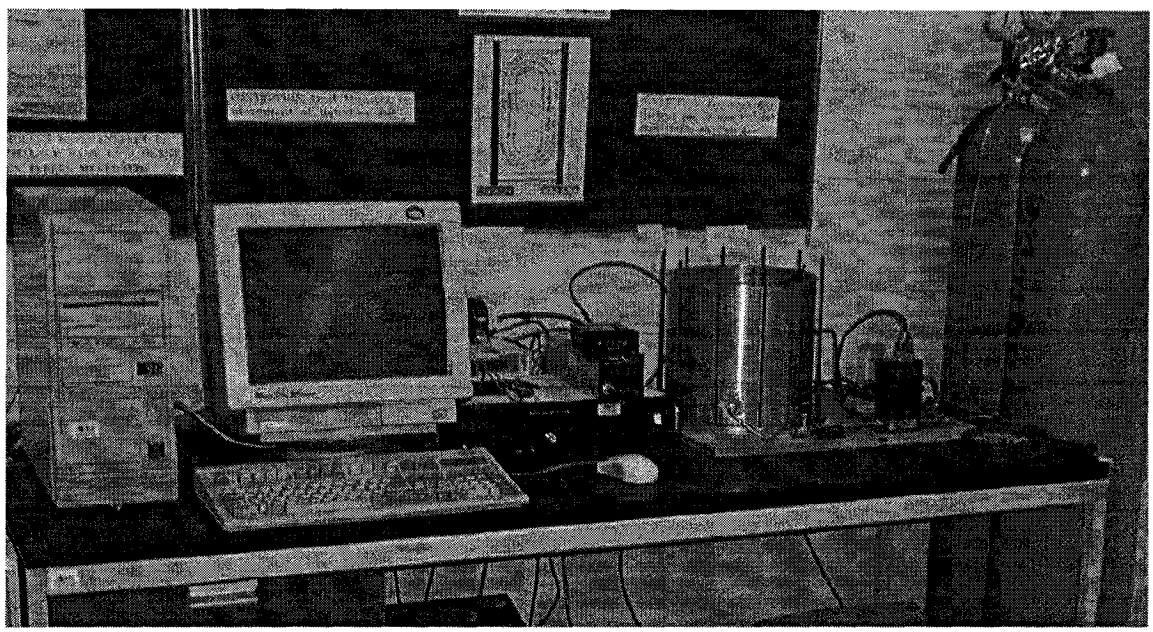

Figure 3.23 Air permeability test apparatus at IRC-NRC

3.7.2 Specimens Preparation and Test Conditions

The specimens used for the air permeability test were the same as the water vapor permeability tests. Molten wax was used to seal the specimen on the mounting plate. The measurements were conducted at 22 °C and 40 % RH.

3.7.3 Air Permeabilities of Building Materials

The dependence of airflow rate on pressure difference for fiberboard is shown in this section, while the data for other products are listed in Appendix A. The summary of the statistical analysis of the data from two sets of measurements for each specimen of fiberboard product is shown in Figure 3.24 as three different sets.

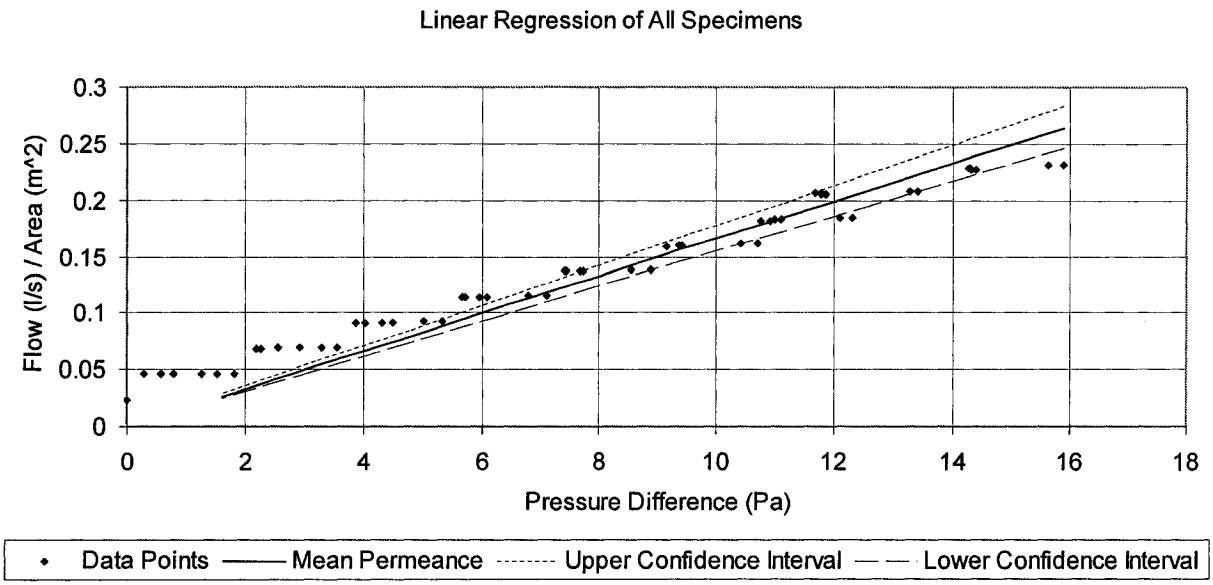

Figure 3.24 The dependence of airflow rate on pressure difference for Fiberboard

At the range of pressure differences from 0 to 16 Pa, the flow rate of all test specimens varies linearly with the pressure difference. The air permeability of the tested fiberboard is (2.2 ± 0.2) E - 07 kg m^{-1} Pa^{-1} s^{-1}.

The measured air permeabilities of the materials are shown in Figure 3.25. Comparison found that the fiberboard is the most air permeable material among them. Three sheathing materials display different air permeabilities. The construction paper, which usually is placed behind the stucco to prevent water entering the wall system, has the lowest air permeability.

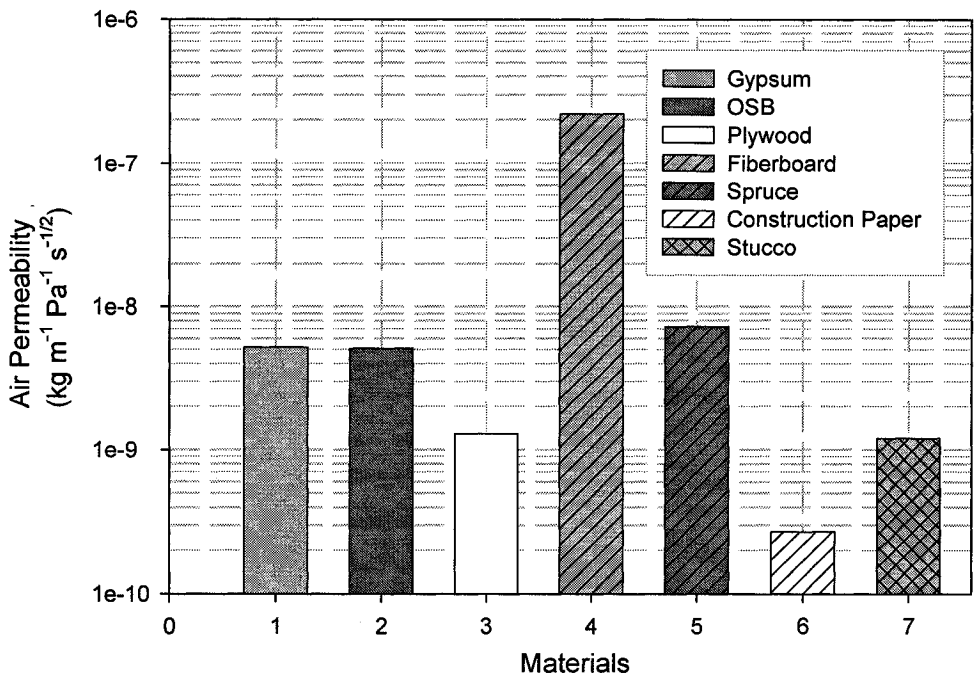

Figure 3.25 Measured air permeabilities of building products

Comparing the measured data with ASHRAE research project 1018 (Kumaran et al. 2002a) found that for fiberboard, plywood and OSB products the air permeabilities have approximately 12%, 30% and 50% difference with recorded results respectively. Rather

large discrepancies in air permeabilities are found for gypsum, spruce and stucco products.

3.8 Summary

The material properties of 10 building products which are widely used in Canada were determined using well-established test procedures. The determined properties include thermal conductivity, sorption/desorption isotherm, retention curve, water vapor permeability, liquid diffusivity, water absorption coefficient, and air permeability. These material properties can be used as input for advanced HAM models. The measured hygrothermal material properties were compared with material database in ASHRAE Research Project 1018 (Kumaran et al 2002a). The comparison found that the differences in the measurement results exist for all the products and for most of cases the differences range from 10% to 50%. The measured hygrothermal properties for stucco product have rather large discrepancies with documented data probably due to their different workmanship and manufactures.

Chapter 4
Moisture Buffering Capacity of Building Materials

This chapter presents the experimental study of the moisture buffering capacity (MBC) of building materials. The MBC tests were carried out for 5 building products. The general information, experimental procedure, and facilities are introduced.

4.1 General Information of MBC

Indoor air humidity level is one of the most important factors that affect the indoor air quality for occupants (Fang et al. 2000). The indoor relative humidity level has significant diurnal variation due to the activities of the occupants. Also seasonal change can be found because of the weather conditions. From the study of hygrothermal properties of the hygroscopic building materials, it can be concluded that those materials can effectively reduce the peaks of indoor humidity level and sequentially improve the indoor air quality. The use of hygroscopic building materials to adjust indoor humidity conditions is effective and is achieved without any external energy input. Hence there has been an increasing interest in this topic recently. The ability of a building material to moderate humidity level in the indoors can be represented by its moisture buffering capacity (MBC).

Earlier studies have shown the potential of using building materials to moderate indoor relative humidity (Padfield, 1998, Salonvaara et al. 2004). One of the researchers experimentally investigated the role of absorbent material in moderating the change of relative humidity (Padfield, 1998). In his work, the moisture buffering capacity was

measured for wood, brick, cellular concrete and unfired clay. He found that wood end grain panels showed the best buffering capacity due to rapid diffusion and high moisture capacity of wood. Some others studied the moisture buffering capacity of building materials by small scale laboratory and full scale single room tests and numerical calculations (Salonvaara et al. 2004). A review (Rode et al. 2004) was carried out for moisture buffering in interior spaces, and also indicated that there is a need to quantify the moisture buffering capacity of building materials. Recently, a workshop was held in Europe with the main purpose to standardize a test method for MBC (Rode et al. 2003). Later, in 2005, a Nordtest standard defining the moisture buffering effect and test method was presented as a result of a Nordic collaboration project (Rode et al. 2005).

In North America, a series of tests on moisture buffering capacity of plywood product was carried out at the University of Saskatchewan (Osanyintola et al. 2005). However, there is no test standard available for MBC of building materials in North America. In addition, the shortage of moisture buffering value data for most building materials will delay research in using absorptive material to improve indoor environmental conditions.

MBC can be defined as the ability of indoor building materials to moderate the humidity level. The term, Moisture buffering Value (MBV), quantifies the moisture buffering capacity of building materials, and it indicates the amount of moisture uptake or release by materials when they are exposed to repeated daily variations in relative humidity between two given levels. Rode et al. (2005) found that besides hygrothermal properties of building materials, MBV depends on air flow velocity, area and thickness of the test specimen.

The experimental principle was based on an environmental chamber test, where the test specimens were exposed under a square wave relative humidity change in daily cycles (see the RH change in Figure 4.1). The indoor humidity level is affected by many factors, such as types of materials, construction methods, ventilation, air movement, thermal condition, and function of buildings. A healthy or target indoor RH conditions might be varied with different types of buildings. The RH range chosen in this study is 33% to 75%, which covers the practical conditions measured in North America wood based residential buildings. During the test the changes in the masses of the specimens were recorded. The change in mass from the beginning of test is calculated as,

$$\Delta m = \frac{m - m_i}{A} \tag{4.1}$$

where m (kg) is the mass of the test specimen at a specific time, m_i (kg) is the mass of the test specimen when the experiment started (i.e. the initial conditions) and A (m^2) is the exposed surface area of the test specimen.

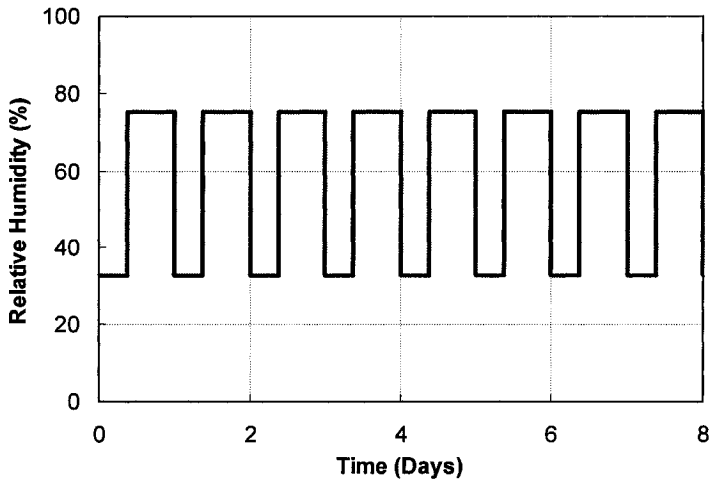

Figure 4.1 Relative humidity changes during the MBC test

The MBV (kg/m^2·% RH) can be calculated as the ratio of the mass change of the specimen during absorption or desorption of a cycle at equilibrium and the change in relative humidity. This ratio is shown in Equation 4.2.

$$MBV = \frac{\Delta m_p}{\Delta RH} \tag{4.2}$$

$$\Delta m_p = \frac{m_{final} - m_{start}}{A} \tag{4.3}$$

where Δm_p (kg) is the mass change of the test specimen during each relative humidity square cycle at equilibrium state, m_{final} (kg) is the mass of the test specimen measured at the end of an adsorption or desorption phase and m_{start} (kg) is the mass of the test specimen when the adsorption or desorption phase started.

4.2 Experimental Setting

4.2.1 Experimental Building Materials

The building products under testing were gypsum board, plywood, OSB, fiberboard, and cement stucco. The specimens were cut into 140 mm x 140 mm rectangular sheets. The edges and one surface of each specimen were sealed with molten wax, and there was only one surface exposed to the air. This setup simulated the situation in practice. Before the test, all the specimens were conditioned in the climate chamber where the indoor temperature and relative humidity was 22 °C and 50 % RH for a month until the equilibrium condition was reached (i.e. mass change of the specimen is less than 0.1 % for two weeks). The information on the experimental material is listed in Table 4.1. In

Table 4.1, the term, initial moisture content, represents the moisture content of the pre-conditioned specimen.

Table 4.1 The tested building materials

Test material	Area (cm^2)	Thickness (mm)	Dry density (kg/m^3)	Initial Moisture Content (k/kg)
Gypsum board	148.48	12.53	569	53.73
Plywood	148.78	12.65	428	134.61
OSB	148.72	11.407	634	71.46
Fiberboard	148.43	10.89	270	71.46
Stucco	99.94	19.47	1353	124.56

4.2.2 Experimental Facilities

Envirotronics standard temperature/humidity chamber SH16 was used in this test. The temperature range is – 30 °C to + 177 °C with accuracy of ± 0.3 °C, and it can change relative humidity from 10 % to 98 % with ± 2 %. The workspace of the chamber is 76.2 mm (width) × 76.2 mm (depth) × 76.2 mm (height). The picture of the chamber is shown in Figure 4.2. The climate change inside the chamber was controlled by Envirotronics System Plus Programmer/Controller. This controller also can function as a data logger, which can store the information about the chamber into a diskette or transfer running data to a data acquisition system. The electronic analytical balance with the resolution of 0.001 g was used for recording the mass change of the specimen exposed to the dynamic climate condition. A Vaisala temperature/humidity probe with uncertainty of 2 % was placed in the test chamber to monitor the RH and temperature. The air velocity in the test chamber was measured using TSI Velocicalc plus Air Velocity Meter.

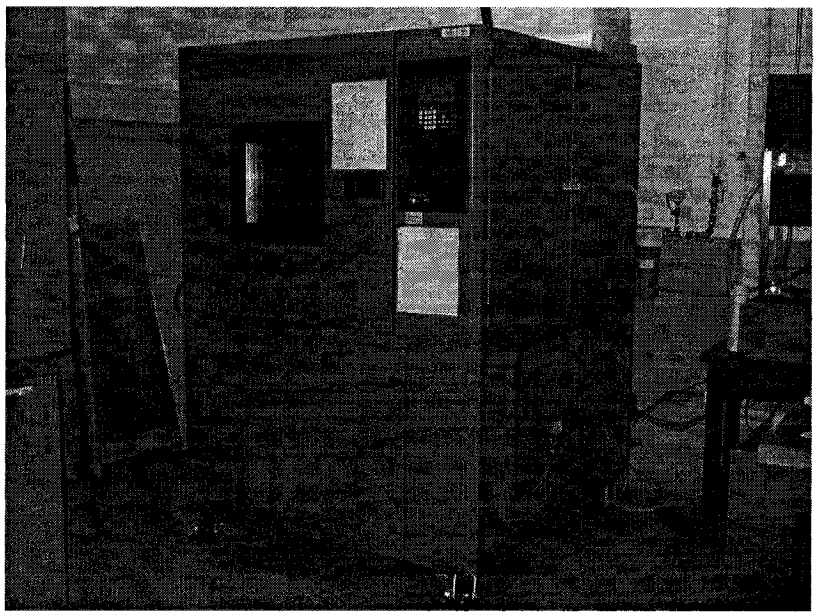

Figure 4.2 Envirotronics standard temperature/humidity chamber at IRC-NRC

4.2.3 Experimental Conditions

The specimens in the test chamber were periodically weighed. The change in mass of the specimens within the humidity cycle represents the moisture accumulated by building products. Test condition can be seen in Table 4.2. The high RH should last for 8 hours and low RH for 16 hours, and those RH set points are the same as the requirement in the Nordtest Standard (Rode et al. 2005).

Table 4.2 Test conditions for moisture buffering test

Temperature (°C)	Low RH (%)	High RH (%)
23 ± 0.3	33 ± 2	75 ± 2

Figure 4.3 presents the temperature and relative humidity measured using the temperature/humidity sensor located in the test chamber during a typical MBC test. Figure 4.3 was recorded every 5 minutes for 4 repeated cycles. Some scattered points can

be found in the RH readings. This scatter was the result from opening the chamber to weigh the specimen at one hour intervals.

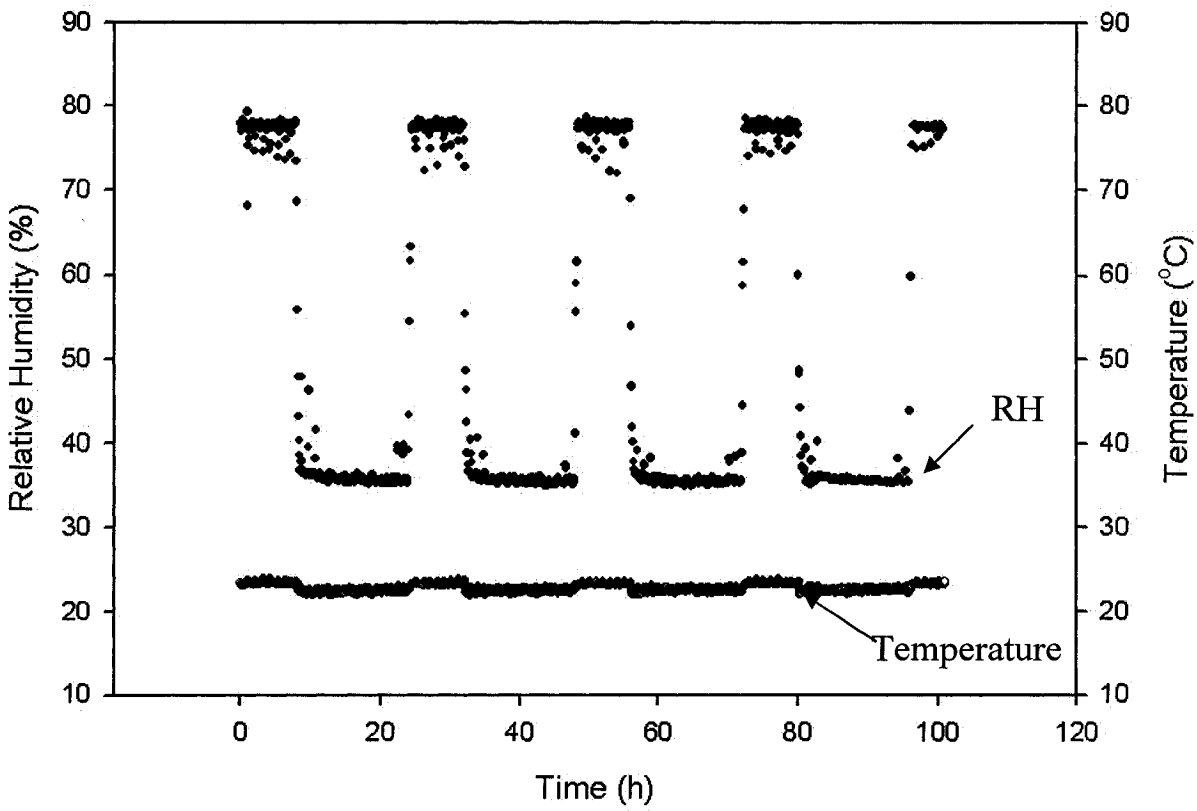

Figure 4.3 Measured relative humidity and temperature of the air entering the test chamber during a typical MBC test

4.3 MBV of Building Materials

This section presents the experimental data from the facilities mentioned above. The moisture accumulation data were used to determine the MBV of six building products. The initial and boundary conditions of the tests were also recorded.

The experimental data for the uncoated gypsum board are presented in Figure 4.4. It shows the mass changes of 3 gypsum board specimens for four 24-hour cycles. The mass change Δm_p from the beginning of the test is calculated using Equation 4.3

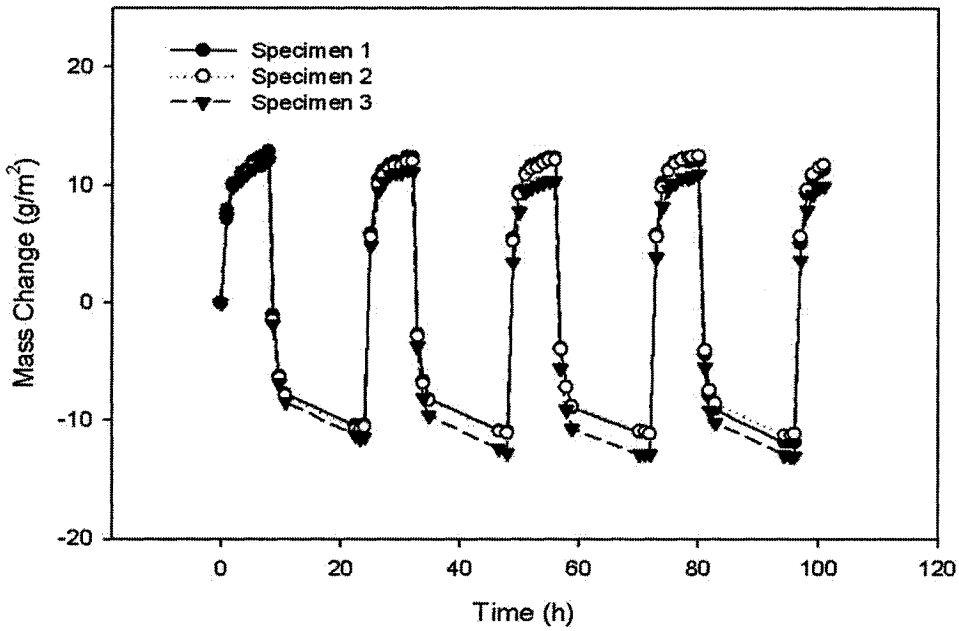

Figure 4.4 Mass changes of three identical uncoated gypsum board specimens over four 24-hour cycles for 3 specimens

It can be seen that the mass changes of three uncoated gypsum specimens under stepwise relative humidity circles followed a similar pattern of moisture absorption and desorption. During the first three cycles, the average mass change of three gypsum board specimens for the absorption process, Δm_{ads}, is 23.31 ± 0.33 g/m^2, and for the desorption process Δm_{des}, is 23.15 ± 0.48 g/m^2. The average mass change, Δm_{avg}, during three humidity cycles is 23.23 ± 0.32 g/m^2, which will be used later to quantify the MBC of building materials.

The measured mass changes of plywood, OSB, fiberboard and stucco products for four 24-hour cycles are plotted in Figure 4.5 to 4.8 respectively.

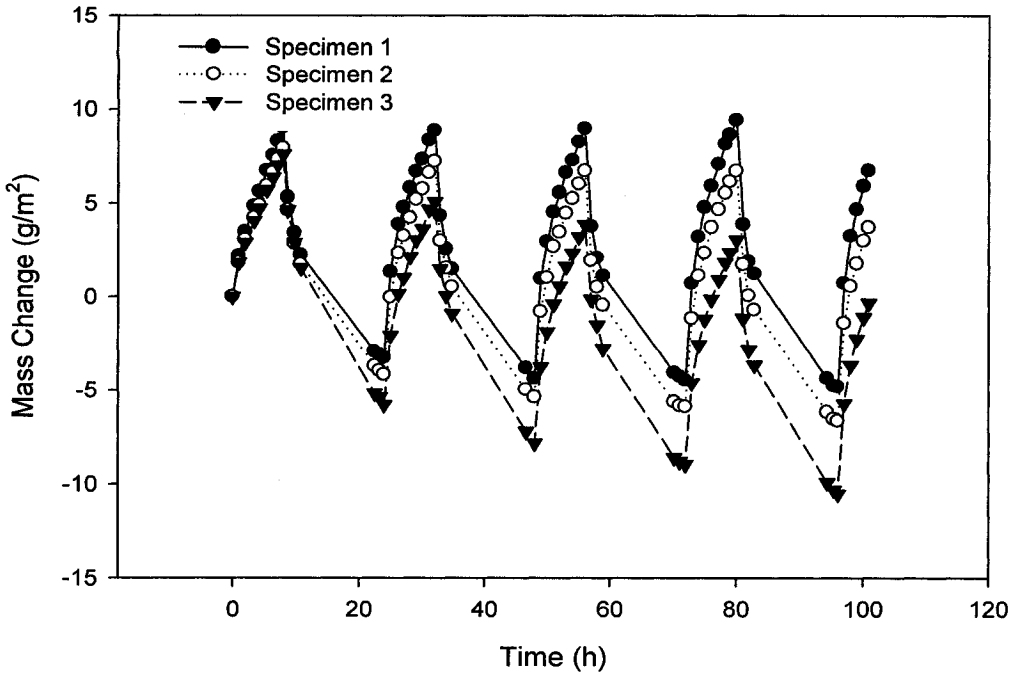

Figure 4.5 Mass changes of three identical plywood specimens over four 24-hour cycles

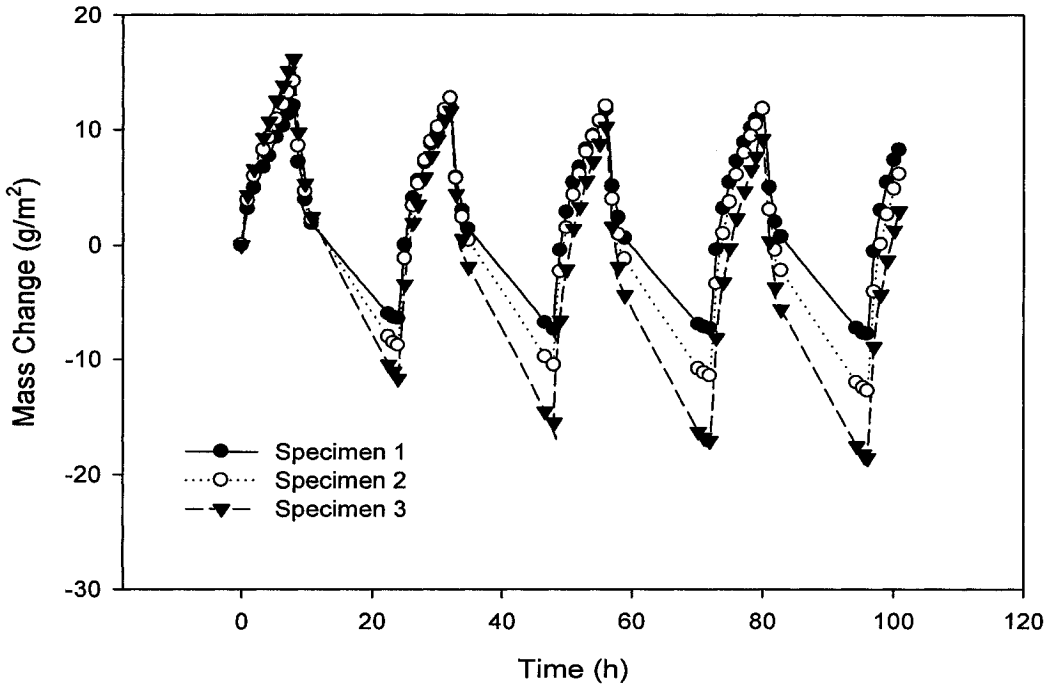

Figure 4.6 Mass changes of three identical OSB specimens over four 24-hour cycles

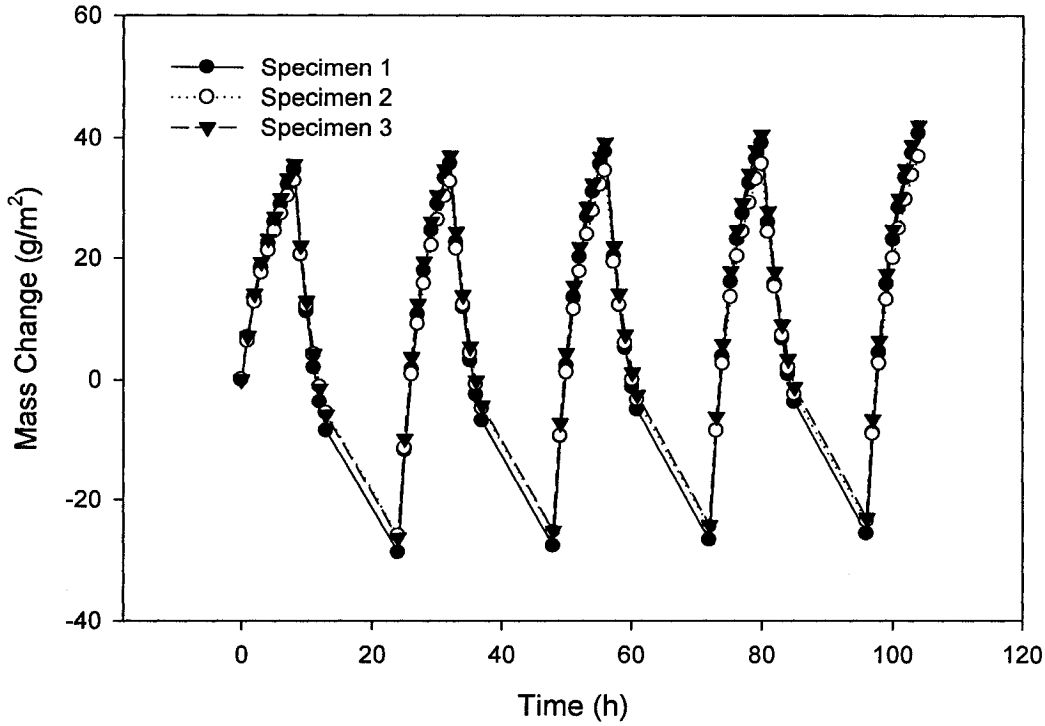

Figure 4.7 Mass changes of three identical fiberboard specimens over four 24-hour cycles

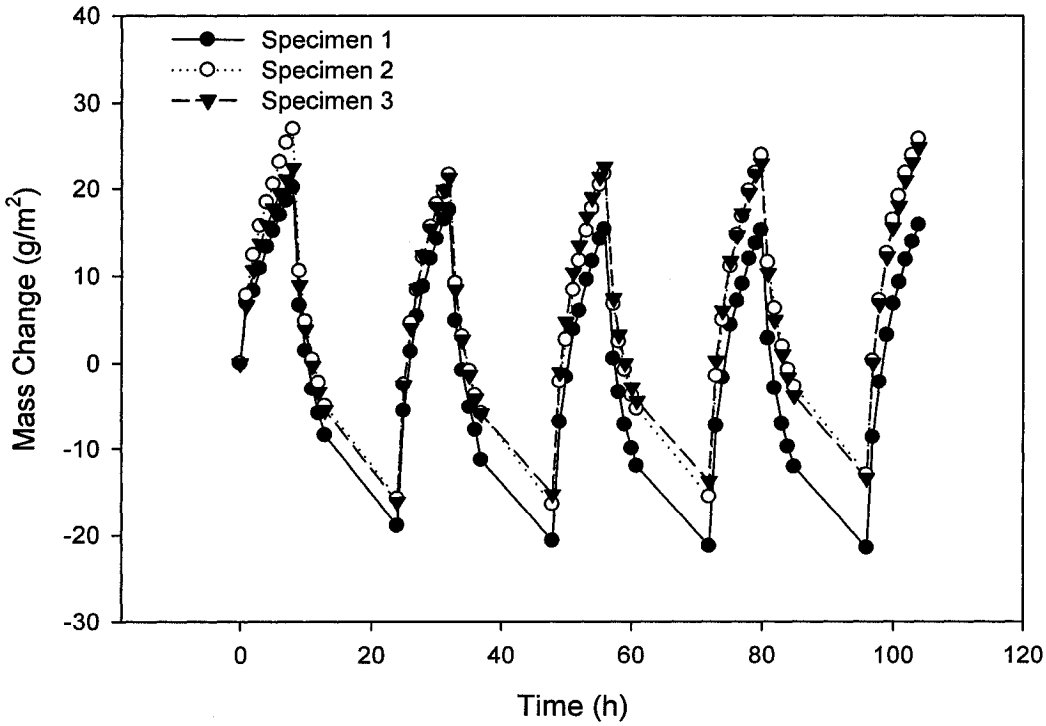

Figure 4.8 Mass changes of three identical stucco specimens over four 24-hour cycles

It can be seen that the mass change in all the tested building products follow similar patterns of moisture uptake and release. The mass changes of the tested building products under absorption and desorption processes during three RH cycles are summarized in Table 4.3. The differences in moisture uptake and release were due to the hysteresis effect, however, this difference decreased in the three RH cycles. At the third cycle, the percentage difference between moisture uptake and release is less than 2 % for all building products. The mass changes listed in Table 4.3 were based on the average value from 3 test specimens under the same test condition.

Table 4.3 The measured mass changes of the tested building products under MBC test

Materials		1st Cycle Mass Change (g/m^2)	2nd Cycle Mass Change (g/m^2)	3rd Cycle Mass Change (g/m^2)	Average Mass Change (g/m^2)
Gypsum	Absorption	22.6 ± 0.1	23.2 ± 0.1	23.6 ± 0.3	23.2 ± 0.5
	Desorption	23.1 ± 0.4	23.5 ± 0.4	23.3 ± 0.1	23.3 ± 0.3
Plywood	Absorption	11.5 ± 0.6	12.4 ± 0.9	12.8 ± 1.0	12.2 ± 0.9
	Desorption	12.6 ± 0.7	12.9 ±0.3	13.0 ± 0.4	12.8 ± 0.5
OSB	Absorption	21.0 ± 2.6	22.5 ± 3.3	22.8 ± 3.6	22.1 ± 2.9
	Desorption	23.1 ± 4.7	23.2 ± 4.0	23.3 ± 4.2	23.2 ± 3.7
Fiberboard	Absorption	60.1 ± 3.1	63.2 ± 3.0	63.5 ± 3.1	62.9 ± 2.7
	Desorption	61.3 ± 2.4	61.1 ± 2.8	62.2 ± 2.9	61.5 ± 2.4
Stucco	Absorption	37.8 ± 0.5	37.3 ± 1.2	37.6 ± 1.7	37.3 ± 1.1
	Desorption	40.0 ± 2.2	37.6 ± 1.0	36.7 ± 0.5	38.1 ± 2.0

The amount of moisture uptakes and releases under RH cycles for building products depends on the materials. MBV of all the tested materials were calculated based on Equation 4.2. The comparison of the MBV for different building products is shown in Figure 4.9 and Table 4.4. The MBVs shown in Figure 4.9 are the average of MBV value and its standard deviation for 3 specimens at the third RH cycle.

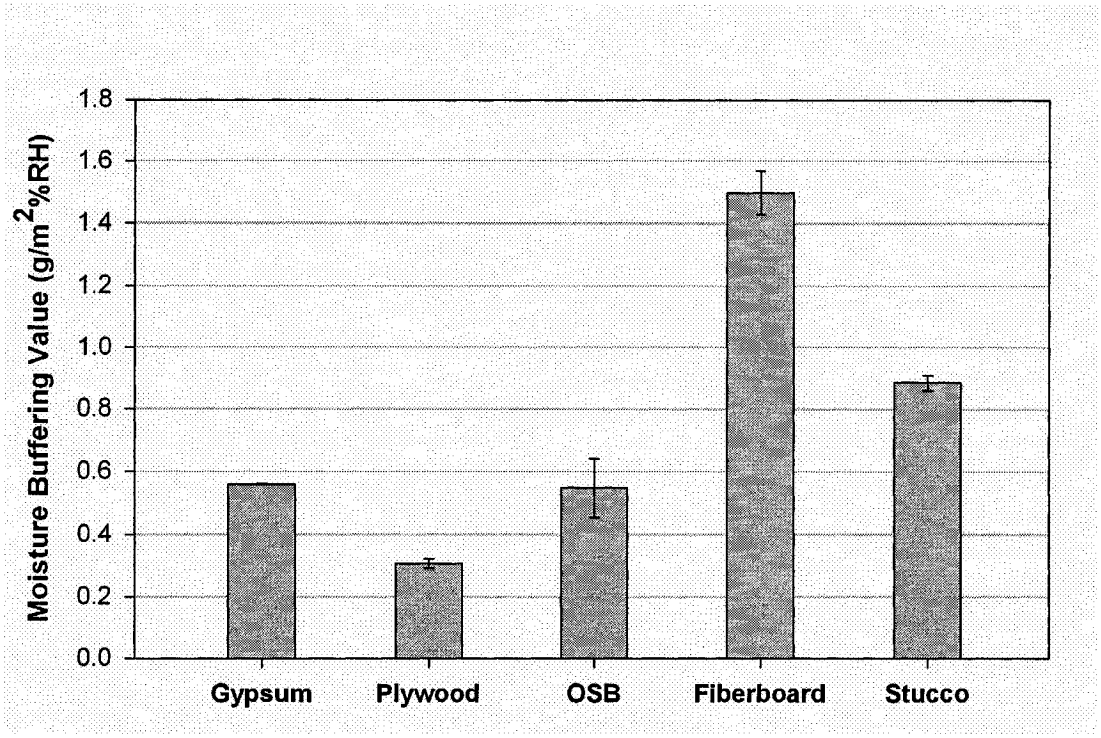

Figure 4.9 The Moisture Buffering Values (MBV) as an average value for all the measurements (3 specimens at the third RH cycles with moisture uptake and release). The thin vertical line-bars indicate standard deviations

Table 4.4 The Moisture Buffering Values (MBV) as an average value for all the measurements (3 specimens at the third RH cycles with moisture uptake and release). Standard deviation is calculated for the same data.

Materials	MBV (g/m^2%RH)		
	Average	Standard Deviation	% Deviation
Gypsum	0.56	0.00	0.3
Plywood	0.31	0.02	5.3
OSB	0.55	0.09	16.9
Fiberboard	1.50	0.07	4.7
Stucco	0.88	0.03	2.9

From the statistics shown in Table 4.4, it can be seen that for most tested building products the standard deviation of measured MBVs are within 5%. The highest standard deviation can be found in OSB product because of its heterogeneous property.

The sorption and desorption processes vary from material to material, but the majority of building materials follow a general sharp curvature. Since during the moisture buffering test building materials up-took and released water with the change of relative humidity, the processes are possibly described by the sorption and desorption curves. The commercial software package, TableCurve2, was used for curve fitting the sorption and desorption of the MBC test, and the relationship between water uptake/release with the time elapse were represented by different equations. The curve fitting results for first and third moisture uptake/release cycles of the tested building product specimens are shown in Figure 4.10. The equations used to describe the fitting curves of each moisture uptake and release process were chosen by the R square values, and all the equations listed in Figure 4.10 have the largest R square values among the ones listed by TableCurve2. The weight of the specimen at the starting point of moisture uptake process was set as the base value to calculate the mass change.

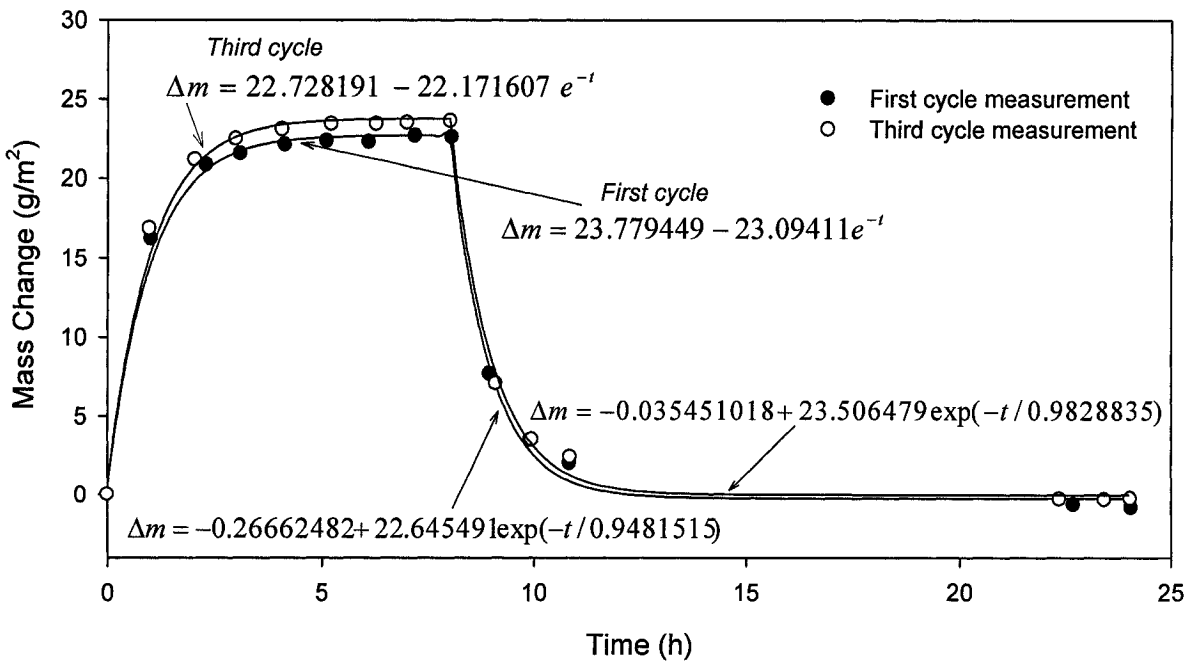

(a)

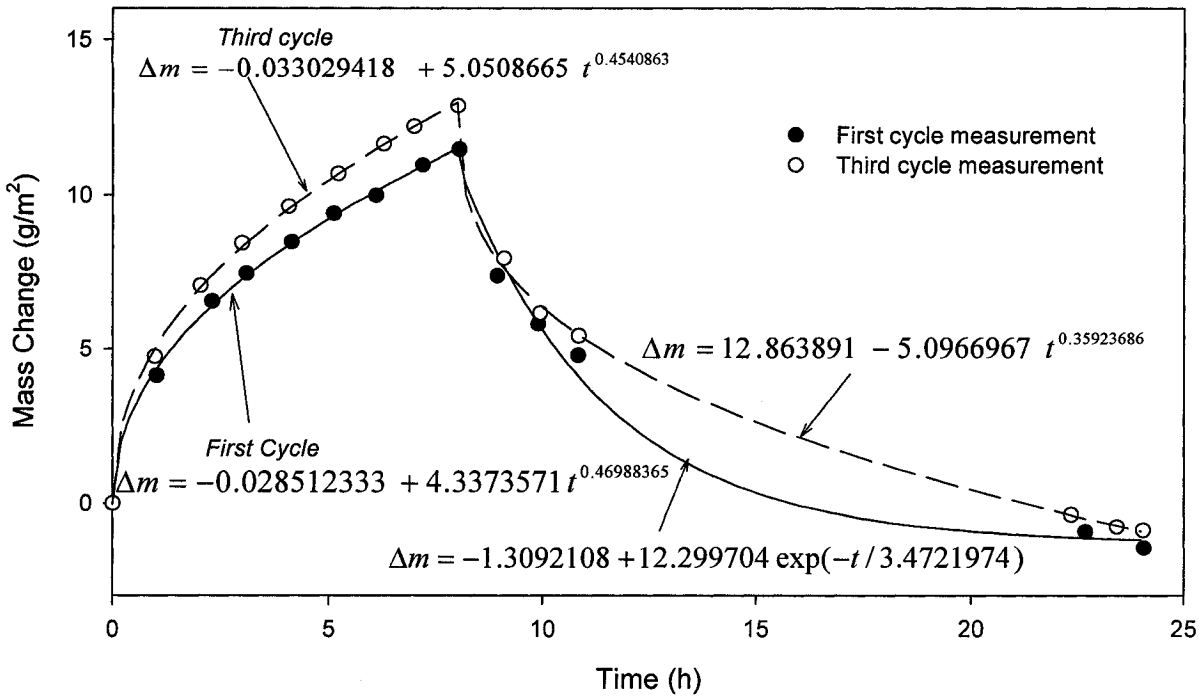
Third cycle
$\Delta m = -0.033029418 + 5.0508665\ t^{0.4540863}$
First cycle measurement
Third cycle measurement
$\Delta m = 12.863891 - 5.0966967\ t^{0.35923686}$
First Cycle
$\Delta m = -0.028512333 + 4.3373571\ t^{0.46988365}$
$\Delta m = -1.3092108 + 12.299704 \exp(-t/3.4721974)$
Mass Change (g/m^2)
Time (h)
0
5
10
15
20
25

(b)

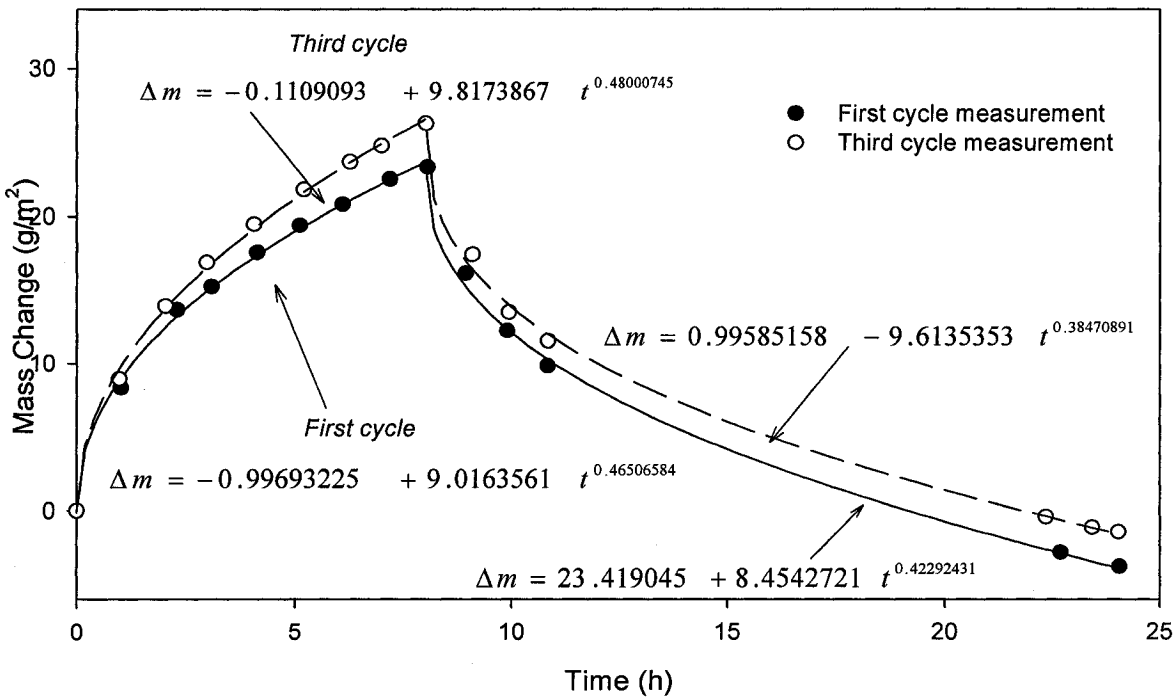
Third cycle
$\Delta m = -0.1109093 + 9.8173867\ t^{0.48000745}$
First cycle measurement
Third cycle measurement
$\Delta m = 0.99585158 - 9.6135353\ t^{0.38470891}$
First cycle
$\Delta m = -0.99693225 + 9.0163561\ t^{0.46506584}$
$\Delta m = 23.419045 + 8.4542721\ t^{0.42292431}$
Mass Change (g/m^2)
Time (h)
0
10
20
30
0
5
10
15
20
25

(c)

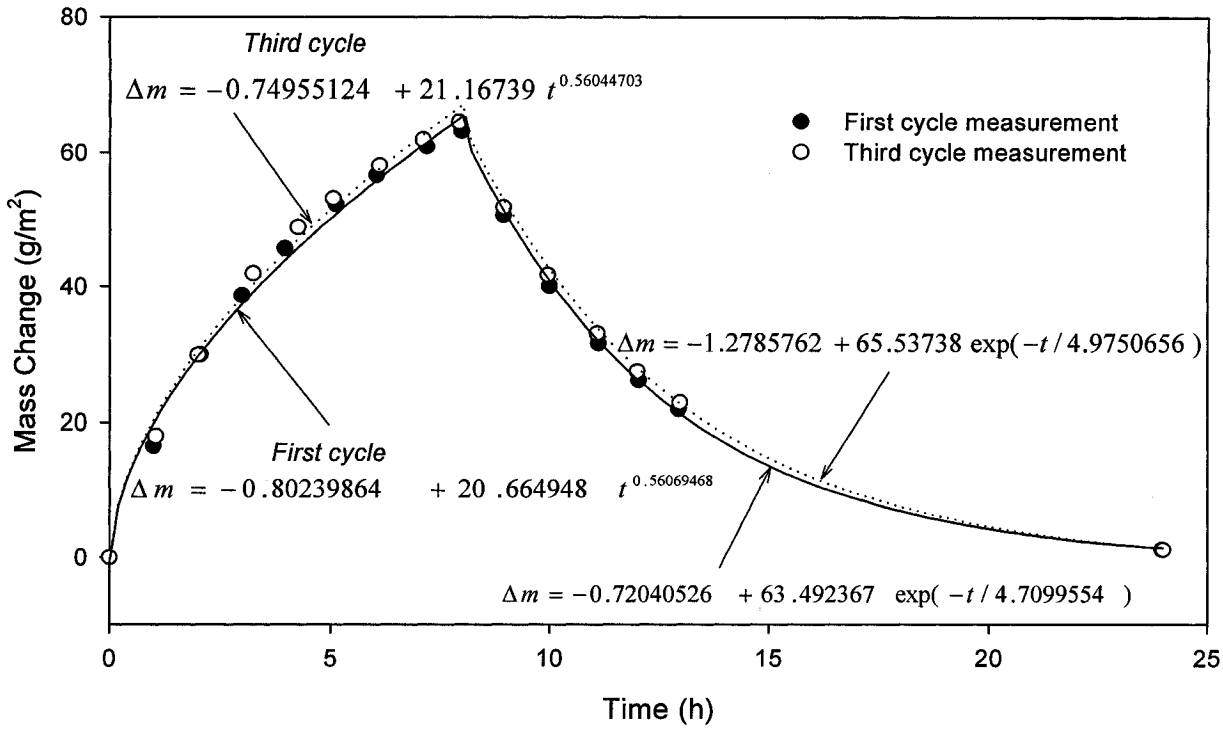

(d)

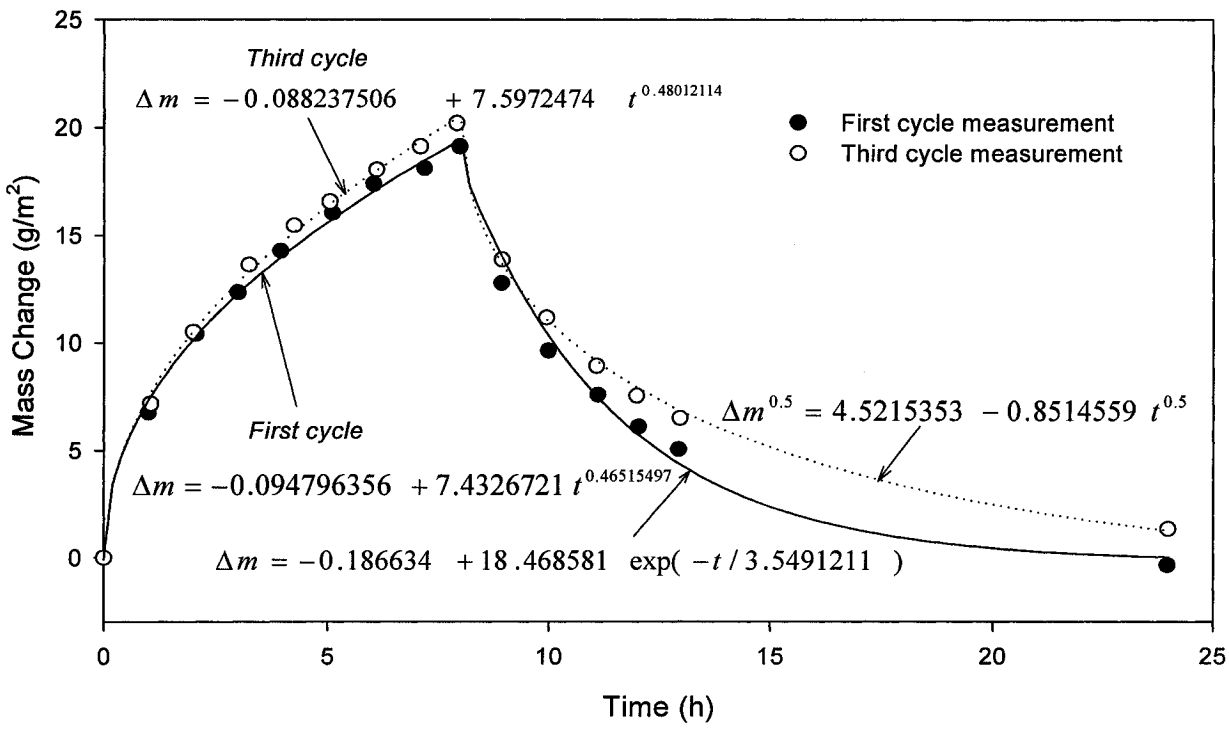

(e)

Figure 4.10 The measured mass change and fitting curves for first and third moisture uptake/release cycles of the tested building products. (a) Gypsum board, (b) Plywood, (c) OSB, (d) Fiberboard, (e) Stucco.

From Figure 4.10, it can be seen that for these building products the mass change during the test varies. However, their curves for sorption and desorption follow similar patterns. A small difference in peak moisture gains can be found at the first and third cycles. For the plywood and OSB products, this difference is more significant than others. The gypsum board and fiberboard products show the most identical curve patterns for two cycles. The gypsum product has a distinctive sorption and desorption curve, which is shown in Figure 4.10(a). In the first four hours, its moisture content changed very fast, after that the curvature tended to be flatter. This reflects that gypsum board has a faster moisture response, and it also can be verified by the first derivative of the fitted curve. The moisture uptake and release process of gypsum in the MBC test can be expressed by Equation 4.4 and 4.5 respectively.

$$\Delta m = a + be^{-t} \tag{4.4}$$

$$\Delta m = a + b\exp(-t/c) \tag{4.5}$$

where a, b and c are fitted coefficients. For the moisture uptake process a linear relationship can be found between mass change Δm and e^{-t}. An exponential fitted equation is used to describe moisture release of gypsum product.

Figure 4.10 (b, c, d) plot the mass change for three sheathing materials, plywood, OSB and Fiberboard. Power and exponential fitted equations are used to depict the sorption and desorption process, which are Equations 4.6 and 4.5.

$$\Delta m = a + bx^{c} \tag{4.6}$$

For plywood and OSB products, Equation 4.6 can also be adopted to describe moisture release in some cases. Obviously, the moisture release process is more diverse than uptake. A proper mathematical description about release could be Equation 4.5 because it can fit for most of building products tested. Compared with moisture release, the uptake process is more consistent. Equation 4.6 can fit the measurement data of tested building products except gypsum board.

Through the curve fitting of measurement data, the relationship of mass change and time elapsed can be represented by mathematical equation. The power and exponential equations can be used to describe the moisture uptake and release for most building products. Gypsum board is a fast moisture response material, therefore, the moisture uptake and release curves are different from others.

Chapter 5
Simulation of Dynamic Moisture Uptake and Release Process for Building Materials

In this chapter, the simulation of the dynamic moisture transport for building materials subjected to the boundary relative humidity changes are conducted. This is representative of the moisture transport processes that occurred in the experiments presented in Chapter 4. The computer model, hygIRC 1-D, was used for this purpose. This model was developed and benchmarked at IRC-NRC, and recently has been extensively used at IRC as the primary analytical tool to conduct parametric studies in assessing the hygrothermal performance of various wall assemblies exposed to different climatic conditions in North America. The simulation were carried out to predict the moisture buffering capacity of building products and to investigate the influences of parameter variations. The results are also compared with experimental data.

5.1 Hygrothermal Mathematical Model

Use of simulation models to predict and simulate the hygrothermal performance of building envelope system has been advanced only recently. With the new simulation models and state-of-the-art test capability, the understanding of new building systems and materials can be faster once the models have been validated against laboratory and field tests. Hygrothermal models have the ability to respond to a variety of boundary conditions and a faster analysis procedure which results from the recent advances in computer technology. Depending upon the complexity of the problem under

consideration, these models can be very simple, one-dimensional, steady state or the more difficult two and three dimensional with the transient methods (Hens 1996).

hgyIRC is an advanced hygrothermal computer model and is used to simulate the dynamic moisture transport in building products. It was developed at IRC-NRC, which has been evolving for past fifteen years. hygIRC 1-D, and is used in this thesis research, is the one dimensional version of hygIRC, and it uses the recently benchmarked hygIRC solver, a climate database containing 30 to 40 years of hourly weather data for 19 Canadian and 6 US cities, a material database containing the hygrothermal properties of more than 100 common construction materials as measured at IRC-NRC (Kumaran 1996, Kumaran et al 2002a and 2002b), and models to derive interior temperature and relative humidity conditions. The model is continuously updated, benchmarked and validated. The earlier version of hygIRC, LATENITE, was benchmarked during the International Energy Agency-Annex 24 by a round robin model comparison (Hens 1996). The hygIRC compared well with the experimental results from small scale lab tests (Kumaran and Wang 1999). More recently, hygIRC was validated in a number of controlled laboratory tests performed under the MEWS (Moisture Management in Exterior Wall System) project (Maref et al 2002a, 2002b). It was also benchmarked during the European HAMSTAD Project (Cornick 2006).

Like many of the hygrothermal simulation models, hygIRC 1D is based on three physical laws, the Fick's law of heat conduction, the Fourier's law of diffusion and the Darcy's laws of fluid flow. Moisture contents and vapor pressure are the moisture transport potentials used in the model. The driving force to calculate energy transport is temperature. The transient moisture content in certain location of the building system can

be obtained by solving vapor diffusion and capillary liquid moisture mass balance. The governing equations in the model are given below.

Moisture balance

$$\rho_d \frac{\partial(u)}{\partial t} = -\nabla\{g_l + g_v\} \tag{5.1}$$

$$g_v = -\underbrace{\delta_p(u,T)\nabla P_v}_{\text{Vapor diffusion}} + \underbrace{\rho_v V_a}_{\text{Vapor airflow}} \tag{5.2}$$

$$g_l = -\underbrace{\rho_d D_w(u,T)\nabla u}_{\text{Liquid diffusion}} + \underbrace{k_w(u)\rho_w g}_{\text{Liquid gravity flow}} \tag{5.3}$$

$$k_w = \rho_d \frac{D_w(u,T)}{\frac{\partial P_c}{\partial u}} \tag{5.4}$$

Energy balance

$$\frac{\partial\left(\rho_T(u,T)C_p(u,T)T\right)}{\partial t} = \underbrace{-\nabla\left(\rho_a(T)C_{P_a}(T)\vec{V}_a T\right)}_{\text{Airflow convective heat}} + \underbrace{\nabla\left(k(u,T)\nabla T\right)}_{\text{Heat conduction}} + \underbrace{L_v\left(\nabla\left(\rho_d\delta_p(u,T)\nabla P_v\right)\right)}_{\text{Evaporation/condensation heat}} - \underbrace{L_{ice}\left(\rho_d u\frac{\partial f_1}{\partial t}\right)}_{\text{Freeze/thaw heat}} \tag{5.5}$$

u Moisture content (kg/kg)
g_l Liquid moisture mass flow rate (kg/s/m^2)
g_v Vapor moisture mass flow rate (kg/s/m^2)
k_w Liquid moisture permeability (kg/m·s·Pa)
P_c Capillary suction pressure (Pa)
P_v Vapor moisture pressure (Pa)
T Temperature (K)
t Time (s)
$\vec{V}_a$ Air velocity vector (m/s)
ρ_d Density of the dry porous material (kg /m^3)
ρ_v Vapor moisture partial density (kg/m^3)
ρ_w Liquid moisture partial density (kg/m^3)
D_w Liquid moisture diffusivity (m^2/s)
δ_p Vapor water permeability (kg/m·s·Pa)
$\vec{g}$ Gravitational vector (m/s^2)
C_p Effective specific heat capacity (J/kg · K)
C_{Pa} Dry-air specific heat capacity (J/kg·K)

f_l Liquid fraction having a value from 0 to 1

k Effective thermal conductivity (W/m · K)

L_v Enthalpy of evaporation/condensation (J/kg)

L_{ice} Enthalpy of freeze/thaw (J/kg)

ρ_T Actual total density of the material including moisture contribution (kg/m^3)

5.2 Results from a Simulation of the MBC Test

The hygIRC 1-D model has been used for calculating mass change of the building products exposed under the periodically changing boundary conditions. The material properties measured in this work have been imported in the model as material property input, which includes air permeability, thermal conductivity, density, liquid diffusivity, heat capacity, sorption isotherms, suction pressure and vapor permeability data. The time step used in the calculations was 6 minutes. Fifty nodes were used along the thickness of the building products. The density of nodes is higher, by a factor of 1.5, in the region near the non-waxed surface exposed to the selected boundary condition than the region near the waxed surface. The initial moisture content in the simulation is set as the measured value. The moisture transfer coefficient can be calculated based on air flow velocity near the surface of the test specimen by the well known approximation, Lewis equation. The measured air velocity is 1.3 m/s, and then through the calculation the moisture transfer coefficient near the specimen surface is determined as $7x10^{-8}$ s/m, which has been used in the simulations. Results from simulation versus MBC test are shown in Figure 5.1.

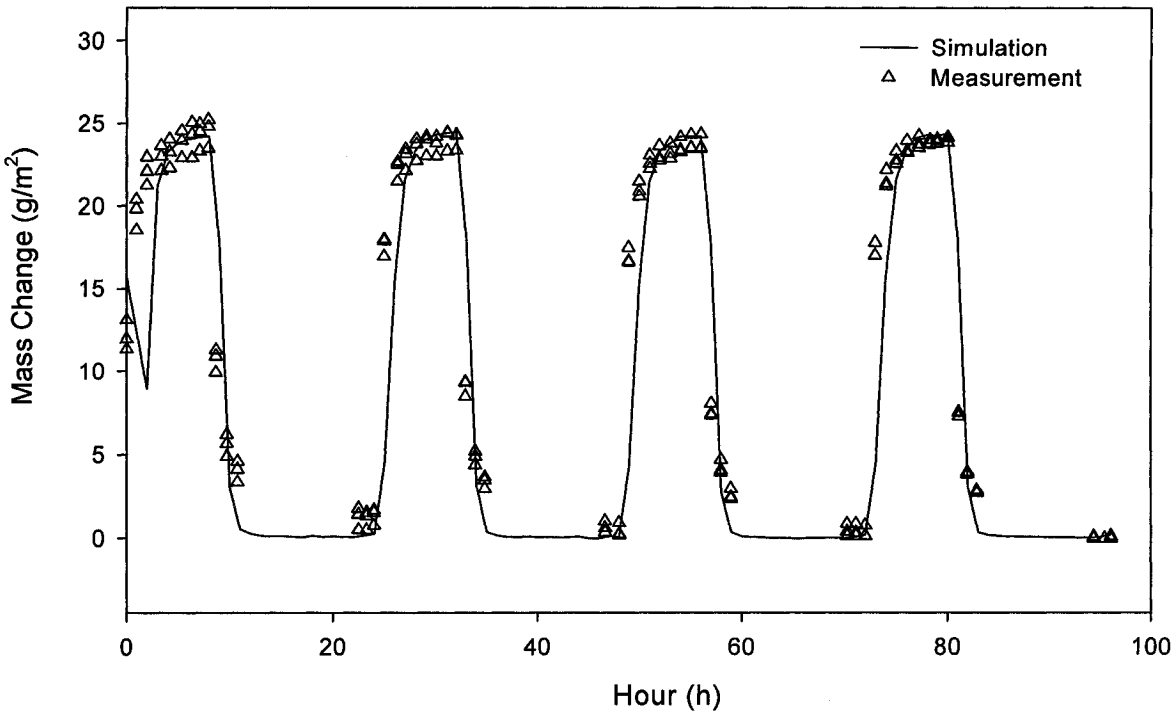

(a) Gypsum

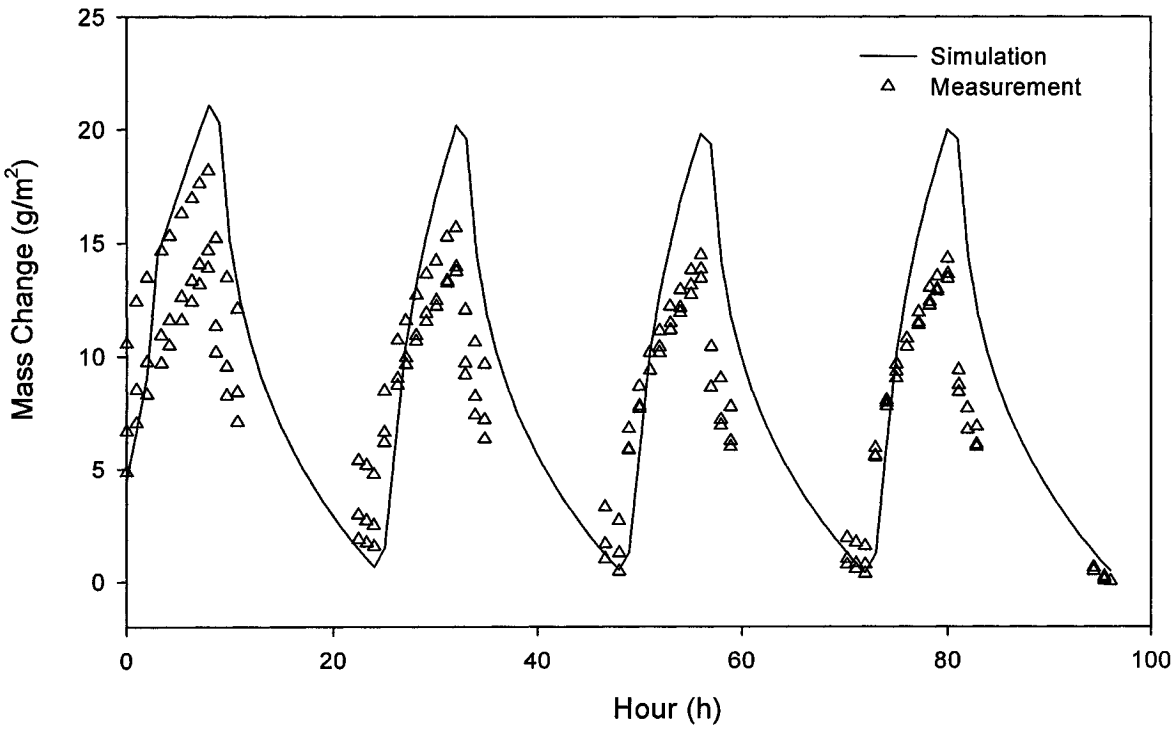

(b) Plywood

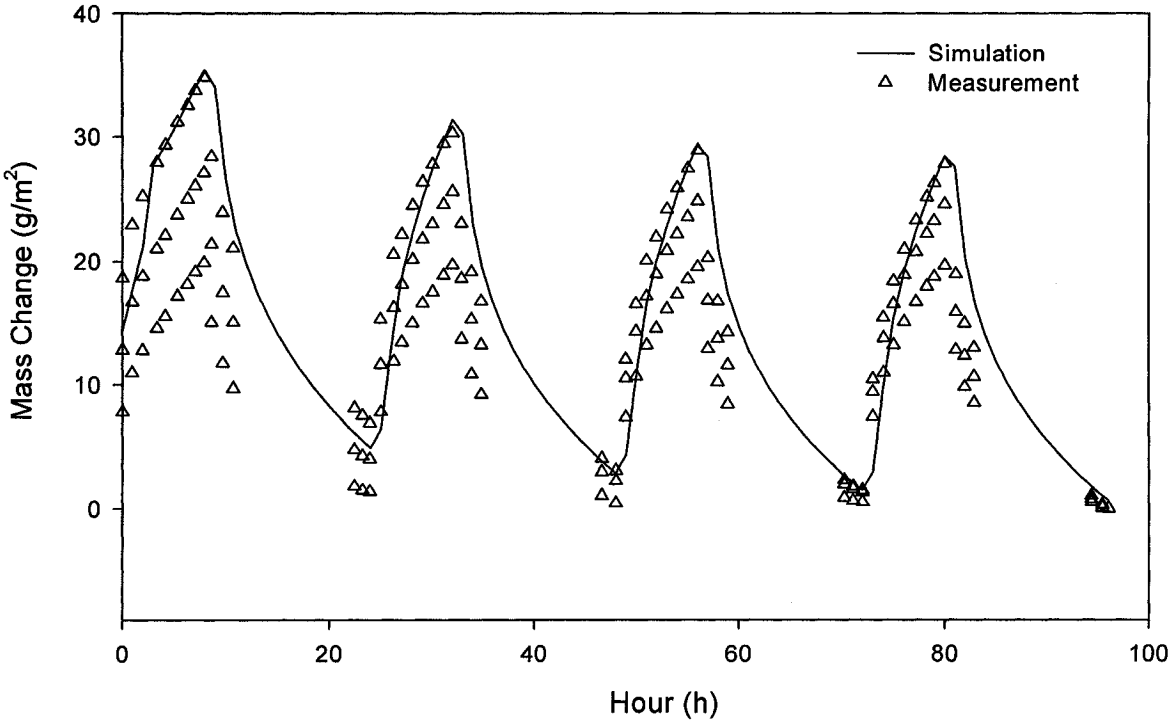

(c) OSB

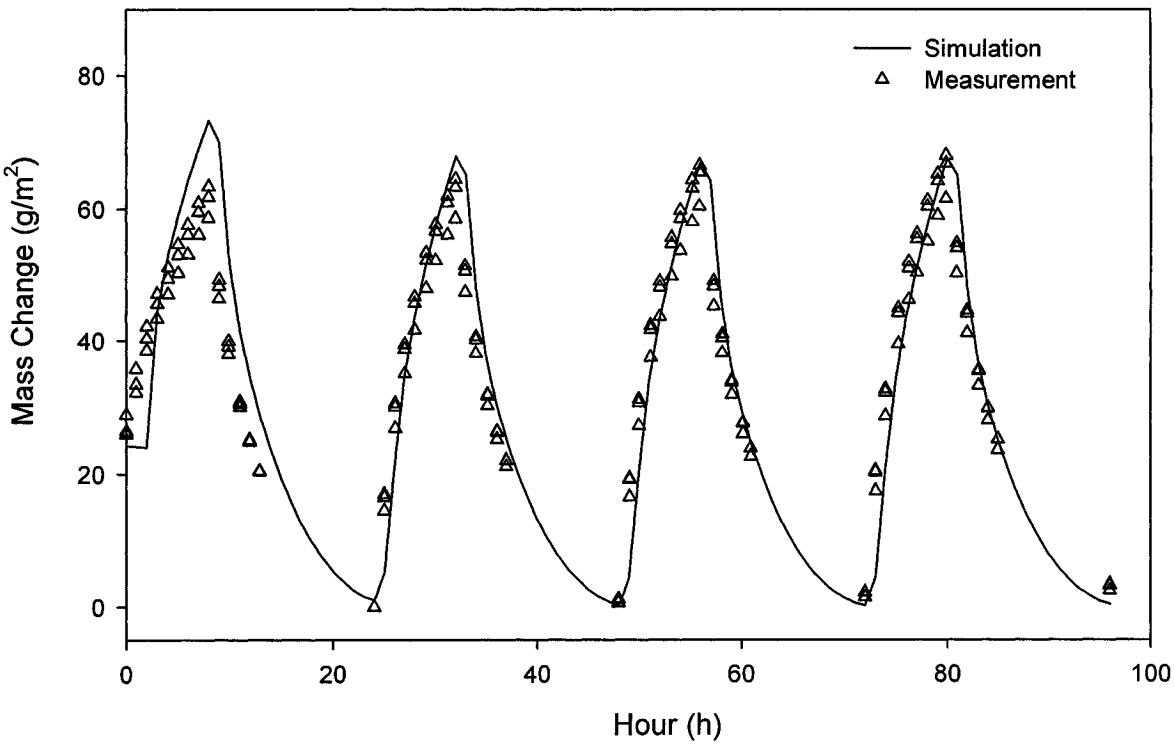

(d) Fiberboard

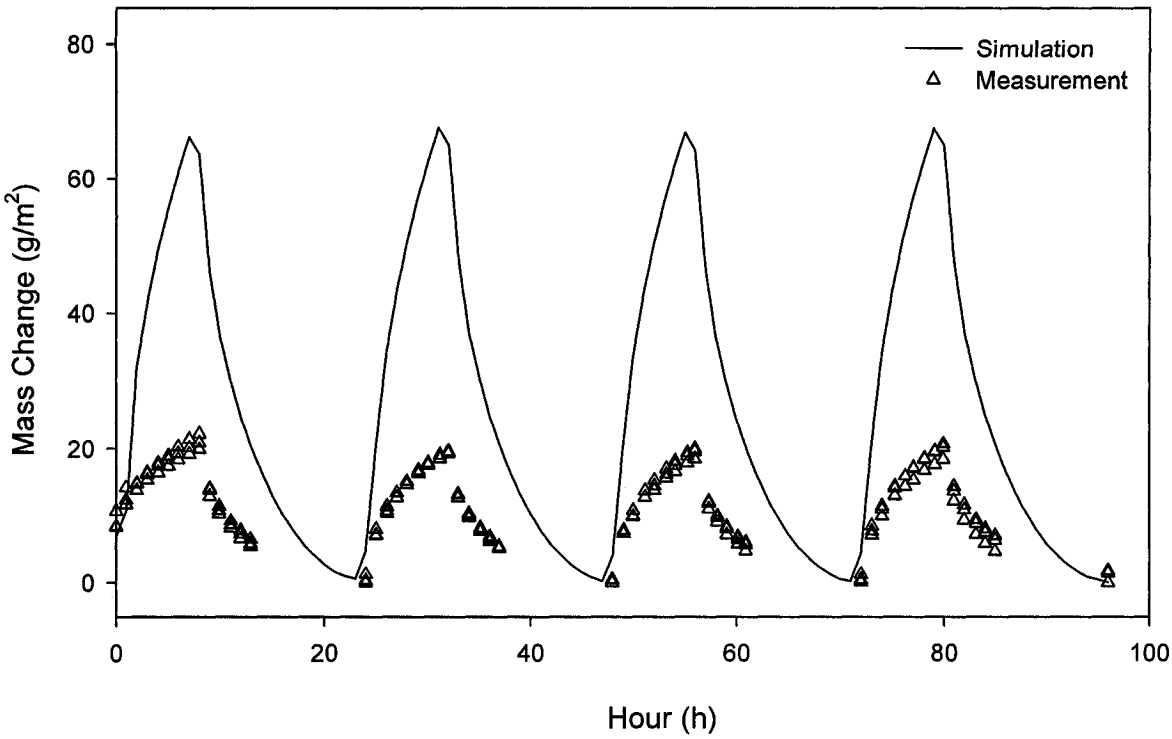

(e) Stucco

Figure 5.1 Measured and simulated mass changes of building materials under MBC test.

In the above figures, the measured and simulated weight changes of the building products during the MBC test are compared. It is shown that for gypsum board, OSB and fiberboard the overall agreements between the experimental and numerical data are very small and the discrepancies are within 8 %, 18 % and 6 % respectively. The simulated weight changes of plywood and stucco are higher than the measured value, and they can be as high as 60 % and 200 % of the experimental data. The cause of this discrepancy could be the variation in material properties of the stucco and the plywood. The building products, such as plywood and stucco, display the incoherent hygrothermal properties especially for their sorption isotherms and vapor permeability, etc. In addition, the finished stucco depends greatly on workmanship and can have large variations in its

physical and hygrothermal properties. Specimens used for MBC tests were not the same specimens as used for material property tests, and some of them were even not cut from the same sheet. As a result, the input material properties in the model can not represent the actual material properties for some of building materials such as the stucco and plywood. Another explanation of the discrepancy could be the uncontrolled air flow in the environmental chamber, which resulted in the various moisture transfer coefficient for each specimen.

The hygrothermal properties can affect the moisture buffering performance of the building products. To understand this effect, several sets of parametric analysis were carried out and the results from those are discussed below.

5.3 Parametric Analysis and Discussion

The results from the parametric analysis of the MBC tests in response to changes in the sorption isotherms, liquid diffusivity and vapor permeability of different building materials and moisture transfer coefficient are presented in this section. The parametric studies are concentrated on the fiberboard product because the simulation results based on this product have the best agreement with the experimental measurement. The codes used for variations of hygrothermal properties are listed in Table 5.1.

Table 5.1 Codes used for parametric analysis

Code	Variation from the hygrothermal properties
sorp 50	The sorption curve was reduced by 50% of the original
sorp 150	The sorption curve was increased by 50% of the original
vap 50	The vapor permeability was reduced by 50% of the original
vap 150	The vapor permeability was increased by 50% of the original
dfl 10	The liquid diffusivity was reduced to 10% of the original
dfl 50	The liquid diffusivity was reduced by 50% of the original
dfl 150	The liquid diffusivity was increased by 50% of the original

5.3.1 Effect of Variations in Sorption Isotherm

In the numerical simulation, the curve fit of the experimental sorption data obtained under a constant temperature is used as sorption isotherm. Figure 5.2 shows the effect of 50% changes downward and upward in the sorption isotherm on the simulated mass change of fiberboard exposed to step-wise change in relative humidity.

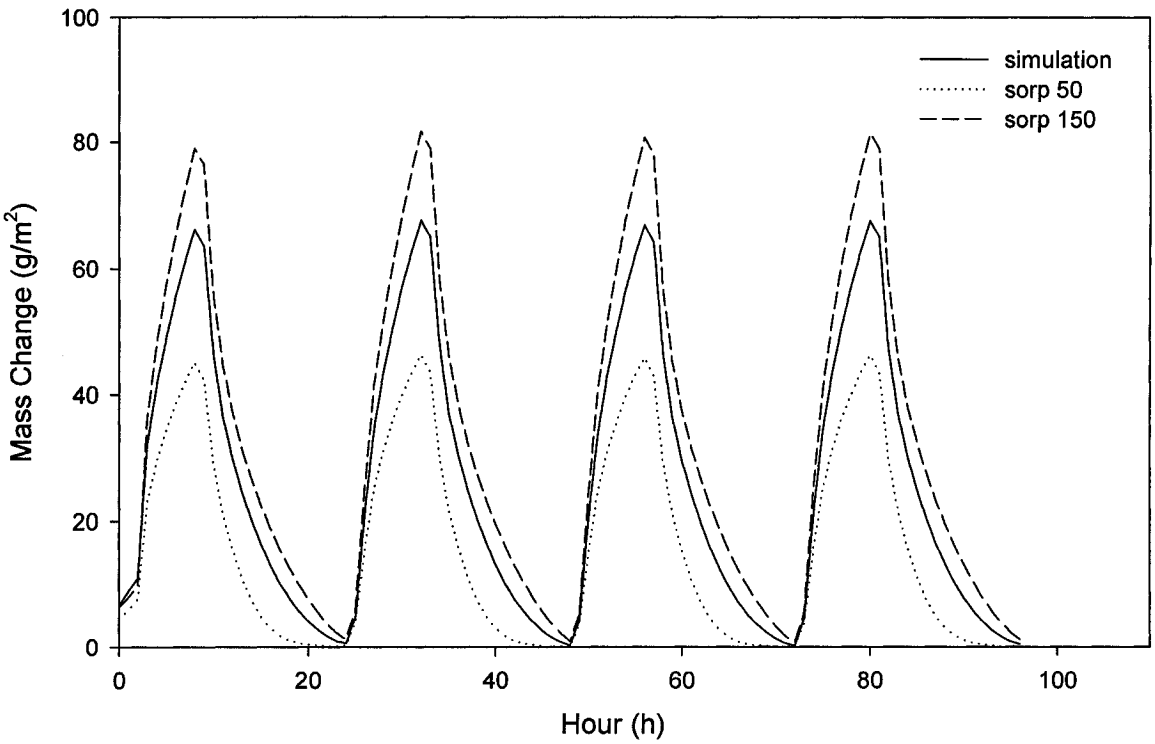

Figure 5.2 Parametric analysis showing the effect of changing the moisture content calculated by the measured sorption isotherm by ±50% for the fiberboard on its sorption and desorption processes

Figure 5.2 indicates that raising the sorption curve by 50 % increases the calculated MBV of fiberboard by 21 %, whereas the 50 % lowering in the sorption curve decreases the calculated MBV by 32 %. The above two percentages are calculated at the end of sorption periods and the start of desorption periods. The sorption isotherm represents the capacity of moisture accumulation; therefore these results make physical sense.

5.3.2 Effect of Variations in Vapor Permeability

The vapor permeability of fiberboard used in the numerical simulation is a curve fit of experimental data. The parametric analysis of the effect of vapor permeability on the simulated mass change of fiberboard exposed to step-wise change in relative humidity is shown in Figure 5.3. Increasing the vapor permeability by 50 % results in a maximum of 17 % increase in the calculated MBV as shown in Figure 5.3. However, reducing 50% only causes 2% difference with the original simulation result.

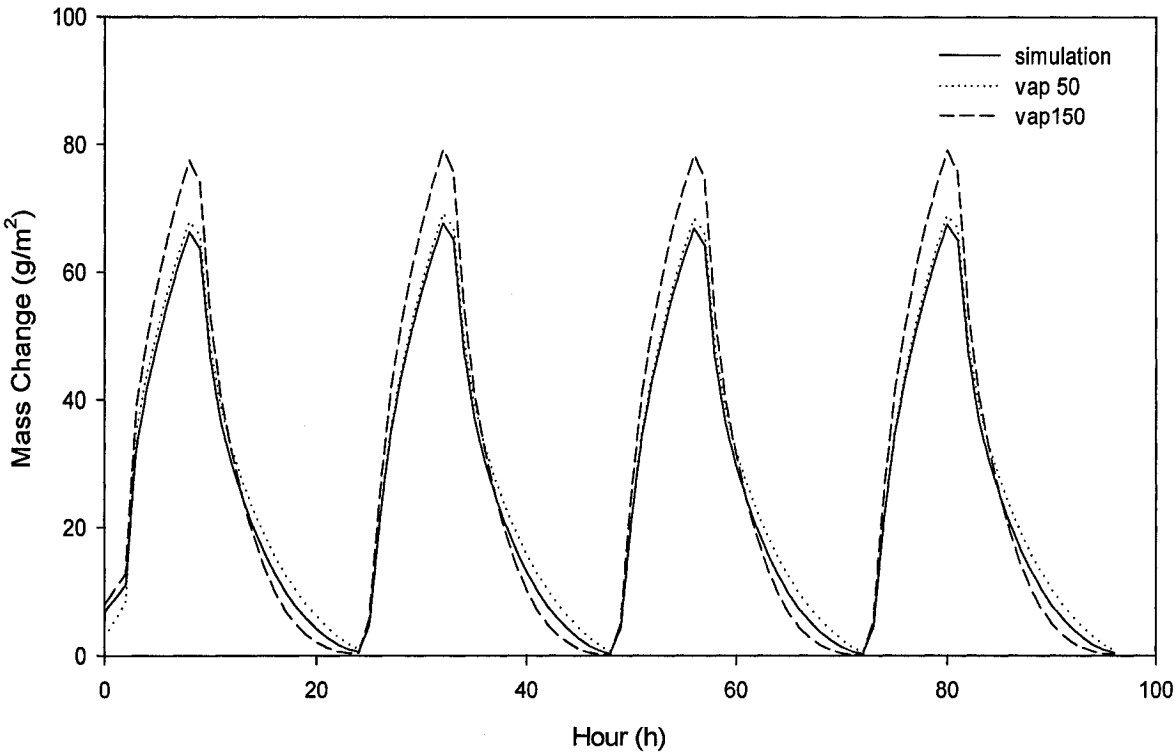

Figure 5.3 Parametric analysis showing the effect of ±50% changes in vapor permeability for fiberboard on its sorption and desorption processes

5.3.3 Effect of Variations in Liquid Diffusivity

The measured liquid diffusivity data of the fiberboard product through the Gamma-ray apparatus is used in the numerical simulation. The parametric analysis of the effect of liquid diffusivity on the simulated mass change of fiberboard exposed to step-wise change in relative humidity is shown in Figure 5.4. It can be noticed from Figure 5.4 that increasing or decreasing the liquid diffusivity by 50 % does not change the calculation result. Moreover, numerical simulation by using 10 % of the liquid diffusivity as input has no effect on the results. These results show that the liquid diffusivity of building products has a very small effect in the simulation of transient moisture sorption and

desorption. The moisture transport in building materials under MBC test had not reached liquid state.

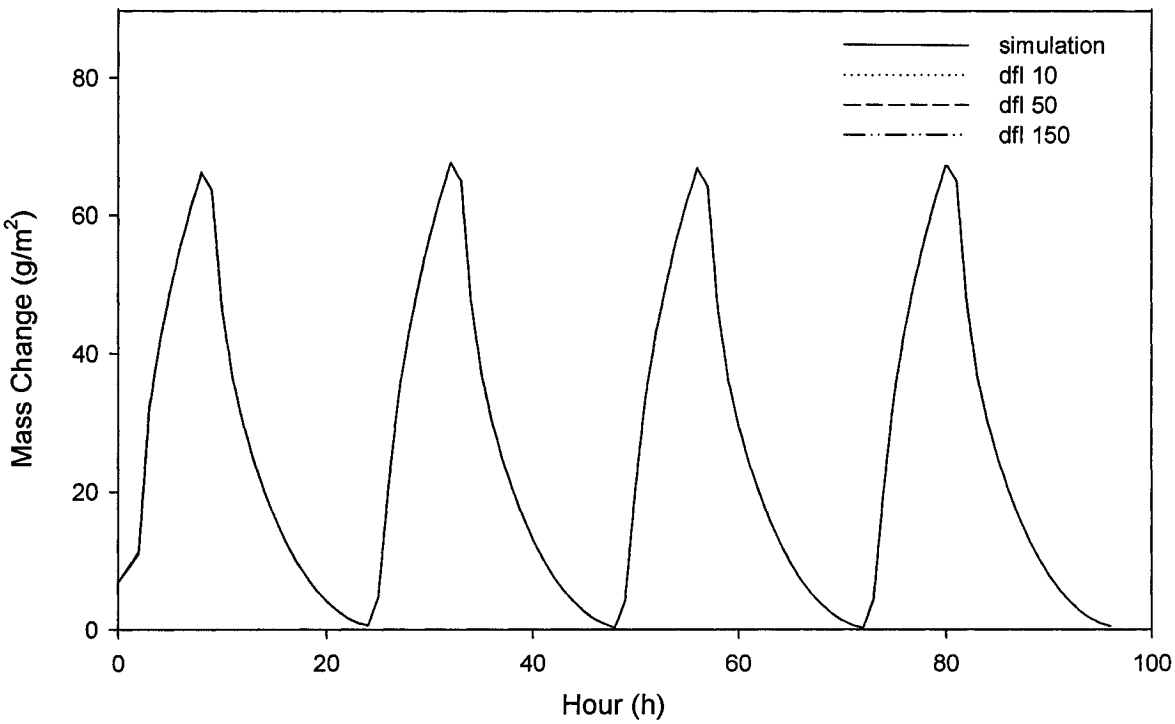

Figure 5.4 Parametric analysis showing the effect of changing liquid diffusivity by 50 %, -50 % and -10 % for fiberboard on its sorption and desorption processes

5.3.4 Effect of Variations in Moisture Transfer Coefficient

Based on the measured air velocity, the moisture transfer coefficient near the specimen surface is determined as $7x10^{-8}$ s/m, which has been used in the simulations. To investigate the effect of the moisture transfer coefficient, additional numerical simulations were done using moisture transfer coefficient of $7x10^{-6}$, $7x10^{-7}$ and $7x10^{-9}$ s/m.

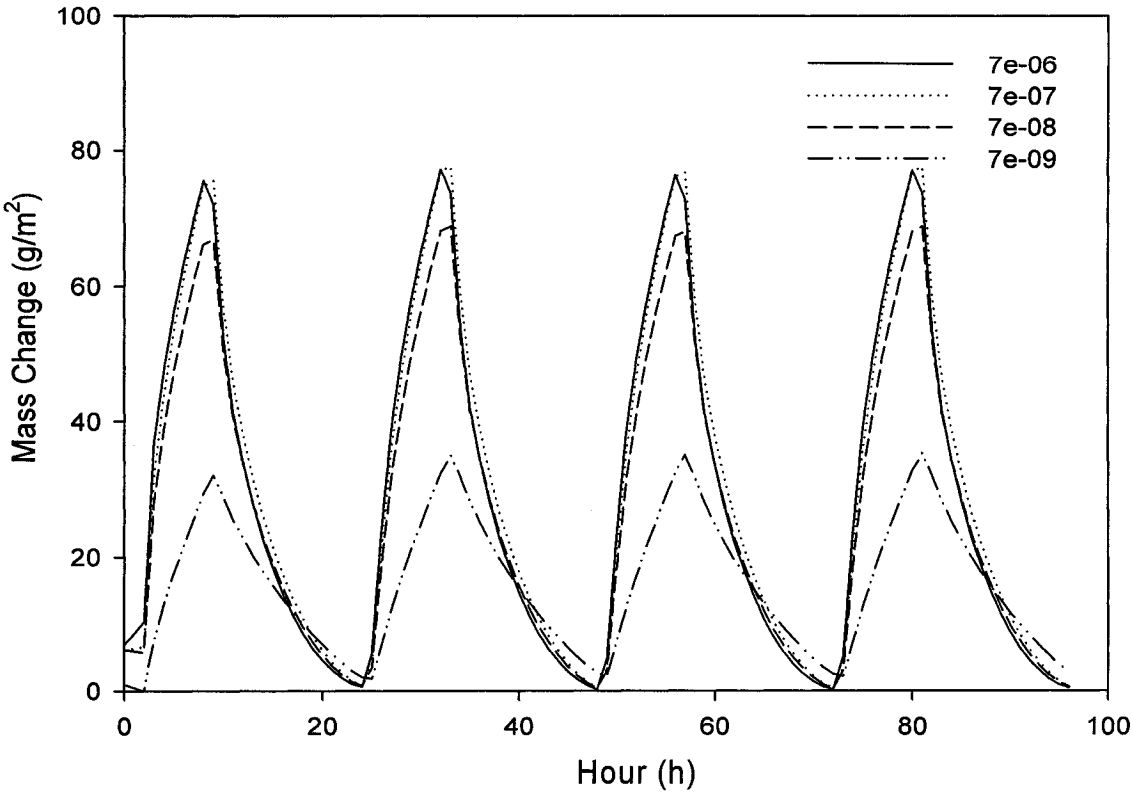

Figure 5.5 Parametric analysis showing the effect of different moisture transfer coefficients for fiberboard on its sorption and desorption processes

As illustrated in Figure 5.5, the simulation results increase the MBV of the fiberboard by 13% when coefficients of $7x10^{-6}$ and $7x10^{-7}$ s/m are used. When the coefficient of $7x10^{-9}$ s/m is adopted in the simulation, the calculated MBV is reduced by more than 50% of the original value. These results show that the moisture transfer coefficient of building products has a significant effect in the simulation of transient moisture sorption and desorption.

5.4 Summary

In this chapter, simulation of transient moisture buffering and transport in building products are carried out and are compared to measurements of mass changes within the

building products exposed to relative humidity cycles. For gypsum board, OSB and fiberboard the overall agreements between the experimental and numerical data are very small and the discrepancies are within 8 %, 18 % and 6 % respectively. The simulated weight changes of plywood and stucco are higher than the measured value, and they can be as high as 60 % and 200 % of the experimental data. These differences could be the resultant of the variation in hygrothermal properties of specimens used for MBC test and material property tests, or inadequate information on the surface transfer coefficients. The comparisons, especially the ones with large discrepancies, call for more data and for better procedure in selecting material property data in simulations.

To determine the sensitivity of the simulated moisture transfer to changes in the material properties used in the model, parametric analysis is carried out. The moisture transfer coefficient has the greatest effect in the numerical simulation of moisture transfer within the fiberboard; the sorption isotherm also gives significant influence. Whereas, the liquid diffusivity has almost no effect.

Chapter 6
Conclusions and Future Work

This thesis presents the results of experimental and numerical research which contribute to a better understanding of the hygrothermal properties of building materials. A state-of-the-art review indicates that the application of existing HAM models is restricted due to the lack of the reliable material property data; meanwhile, development of the reliable material characterization methods is necessary. Series of experiments were conducted on 10 commonly used building materials to provide input for simulation models. The measured building products include several wood-based products, such as OSB, plywood, fiberboard and spruce wood stud; glass fiber insulation; stucco for exterior cladding; interior gypsum board; two other insulation products; one vapor membrane and a construction paper. The measured material properties are essential in engineering analyses and designs using these materials. The properties can also be used directly as property input for the simulation models.

Furthermore, the moisture buffering capacity of gypsum board, plywood, OSB, fiberboard, and cement stucco are measured. These measurements provide data that are used to validate the simulation model HygIRC 1D for one dimensional transient moisture transfer in building materials. In addition, a parametric analysis is carried out to investigate the sensitivity of MBC predictions regarding material properties which include the sorption isotherm, vapor permeability, diffusivity and moisture transfer coefficient.

6.1 Research Summary and Conclusions

The experimental and numerical study provides the knowledge of hygrothermal properties of building materials, which can lead to better understanding and predicting of moisture transport in the building envelope. The following conclusions may be derived in this thesis:

1. The moisture transport theory was explained. The existing test methods for hygrothermal properties of building materials were reviewed and compared. In addition, the history and current situation of HAM study around the world were reported.

2. The material properties of 10 building products which are widely used in Canada were determined using well-established procedures. The determined properties include thermal conductivity, sorption/desorption isotherm, retention curve, water vapor permeability, liquid diffusivity, water absorption coefficient, and air permeability. These material properties can be used as input for advanced HAM models.

3. An experiment to quantify the moisture buffering capacity (MBC) of building materials was developed. The MBC of five building products was determined from moisture accumulation data using analytical balance. Through the measurements, it is found that fiberboard has the greatest moisture buffering value (MBV) while plywood has the least MBV. Through the curve fitting of measurement data, the relationship of mass change and time elapsed have been represented by mathematical equations. The power and exponential equations were used to describe the moisture uptake and release for most building products.

4. The HAM model, hygIRC 1D, was used to simulate the MBC experiment. The measured material properties from current work were used as the input for the simulation model. For gypsum board, OSB and fiberboard the overall agreements between the experimental and numerical data are very small and the discrepancies are within 8%, 18% and 6% respectively. The simulated weight changes of plywood and stucco are higher than the measured value, and they can be as high as 60% and 200% of the experimental data. These differences could be the resultant of the variation in hygrothermal properties of specimens used for MBC test and material property tests, or inadequate information on the surface transfer coefficients. The comparisons, especially the ones with large discrepancies, call for more data and for better procedure in selecting material property data in simulations.

5. A parametric analysis was carried out to determine the sensitivity of the simulated moisture transfer within fiberboard product to changes in the material properties used in the model. This analysis shows that the moisture transfer coefficient has the greatest effect on the numerical simulation of moisture transfer within fiberboard; the sorption isotherm also gives significant influence. Whereas, the liquid diffusivity has almost no effect.

6.2 Recommendations for Future Work

The experimental and numerical investigation into hygrothermal properties of building materials in this thesis has resulted in the identification of several areas for future work, which are listed below:

1. The development and improvement of standard testing method for building materials are recommended. A systematical evaluation of factors affecting the precision of the current test methods should be performed.

2. Further experimental and numerical studies are required to understand the moisture buffering capacity for other building materials. Comprehensive MBV property databases of different building materials obtained under more test conditions can help in selecting the right materials that are best suitable to both adept to different indoor humidity conditions and lower the total building energy consumption. Moreover, the MBV of different building materials should be added in simulation models.

3. Research, including this thesis work, has shown that the moisture transfer coefficient has significant effect on the simulation of moisture buffering performance. Further numerical and experimental investigations of convection vapor transfer are required to better predict MBC of building materials.

Bibliography

Abell, A.B., Willis, K.L., and Lange, D.A., 1999, Mercury porosimetry and image analysis of cement-based materials, Journal of Colloid and Interface Science 221(1): 39-44.

ASTM C177-04, 2004, Standard test method for steady-state heat flux measurements, American Society for Testing and Materials, Philadelphia.

ASTM C518-04, 2004, Standard test method for steady-state thermal transmission properties by means of the heat flow meter apparatus, American Society for Testing and Materials, Philadelphia.

ASTM C 522-03, 2003, Standard test method for airflow resistance of acoustical materials, American Society for Testing and Materials, Philadelphia.

ASTM C1498-01, 2001, Standard test method for hygroscopic sorption isotherms of building materials, American Society for Testing and Materials, Philadelphia.

ASTM E96-00, 2000, Standard test method for water vapor transmission of materials, American Society for Testing and Materials, Philadelphia.

Burch, D.M., Thomas, W.C., and Fanney A.H., 1992, Water vapor permeability measurements of common building materials, ASHRAE Transactions, 98(2), pp. 486-494.

Bomberg, M. and Kumaran, M.K., 1986, A test method to determine air flow resistance of exterior membranes and sheathings, Journal of Thermal Insulation, Vol. 9, pp. 224-235.

Bomberg, M., Pazera, M., Haghighat, F. and Grunewald, J., 2002, Modified cup for testing of water vapor transmission through thick, permeable materials, 6th Symposium on Building Physics in the Nordic Countries, Trondheim.

Bomberg, M., Pazera, M., Zhang, J., 2006, On validation of hygric characteristics for heat air moisture model, Proceedings of the 3rd International Building Physics Conference, pp. 55-63, Concordia University, Montreal Canada, 27-31 August 2006.

Brocken, H. J. O., 1998, Moisture transport in brick masonry: The grey area between bricks, PhD thesis, Eindhoven University of Technology, Eindhoven, The Netherlands.

Carmeliet J., Van Besien T., Roels S., 2003, New indirect estimation technique for the determination of the moisture diffusivity from transient moisture content profiles measured by means of X-ray radiography, 2nd International conference on Research in Building Physics, Sept. 14-18, Leuven, Belgium.

Carmeliet, J., Adan, O., Brocken, H., Cerny, R., Hall, C., Hens, H., Kumaran, K., Pavlik, Z., Pel, L., Plagge, R. and Roels, S., 2004, Determination of the liquid water diffusivity from transient moisture transfer experiments, Journal of Thermal Envelope and Building Science, 27(4), pp. 277–305.

CEN TC89, 1994, Building materials-Determination of water absorption coefficient, WG 10 N95.

Cornick, S., 2006, Results of the HAMSTAD benchmarking exercises using hygIRC 1-D version 1.1, National Research Council of Canada Research Report IRC-RR-222.

Crank, J., 1989, The mathematics of diffusion, Oxford University Press, Oxford, United Kingdom.

Descamps, F., 1997, Continuum and discrete modelling of isothermal water and air transfer in porous materials, PhD-Dissertation, Catholic University of Leuven.

Fagerlund, G., 1973a, Determination of pore size distribution by suction porosimetry, Material and Structure, Paris, 6(33), pp. 191–201.

Fagerlund, G., 1973b, Determination of pore-size distribution from freezing-point depression, Material and Structure, Paris, 6(33), pp. 215–225.

Fang, L., Clausen, G., and Fanger, P.O., 2000, Temperature and humidity: important factors for perception of air quality and for ventilation requirements. ASHRAE Transactions 2, 106.

Ferguson, H. and Gardner, W.H., 1962, Water content measurement in soil columns by Gamma ray absorption, Soil Science American Proceedings, Vol. 26, pp 11-14.

Fick, A., 1855, Über diffusion, Annalen der Physik und Chemie 94, pp. 59–86.

Freitas, V. P. De, Krus, M., Künzel, H. and Quenard, D., 1995, Determination of the water diffusivity of porous materials by gamma-ray attenuation and NMR, Proceeding of the International symposium on Moisture Problems in Building Walls, Porto, 11-13 Sept, pp. 445-460.

Galbraith, G.H., Mclean, R.C., 1986, Realistic vapor permeability values, Building Research & Practice, 14(2), pp. 98-103

Galbraith, G.H., Guo, J. S., and McLean, R. C., 2000, The effect of temperature on the moisture permeability of building materials, Building Research & Information, Volume 28, Number 4, pp. 245 – 259.

Galbrarth, G.H., Kelly, D.J. and McLean, R.C., 2003, Alternative methods for measuring moisture transfer coefficients of building materials. Proceeding of the 2nd International Conference on building Physics, Leuven, Belgium, pp. 249-254.

Gummerson, R.J., Hall, C., Hoff, W.D., Hawkes, R., Holland, G.N. and Moore, W.S., 1979, Unsaturated water flow within porous materials observed by NMR imaging, Nature, 281, pp. 56–57.

HAMSTAD Reports: Adan, O., Brocken, H., Abl-Zarrabi, B., Becker, R., Carmeliet, J., Cerny, R., Grunewald, J., Hagentoft, C., Hall, C., Hau¨ pl, P., Hens, H., Huinink, H., Kumaran, K., Pavlik, Z., Pel, L., Plagge, R., Roels, S., Sasic-Kalagasidis, A. and Toman, J., 2003, Determination of liquid water transfer properties of porous building material and development of numerical assessment methods, HAMSTAD Final Technical Report, EU Contract G6RD-2000-00260, p. 32.

Hansen, K. K. and Lund, H. B., 1990, Cup method for determination of water vapor transmission properties of building materials-Sources of uncertainty in the methods, Proceedings of the 2nd Symposium, Building Physics in the Nordic Countries, Trondheim, pp. 291-298.

Hansen, M. H., 1997, Retention curves measured using pressure plate and pressure membrane appratus: Description of methods and interlaboratory comparison, Nordtest Tech. Rep. No. 367, SBI Rep. No.295, Danish Building Research Institute, Hørsholm, Denmark.

Hansen, M. H., Houvenagehl, G., Janz, M., Krus, M., and Strømdahl, K., 1999, Interlaboratory comparison of the measurement of retention curves, Journal of Thermal Envelope and Building Science, 22, pp. 334–348.

Hansen, K. K., Rode, C., and Hansen, E., 2001, Experimental investigation of the hygrothermal performance of insulation materials, Proceedings for Performance of Exterior Envelopes of Whole Buildings VIII: Integration of Building Envelopes, December 2-7, Clearwater Beach, Florida

Hens, H., 1996, Heat. Air and moisture transport, final report: volume 1, Task 1: Modeling, IEA Annex 24, Laboratorium Bouwfysica, K.U.-Leuven, Belgium.

IEA-ANNEX XIV, 1991, Condensation and Energy: Catalogue of Material Properties, KU Leuven, Belgium.

Janz, M., 1997, Methods of measuring the moisture diffusivity at high moisture levels, Report TVBM-3076, Division of Building Materials, Lund Institute of Technology, Lund.

Janz, M. and Johannesson, B.F., 2001, Measurement of the moisture storage capacity using sorption balance and pressure extractors, Journal of Thermal Envelope and Building Science 2001 24, pp. 316-334.

Johannesson, B.F and Janz, M., 2002, Test of four different experimental methods to determine sorption isotherms, Journal of Materials in Civil Engineering, Volume 14, Issue 6, pp. 471-477.

Joy, F.A. and Wilson, A.G., 1963, Standardization of the dish method for measuring water vapor transmission, Proceeding of the International Symposium on Humidity and Moisture, Washington, D.C., Vol.4, Chapter 31, pp 259-270.

Karagiozis, A., 1993, Overview of the 2D hygrothermal heat-moisture transport model LATENITE, IRC-NRC, Canada.

Karagiozis, A., Künzel, H. and Holm, A., 2001, WUFI ORNL/IBP hygrothermal model, in solutions to moisture problem in building enclosures, Proceedings of the 8th Conference on Building Science and Technology, pp. 119-138. Toronto, Canada.

Kohonen, R., 1984, A method to analyze the transient hygrothermal behavior of building materials and components, Des-Dissertation VTT, Publication 21, Espoo.

Krus, M., 1995, Moisture transport and storage coefficients of porous mineral building materials, Ph.D. Thesis, University of Stuttgart, Germany.

Krus, M., and Kießl, K., 1998, Determination of the moisture storage characteristics of porous capillary active materials, Material and Structure, Paris, 31, pp. 522–529.

Kumaran, M.K. and Bomberg, M., 1985, A gamma spectrometer for determination of density distribution and moisture distribution in building materials, Proceedings of the International Symposium on Moisture and Humidity, Washington, D.C., pp. 485-490.

Kumaran, M.K., Mitalas, G. P., Kohonen, R. and Ojanen, T., 1989, Moisture transport coefficient of pine from gamma ray absorption measurements, American Society of Mechanical Engineers, Heat Transfer Division, (Publication) HTD, v 123, pp. 179-183.

Kumaran, M.K., Mitalas, G.P., and Bomberg, M.T., 1994, Fundamentals of transport and storage of moisture in building materials and components, ASTM Manual Series: MNL 18, Moisture Control in Buildings, ISBN 0-8031-2051-6, Philadephia.

Kumaran, M.K., 1996, Final Report Task 3: material properties IEA, annex 24 HAMTIE, laboratorium Bouwfysica, K.U.-Leuven, Belgium

Kumaran, M.K., 1998a, Interlaboratory comparison of the ASTM standard test methods for water vapor transmission of materials (E 96-95), ASTM Journal of Testing and Evaluation (USA). Vol. 26, no. 2, pp. 83-88.

Kumaran, M.K., 1998b, An alternative procedure for the analysis of data from the cup method measurements for determination of water vapor transmission properties, Journal of Testing and Materials, Volume 26, No. 6, pp. 575-581.

Kumaran, M.K., 1999, Moisture diffusivity of building materials from water absorption measurements, Journal of Thermal Envelope & Building Science, Vol. 22, No. 4, 349-355.

Kumaran, M.K. and J. Wang 1999. How well should one know the hygrothermal properties of building materials?, Proceeding of CIB W40 meeting, Prague, Czech Republic, August 30, 1999, pp. 47-52.

Kumaran, M.K., Lackey, J. C., Normandin, N., van Reenen, D & Tariku, F., 2002a, A thermal and moisture transport property database for common building and insulating materials, Final report of ASHRAW Research Project, RP1018.

Kumaran, M.K., Lackey, J., Normandin, N., van Reenen, D., Tariku, F., 2002b, Summary report from task 3 of MEWS project at the Institute for Research in Construction - Hygrothermal properties of several building materials, Research Report, Institute for Research in Construction, 73 pages, IRC-RR-110.

Kumaran, M.K., Mukhopadhyaya, P., Normandin, N, 2006, Determination of equilibrium moisture contents of building materials: some practical difficulties, Symposium on Heat, Air and Moisture Transport Properties of Building Materials, ASTM Toronto, Ontario, Canada.

Künzel, H.M., 1995, Simultaneous heat and moisture transport in building components, Ph.D. Thesis, University of Stuttgart, Germany.

Künzel, H.M. and Kiessl, K., 1997, Calculation of heat and moisture transfer in exposed building components, International Journal of Heat and Mass Transfer 40(1): pp. 159-167.

Luikov, A.V., 1966, Heat and mass transfer in capillary-porous bodies, Pergamon Press, London.

Marchand, R.G. and Kumaran, M.K., 1994, Moisture diffusivity of cellulose insulation, Journal of Thermal Insulation and Building Envelope, Vol. 17, pp. 362-377.

Maref, W., Lacasse, M.A., Booth, D.G., 2002a, Executive summary of research contributions related to moisture management of exterior wall systems (MEWS) - modeling, experiments, and benchmarking, Research Report, Institute for Research in Construction, National Research Council Canada, 127, pp. 15.

Maref, W., Lacasse, M.A., Booth, D.G., 2002b, Benchmarking of IRC's advanced hygrothermal model- hygIRC using mid- and large-scale experiments, Research Report, Institute for Research in Construction, National Research Council Canada, 126, pp. 38.

Mclean, R.C., Galbraith, G.H., Sanders, C.H., 1992, Moisture transmission testing of building materials and the presentation of vapor permeability values, Building Research and Practice, 18(2), pp. 82-91

Mukhopadhyaya, P., Kumaran, K. and Normandin, N., 2002, Effect of surface temperature on water absorption coefficient of building materials, Journal of Thermal Envelope and Building Science, 26(02), pp179-195.

Mukhopadhyaya, P., Kumaran, K., Tariku, F., and van Reenen, D., 2003, Report from Task 6 of MEWS Project: Experimental assessment of water penetration and entry into wood-frame wall specimens - final report, Research Report, Institute for Research in Construction, pp. 384, IRC-RR-132.

Nielsen, A., 1972, Gamma-ray attenuation used for measuring the moisture content and homogeneity of porous concrete, Building Science, 7: pp. 257–263.

Nordtest Standard, 1997, Retention curve and pore size distribution, NT BUILD 481.

Osanyintola, O.F., 2005, Transient moisture characteristics of spruce plywood, MASc Thesis, University of Saskatchewan, Department of Mechanical Engineering, pp.170.

Pedersen, C. R., 1990, Combined heat and moisture transfer in building constructions, Ph.D. thesis (Report no.214), Thermal Insulation Laboratory, Technical University of Denmark.

Pel, L., Ketelaars, A.A.J., Odan, O.C.G. and Well, A.A., 1993, Determination of moisture diffusivity in porous media using scanning neutron radiography, International Journal of Heat and Mass Transfer, 36: pp. 1261–1267.

Pedersen, C.R., 1992, Prediction of moisture transfer in building constructions, Building and Environment 27(3): pp. 387-397.

Pel, L., 1995, Moisture transport in porous building materials, Ph.D. Thesis, Technical University Eindhoven, the Netherlands.

Philip, J.R. and de Vries, D.A., 1957, Moisture movement in porous materials under temperature gradients, Transactions, American Geophysical Union, 38: pp. 222–232.

Plagge, R., Grunewald, J. and Haüpl, P., 1999, Application of time domain reflectometry to determine water content and electrical conductivity of capillary porous media, Proceedings of the 5th Symposium on Building Physics in the Nordic Countries, pp. 337–344.

Prazak, J., Tywoniak, J., Peterka, F. and Slonc, T., 1990, Description of transport of liquid in porous media – A study based on neutron radiography, International Journal of Heat and Mass Transfer, 33: pp. 1105–1120.

Richards, L. A., 1948, Porous plate apparatus for measuring moisture retention and transmission by soil, Soil Science, 66, pp.105-109.

Richards, R.F., Burch, D.M. and Thomas, W.C., 1992, Water vapor sorption measurements of common building materials, ASHRAE Transactions, 98(2), pp. 475-485.

Rode, C., 2003, Workshop on moisture buffer capacity –summary report, Sagsrapport R-067, Technical University of Denmark, Department of Civil Engineering.

Rode, C., Peuhkuri, R., Hansen, K.K., Time, B., Svennberg, K., Arfvidsson, J., and Ojanen, T., 2005, Moisture buffer value of materials in buildings. In 7th Nordic Symposium on Building Physics, Reykjavík, pp. 108–115.

Roels, S., Vandersteen, K. and Carmeliet, J., 2003, Measuring and simulating moisture uptake in a fractured porous medium, Advances in Water Resources, 26: pp. 237–246.

Roels, S., Carmeliet, J., Hens, H., Adan, O., Brocken, H., Cerny, R., Pavlik, Z., Ellis, A.T., Hall, C., Kumaran, K., Pel, L., and Plagge, R., 2004a, A comparison of different techniques to quantify moisture content profiles in porous building materials, Journal of Thermal Envelope and Building Science 27: pp. 261-276.

Roels, S., Adan, O., Brocken, H., Carmeliet, J., Cerny, R., Hall, Ch., Hens, H., Kumaran, K., Pavlik, Z., Pel, L. and Plagge, R., 2004b, Interlaboratory comparison of the measurement of basic hygric properties of porous building materials, Journal of Thermal Envelope and Building Science, 27(4): pp. 307–325.

Schirmer, R., ZVDI, Beiheft Verfahrenstechnik, Nr. 6, S. 170, 1938.

Wadsö, I. and Wadsö, L., 1996, A new method for determination of vapor sorption isotherms using a twin double microcalorimeter, Thermochimica Acta, Vol. 271, pp. 179–187.

Wadsö, L., 1997, A reviewof methods to measure sorption isotherms and heats of sorption, paper presented at the International Conference on Wood–Water Relations, Copenhagen, 16–17 June.

Wadsö, I. and Wadsö, L., 1997, A second generation twin double microcalorimeter: Measurements of sorption isotherms, heats of sorption and sorption kinetics, Journal of Thermal Analysis, Vol. 49, pp. 1045–1052.

Wilkes, K.E. and Karagiozis, A., 2004, The importance of measured method for gypsum sorption isotherm, IEA (International Energy Agency), Annex 41, 2004.

Wormald, R. and Britch, A.L., 1969, Methods of measuring moisture content applicable to building materials, Building Science, Vol. 3, pp.135-145.

Appendix A

Measured Hygrothermal Properties of Building Materials

The measured hygrothermal properties are presented in this appendix.

A.1. Hygrothermal Properties of Gypsum Board

Thickness: (12.60 ± 0.11) mm

Density: (592 ± 5) kg/m^3

Table A.1 Thermal conductivity of gypsum board

Specimen thickness (mm)	Hot Surface Temperature (°C)	Cold Surface Temperature (°C)	Mean Temperature (°C)	Conductivity ($Wm^{-1}K^{-1}$)
12.43	6.60	-3.14	1.73	0.15
12.43	29.60	19.25	24.43	0.15
12.51	5.27	-3.49	0.89	0.15
12.51	29.59	19.02	24.31	0.14

Table A.2 Results from sorption isotherm measurement of gypsum board

RH, %	Temperature, °C	Moisture Content, kg/kg
100, Vacuum Saturation	Lab at 22 (1)	1.36 (0.12), 29 specimens
96.1 (1)	22.8 (0.1)	0.027 (0.001), 4 specimens
89.2 (1)	23.2 (0.1)	0.014 (0.0002), 4 specimen
70.4 (1)	23.2 (0.1)	0.0082 (0.0001), 4 specimen
50.1 (1)	23.2 (0.1)	0.0048 (0.0001), 4 specimen
33.5 (1)	22.4 (0.1)	0.0035 (0.0001), 4 specimen

Table A.3 Results from desorption isotherm measurement of gypsum board

RH, %	Temperature, °C	Moisture Content, kg/kg
93.8 (1)	23.1 (0.1)	0.126 (0.001), 4 specimens
91.1(1)	23.1 (0.1)	0.028 (0.0002), 4 specimen
70.8 (1)	23.2 (0.1)	0.024 (0.0001), 4 specimen
49.5 (1)	23.3 (0.1)	0.020 (0.0001), 4 specimen
33.1 (1)	22.4 (0.1)	0.019 (0.0001), 4 specimen

Table A.4 Dry cup measurements of gypsum board

Specimen Thickness mm	Chamber RH %	Chamber Temperature °C	WVT Rate kg/s·m^2
12.62	50.0 (1)	23.2 (0.1)	3.08E-06 (2.8E-08)
12.48	50.0 (1)	23.2 (0.1)	2.94E-06 (1.8E-08)
12.63	50.0 (1)	23.2 (0.1)	2.94E-06 (2.4E-08)
12.62	70.4 (1)	23.1 (0.1)	4.71E-06 (7.1E-08)
12.48	70.4 (1)	23.1 (0.1)	4.53E-06 (5.4E-08)
12.63	70.4 (1)	23.1 (0.1)	4.50E-06 (5.9E-08)
12.62	89.8 (1)	23.1 (0.1)	5.72E-06 (5.7E-08)
12.48	89.7 (1)	23.1 (0.1)	5.57E-06 (3.9E-08)
12.63	89.8 (1)	23.1 (0.1)	5.46E-06 (1.1E-08)

Table A.5 Wet cup measurements of gypsum board

Specimen Thickness mm	Chamber RH %	Chamber Temperature °C	WVT Rate kg/s·m^2
12.46	70.5 (1)	23.1 (0.1)	2.28E-06 (2.1E-09)
12.55	70.5 (1)	23.1 (0.1)	2.28E-06 (3.2E-09)
12.48	70.5 (1)	23.1 (0.1)	2.34E-06 (8.3E-09)
12.46	89.7 (1)	23.1 (0.1)	1.06E-06 (1.6E-08)
12.55	89.7 (1)	23.1 (0.1)	1.12E-06 (1.5E-08)
12.48	89.7 (1)	23.1 (0.1)	1.10E-06 (9.8E-09)

Table A.6 Derived water vapor permeability of gypsum board

RH %	Permeability kg/m·s·Pa	RH %	Permeability kg/m·s·Pa
10	3.00E-11	60	3.94E-11
20	3.17E-11	70	4.17E-11
30	3.34E-11	80	4.42E-11
40	3.53E-11	90	4.68E-11
50	3.73E-11	100	4.96E-11

Table A.7 Water absorption of gypsum board

Square Root of Time, $s^{1/2}$	Water Absorption Kg/m^2
7.8	0.08 (0.04)
13.4	0.27 (0.11)
19.0	1.00 (0.28)
23.2	1.55 (0.40)
26.8	2.17 (0.48)
30.0	2.80 (0.59)
32.9	3.14 (0.61)
35.5	3.51 (0.64)
40.3	4.02 (0.60)
44.5	4.33 (0.45)
50.2	4.62 (0.27)
55.3	4.80 (0.22)
66.2	5.08 (0.22)
78.6	5.36 (0.23)

Through the linear regression of the first linear part of the absorption curve, the absorption coefficient of gypsum board is calculated, and the value is 0.16 ± 0.04 $kg/m^2s^{1/2}$.

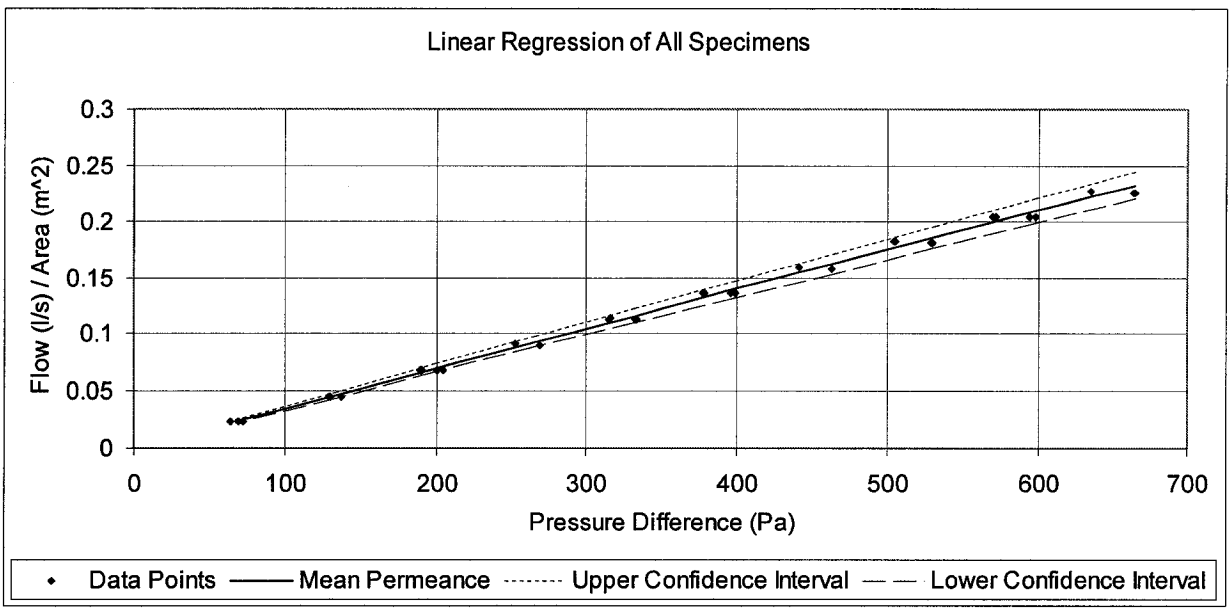

Figure A.1 The dependence of airflow rate on pressure difference for gypsum board

At the range of pressure differences from 100 to 700 Pa, the flow rate varies with pressure difference. The air permeability of gypsum board under test is (5.2 ± 0.3) E-08 kg/m·Pa·s.

A.2. Hygrothermal Properties of Oriented Strand Board

Thickness: (11.64 ± 0.72) mm

Density: (664 ± 46) kg/m^3

Table A.8 Thermal conductivity of OSB

Specimen thickness (mm)	Hot Surface Temperature (°C)	Cold Surface Temperature (°C)	Mean Temperature (°C)	Conductivity ($Wm^{-1}K^{-1}$)
11.41	12.10	0.26	6.18	0.087
11.41	31.89	18.54	25.21	0.091
11.37	12.08609	0.366293	6.23	0.088
11.37	31.82672	18.57836	25.20	0.091

Table A.9 Results from sorption isotherm measurement of OSB

RH, %	Temperature, °C	Moisture Content, kg/kg
96.1 (1)	22.8 (0.1)	0.25 (0.02), 4 specimens
89.2 (1)	23.2 (0.1)	0.16 (0.002), 4 specimen
70.4 (1)	23.2 (0.1)	0.11 (0.002), 4 specimen
50.1 (1)	23.2 (0.1)	0.062 (0.0003), 3 specimen
33.5 (1)	22.5 (0.1)	0.047 (0.001), 4 specimen

Table A.10 Results from desorption isotherm measurement of OSB

RH, %	Temperature, °C	Moisture Content, kg/kg
100, Vacuum Saturation	Lab at 22 (1)	1.36 (0.12), 29 specimens
93.7 (1)	23.1 (0.1)	0.25 (0.008), 4 specimens
91.2 (1)	23.0 (0.1)	0.19 (0.002), 4 specimen
70.4 (1)	23.1 (0.1)	0.12 (0.002), 4 specimen
49.7 (1)	23.3 (0.1)	0.084 (0.001), 3 specimen
32 (1)	22.4 (0.1)	0.058 (0.001), 4 specimen

Table A.11 Dry cup measurements of OSB

Specimen Thickness mm	Chamber RH %	Chamber Temperature °C	WVT Rate kg/s·m^2
11.54	49.95 (1)	23.25 (0.1)	8.60E-08 (1.75E-09)
11.65	49.95 (1)	23.25 (0.1)	1.07E-07 (1.87E-09)
11.59	49.95 (1)	23.25 (0.1)	1.02E-07 (1.91E-09)
11.54	70.38 (1)	23.21 (0.1)	1.69E-07 (1.81E-09)
11.65	70.38 (1)	23.21 (0.1)	1.99E-07 (1.88E-09)
11.59	70.38 (1)	23.21 (0.1)	1.87E-07 (2.18E-09)
11.54	89.88 (1)	23.07 (0.1)	2.03E-07 (4.10E-09)
11.65	89.88 (1)	23.07 (0.1)	2.27E-07 (2.73E-09)
11.59	89.88 (1)	23.07 (0.1)	2.20E-07 (4.58E-09)

Table A.12 Wet cup measurements of OSB

Specimen Thickness mm	Chamber RH %	Chamber Temperature °C	WVT Rate kg/s·m^2
11.54	70.38	23.18	3.12E-07 (3.09E-09)
11.65	70.38	23.18	2.43E-07 (4.18E-09)
11.59	70.38	23.18	1.82E-07 (5.52E-09)
11.54	89.88	23.06	3.23E-07 (5.48E-09)
11.65	89.88	23.06	2.90E-07 (5.53E-09)
11.59	89.88	23.06	2.58E-07 (5.68E-09)

Table A.13 Derived water vapor permeability for OSB

RH %	Permeability kg/m·s·Pa	RH %	Permeability kg/m·s·Pa
10	2.95E-13	60	1.46E-12
20	4.05E-13	70	2.01E-12
30	5.58E-13	80	2.78E-12
40	7.67E-13	90	3.85E-12
50	1.06E-12	100	5.35E-12

Table A.14 Water absorption of OSB

Square Root of Time, s$^{1/2}$	Water Absorption Kg/m^2
7.7	0.020 (0.002)
13.4	0.030 (0.002)
17.3	0.037 (0.002)
20.5	0.045 (0.004)
24.5	0.050 (0.005)

Table A.14 Water absorption of OSB (Cont'd)

Square Root of Time, $s^{1/2}$	Water Absorption Kg/m^2
30.0	0.061 (0.59)
34.6	0.074 (0.008)
38.7	0.078 (0.007)
42.4	0.082 (0.008)
49.0	0.094 (0.007)
54.8	0.103 (0.008)
60.0	0.111 (0.008)
64.8	0.118 (0.011)
81.2	0.141 (0.014)
94.9	0.166 (0.016)
112.2	0.194 (0.021)
135.7	0.237 (0.028)
155.9	0.275 (0.034)
291.4	0.686 (0.109)
312.8	0.754 (0.115)

Through the linear regression of the first linear part of the absorption curve, the absorption coefficient of OSB is calculated, and the value is 0.0018 ± 0.0002 $kg/m^2s^{1/2}$.

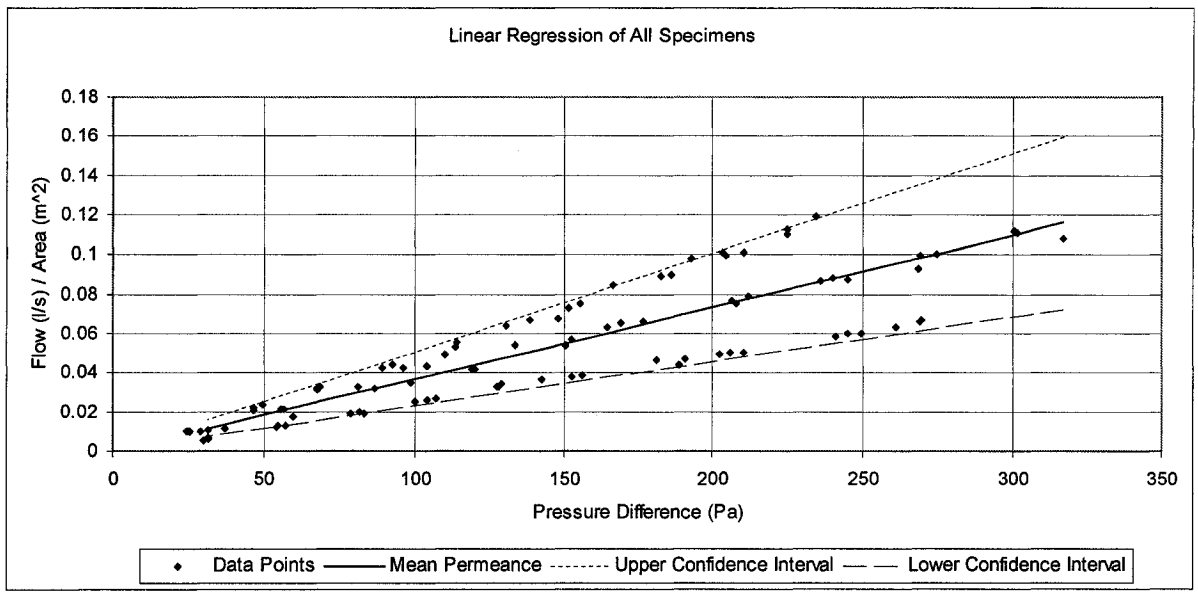

Figure A.2 The dependence of airflow rate on pressure difference for OSB

At the range of pressure differences from 20 to 300 Pa, the flow rate varies with pressure difference. The air permeability of gypsum board under test is (5.1 ± 1.9) E-09 kg/m·Pa·s.

A.3. Hygrothermal Properties of Plywood

Thickness: (12.57 ± 0.37) mm

Density: (456 ± 30) kg/m^3

Table A.15 Thermal conductivity of plywood

Specimen thickness (mm)	Hot Surface Temperature (°C)	Cold Surface Temperature (°C)	Mean Temperature (°C)	Conductivity ($Wm^{-1}K^{-1}$)
12.69	2.86	-3.51	-0.32	0.084
12.69	32.51	19.62	26.07	0.089
12.49	2.86	-3.68	-0.41	0.081
12.49	31.81	19.70	13.11	0.086

Table A.16 Results from adsorption isotherm measurement of plywood

RH, %	Temperature, °C	Moisture Content, kg/kg
100, Vacuum Saturation	Lab at 22 (1)	1.29 (0.11), 29 specimens
96.2 (1)	22.7 (0.1)	0.28 (0.027), 4 specimens
89.2 (1)	23.2 (0.1)	0.17 (0.005), 4 specimen
70.5 (1)	23.2 (0.1)	0.12 (0.002), 4 specimen
50.1 (1)	23.2 (0.1)	0.072 (0.0003), 4 specimen
33.5 (1)	22.5 (0.1)	0.058 (0.0003), 4 specimen

Table A.17 Results from desorption isotherm measurement of plywood

RH, %	Temperature, °C	Moisture Content, kg/kg
93.7 (1)	23.1 (0.1)	0.27 (0.005), 4 specimens
90.0 (1)	22.9 (0.1)	0.20 (0.001), 4 specimen
70.4 (1)	23.1 (0.1)	0.14 (0.001), 4 specimen
49.7 (1)	23.3 (0.1)	0.095 (0.002), 4 specimen
33.0 (1)	22.4 (0.1)	0.066 (0.001), 4 specimen

Table A.18 Dry cup measurements of plywood

Specimen Thickness mm	Chamber RH %	Chamber Temperature °C	WVT Rate kg/s·m2
13.04	49.98 (1)	23.21 (0.1)	8.69E-08 (1.07E-09)
13.15	49.98 (1)	23.21 (0.1)	1.41E-07 (3.02E-10)
12.08	49.98 (1)	23.21 (0.1)	6.67E-08 (4.09E-10)
13.04	70.40 (1)	23.15 (0.1)	1.83E-07 (9.58E-10)
13.15	70.40 (1)	23.15 (0.1)	2.94E-07 (4.52E-09)
12.08	70.40 (1)	23.15 (0.1)	1.69E-07 (9.75E-10)
13.04	89.15 (1)	23.18 (0.1)	3.63E-07 (6.05E-09)
13.15	89.15 (1)	23.18 (0.1)	4.97E-07 (1.00E-08)
12.08	89.15 (1)	23.18 (0.1)	3.72E-07 (4.59E-09)

Table A.19 Wet cup measurements of plywood

Specimen Thickness mm	Chamber RH %	Chamber Temperature °C	WVT Rate kg/s·m^2
12.18	70.36 (1)	23.13 (0.1)	6.13E-07 (5.51E-09)
12.09	70.36 (1)	23.13 (0.1)	6.12E-07 (8.65E-09)
12.06	70.36 (1)	23.13 (0.1)	5.19E-07 (9.87E-09)
12.18	89.08 (1)	23.19 (0.1)	4.57E-07 (7.02E-09)
12.09	89.08 (1)	23.19 (0.1)	4.76E-07 (5.68E-09)
12.06	89.08 (1)	23.19 (0.1)	3.95E-07 (4.66E-09)

Table A.20 Derived water vapor permeability for plywood

RH %	Permeability kg/m·s·Pa	RH %	Permeability kg/m·s·Pa
10	1.01E-13	60	1.86E-12
20	1.80E-13	70	3.37E-12
30	3.22E-13	80	6.18E-12
40	5.77E-13	90	1.16E-11
50	1.03E-12	100	2.26E-11

Table A.21 Water absorption of plywood

Square Root of Time, $s^{1/2}$	Water Absorption Kg/m^2
7.8	0.026 (0.004)
11.0	0.042 (0.004)
15.5	0.055(0.018)
20.5	0.065 (0.038)
24.5	0.075 (0.041)
27.9	0.081 (0.047)
32.9	0.089 (0.055)
37.2	0.099 (0.061
44.5	0.115 (0.073)
52.0	0.129 (0.082)
60.0	0.143 (0.090)
64.3	0.152 (0.097)
73.1	0.169 (0.110)
89.7	0.195 (0.125)
109.5	0.239(0.147)
127.0	0.275 (0.160)
150.6	0.343 (0.170)
168.6	0.406 (0.191)
295.4	1.018 (0.533)
309.4	1.095 (0.563)
323.2	1.174 (0.588)
336.3	1.260 (0.599)

Through the linear regression of the first linear part of the absorption curve, the absorption coefficient of plywood is calculated, and the value is 0.0020 ± 0.0013 $kg/m^2s^{1/2}$.

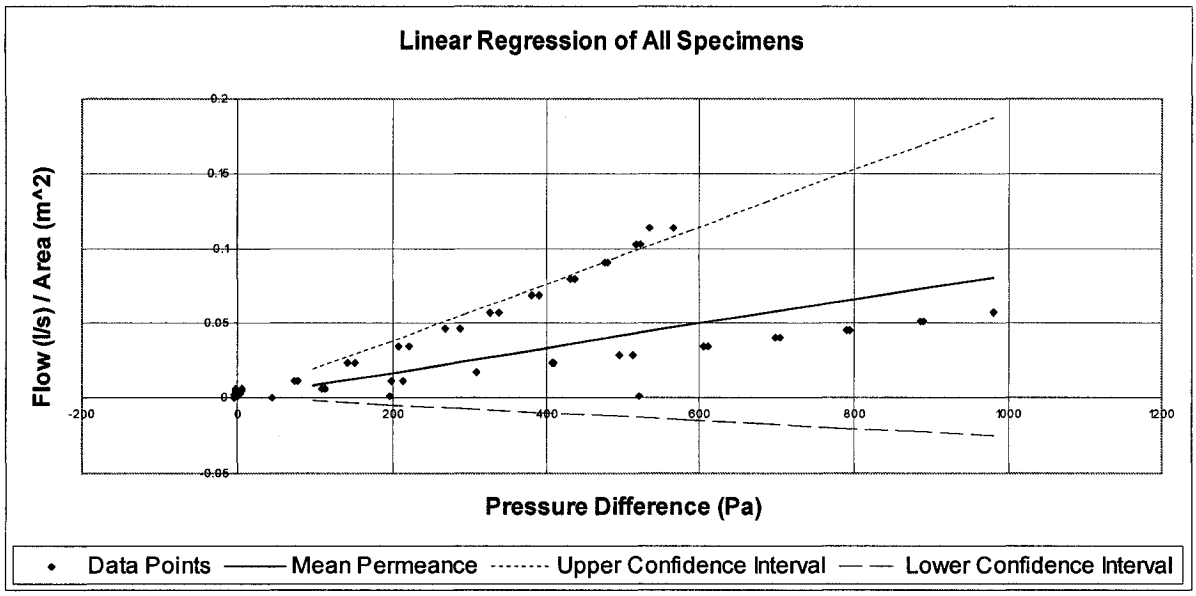

Figure A.3 The dependence of airflow rate on pressure difference for plywood

At the range of pressure differences from 20 to 1000 Pa, the flow rate varies with pressure difference. The air permeability of gypsum board under test is (1.3 ± 1.7) E-09 kg/m·Pa·s.

A.4. Hygrothermal Properties of wood fiberboard

Thickness: (10.84 ± 0.11) mm

Density: (279 ± 3) kg/m^3

Table A.22 Thermal conductivity of fiberboard

Specimen thickness (mm)	Hot Surface Temperature (°C)	Cold Surface Temperature (°C)	Mean Temperature (°C)	Conductivity ($Wm^{-1}K^{-1}$)
10.66	4.62	-2.94	0.84	0.0457
10.66	14.90	7.17	11.03	0.0463
10.72	15.67	7.22	11.44	0.0471
10.72	32.01	17.86	24.93	0.0485

Table A.23 Results from sorption isotherm measurement of fiberboard

RH, %	Temperature, °C	Moisture Content, kg/kg
100, Vacuum Saturation	Lab at 22 (1)	3.597 (0.046), 29 specimens
96.2 (1)	22.7 (0.1)	0.276 (0.027), 4 specimens
89.2 (1)	23.2 (0.1)	0.174 (0.005), 4 specimen
70.5 (1)	23.2 (0.1)	0.119 (0.002), 4 specimen
50.1 (1)	23.2 (0.1)	0.072 (0.0003), 4 specimen
33.5 (1)	22.5 (0.1)	0.058 (0.0003), 4 specimen

Table A.24 Results from desorption isotherm measurement of fiberboard

RH, %	Temperature, °C	Moisture Content, kg/kg
93.7 (1)	23.1 (0.1)	0.297 (0.01)
91.2 (1)	23.0 (0.1)	0.188 (0.002)
70.4 (1)	23.1 (0.1)	0.120 (0.001)
49.5 (1)	23.2 (0.1)	0.083 (0.001)
33.0 (1)	22.4 (0.1)	0.055 (0.001)

Table A.25 Dry cup measurements of fiberboard

Specimen Thickness mm	Chamber RH %	Chamber Temperature °C	WVT Rate kg/s·m2
11.00	50.05 (1)	23.20 (0.1)	2.00E-06 (1.28E-08)
11.11	50.05 (1)	23.20 (0.1)	2.06E-06 (1.93E-08)
11.02	50.05 (1)	23.20 (0.1)	2.12E-06 (2.11E-08)
11.00	70.39 (1)	23.15 (0.1)	2.78E-06 (7.71E-09)
11.11	70.39 (1)	23.15 (0.1)	2.87E-06 (8.98E-09)
11.02	70.39 (1)	23.15 (0.1)	2.94E-06 (8.51E-09)
11.00	89.74 (1)	23.07 (0.1)	3.70E-06 (2.27E-08)
11.11	89.74 (1)	23.07 (0.1)	3.79E-06 (2.99E-08)
11.02	89.74 (1)	23.07 (0.1)	3.84E-06 (2.76E-08)

Table A.26 Wet cup measurements of fiberboard

Specimen Thickness mm	Chamber RH %	Chamber Temperature °C	WVT Rate kg/s·m2
10.94	70.46	23.10	1.25E-06 (2.16E-08)
10.93	70.46	23.10	1.24E-06 (1.81E-08)
11.00	70.46	23.10	1.28E-06 (2.05E-08)
10.94	89.52	23.11	5.09E-07 (1.23E-08)
10.93	89.52	23.11	5.13E-07 (1.22E-08)
11.00	89.52	23.11	5.11E-07 (1.48E-08)

Table A.27 Derived water vapor permeability for fiberboard

RH %	Permeability kg/m·s·Pa	RH %	Permeability kg/m·s·Pa
10	1.82E-11	60	1.88E-11
20	1.85E-11	70	1.89E-11
30	1.86E-11	80	1.89E-11
40	1.87E-11	90	1.89E-11
50	1.88E-11	100	1.89E-11

Table A.28 Water absorption of fiberboard

Square Root of Time, $s^{1/2}$	Water Absorption Kg/m^2
7.75	0.012 (0.006)
13.42	0.022 (0.008)
18.97	0.028 (0.008)
25.69	0.035 (0.008)
35.50	0.042 (0.008)
43.13	0.049 (0.010)
55.32	0.065 (0.009)
70.57	0.084 (0.010)
84.14	0.106 (0.011
94.55	0.129 (0.015)
112.78	0.183 (0.029)
129.38	0.255 (0.046)
148.19	0.353 (0.069)
161.37	0.428 (0.078)

Through the linear regression of the first linear part of the absorption curve, the absorption coefficient of plywood is calculated, and the value is 0.0012 ± 0.0001 $kg/m^2s^{1/2}$.

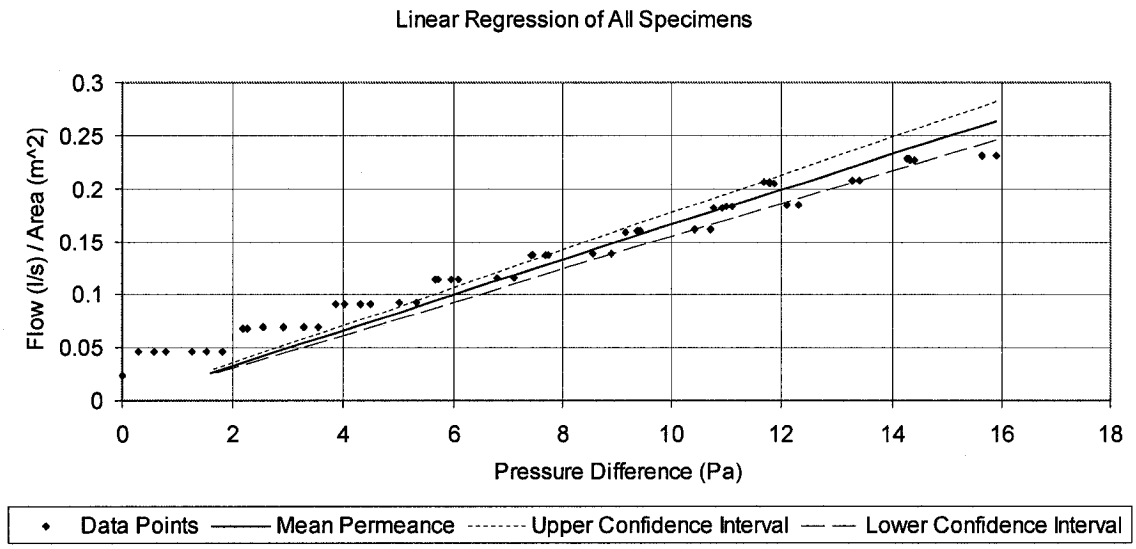

Figure A.4 The dependence of airflow rate on pressure difference for fiberboard

At the range of pressure differences from 0 to 16 Pa, the flow rate of all test specimens linearly varies with the pressure difference. The air permeability of fiberboard under test is (2.2 ± 0.2) E-07 kg/m·Pa·s.

A.5. Hygrothermal Properties of spruce wood stud

Density: (465 ± 20) kg/m^3

Table A.29 Thermal conductivity of spruce wood stud

Specimen thickness (mm)	Hot Surface Temperature (°C)	Cold Surface Temperature (°C)	Mean Temperature (°C)	Conductivity ($Wm^{-1}K^{-1}$)
37.48	12.25	-2.69	4.78	0.095
37.48	34.89	15.27	25.08	0.099
37.45	14.64	-2.33	6.16	0.096
37.45	34.90	15.32	25.11	0.098

Table A.30 Results from sorption isotherm measurement of spruce wood stud

RH, %	Temperature, °C	Moisture Content, kg/kg
93.7 (1)	23.1 (0.1)	0.24 (0.006), 4 specimens
91.2 (1)	23.0 (0.1)	0.17 (0.002), 4 specimens
70.4 (1)	23.2 (0.1)	0.12 (0.001), 4 specimens
49.7 (1)	23.1 (0.1)	0.08 (0.0005), 4 specimens
33.1 (1)	22.4 (0.1)	0.054 (0.001), 4 specimens

Table A.31 Results from desorption isotherm measurement of spruce wood stud

RH, %	Temperature, °C	Moisture Content, kg/kg
100, Vacuum Saturation	Lab at 22 (1)	1.57 (0.13), 29 specimens
93.7 (1)	23.1 (0.1)	0.28 (0.03), 4 specimens
90.0 (1)	23.2 (0.1)	0.19 (0.004), 4 specimens
70.4 (1)	23.1 (0.1)	0.14 (0.002), 4 specimens
49.9 (1)	23.3 (0.1)	0.10 (0.001), 4 specimens
33.1 (1)	22.4 (0.1)	0.071 (0.001), 4 specimens

Table A.32 Dry cup measurements of spruce wood stud

Specimen Thickness mm	Chamber RH %	Chamber Temperature °C	WVT Rate kg/s·m2
38.48	50.06	23.30	5.41E-08 (5.91E-10)
38.35	50.06	23.30	4.03E-08 (6.06E-10)
38.05	50.06	23.30	3.89E-08 (5.77E-10)
38.48	70.59	23.19	1.02E-07 (7.38E-10)
38.35	70.59	23.19	8.62E-08 (7.91E-10)
38.05	70.59	23.19	8.94E-08 (1.76E-09)
38.48	90.82	22.99	2.36E-07 (3.42E-09)
38.35	90.82	22.99	2.12E-07 (2.57E-09)
38.05	90.82	22.99	2.29E-07 (3.48E-09)

Table A.33 Wet cup measurements of spruce wood stud

Specimen Thickness mm	Chamber RH %	Chamber Temperature °C	WVT Rate kg/s·m^2
38.90	70.54	23.23	3.00E-07 (4.68E-09)
38.63	70.54	23.23	2.74E-07 (4.63E-09)
38.75	70.54	23.23	2.81E-07 (3.97E-09)
38.90	90.82	23.00	2.25E-07 (4.14E-09)
38.63	90.82	23.00	2.45E-07 (4.45E-09)
38.75	90.82	23.00	2.04E-07 (5.60E-08)

Table A.34 Derived water vapor permeability for spruce wood stud

RH %	Permeability kg/m·s·Pa	RH %	Permeability kg/m·s·Pa
10	2.92E-13	60	3.23E-12
20	5.05E-13	70	5.32E-12
30	8.02E-13	80	9.00E-12
40	1.26E-12	90	1.56E-11
50	2.00E-12	100	2.81E-11

Table A.35 Water absorption of spruce stud

Square Root of Time $s^{1/2}$	Water Absorption (Average of 4 specimens) Kg/m^2
7.7	0.34 (0.03)
15.5	0.38 (0.02)
20.5	0.45 (0.03)
24.5	0.53 (0.03)
30.0	0.58 (0.05)
34.6	0.64 (0.03)
38.7	0.68 (0.03)
42.4	0.75 (0.04)
49.0	0.83 (0.03)
60.0	0.95 (0.05)
73.5	1.07 (0.05)
84.9	1.20 (0.03)
94.9	1.31 (0.03)
112.2	1.54 (0.04)
127.3	1.69 (0.05)
140.7	1.86 (0.04)
153.0	2.02 (0.05)
296.0	3.89 (0.01)
302.3	3.97 (0.05)
325.2	4.36 (0.05)
723.0	5.11 (0.30)

Through the linear regression of the first linear part of the absorption curve, the absorption coefficient of spruce is calculated, and the value is 0.0124 ± 0.0001 $kg/m^2s^{1/2}$.

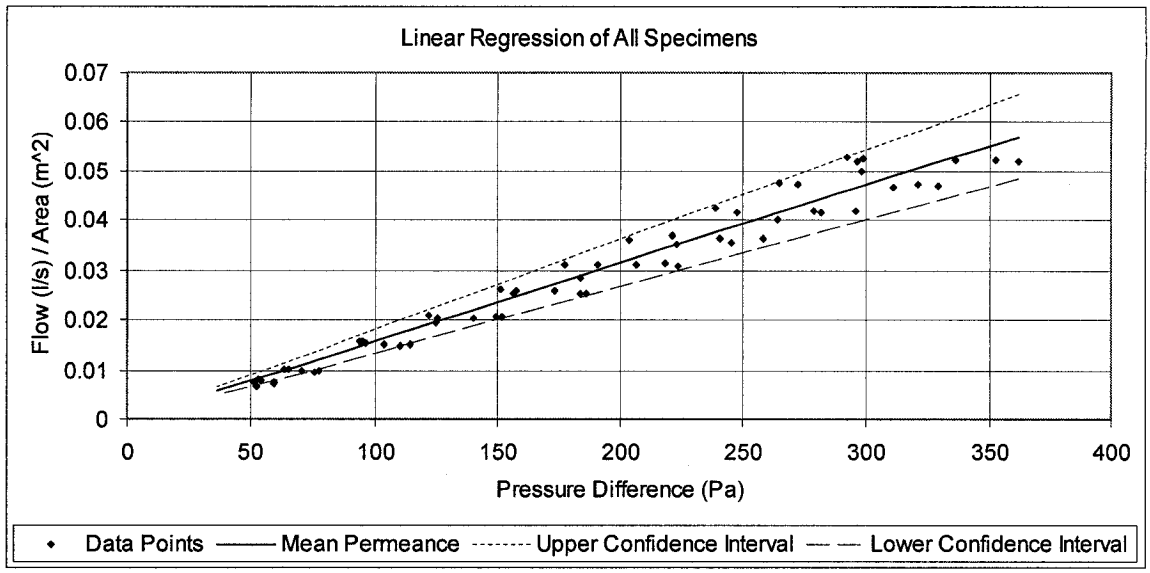

Figure A.5 The dependence of airflow rate on pressure difference for spruce stud

At the range of pressure differences from 50 to 350 Pa, the flow rate of two specimens increases with the pressure difference. The air permeability of spruce stud under test is (7.2 ± 1.0) E-9 kg/m·Pa·s.

A.6. Hygrothermal Properties of extruded polystyrene foam sheathing

Density: (27.2 ± 0.5) kg/m^3

Thickness: (26.3 ± 0.7) mm

Table A.36 Thermal conductivity of EPS

Specimen thickness (mm)	Hot Surface Temperature (°C)	Cold Surface Temperature (°C)	Mean Temperature (°C)	Conductivity ($Wm^{-1}K^{-1}$)
25.88	16.29	-6.17	5.61	0.0258
25.88	34.60	13.47	24.04	0.0279
26.51	14. 89	−4. 99	4.95	0.0259
26.51	36. 41	15. 80	26.11	0.0280

Table A.36 Results from sorption isotherm measurement of EPS

RH, %	Temperature, °C	Moisture Content, kg/kg
96.2 (1)	22.7 (0.1)	0.003 (0.001), 3 specimens
89.2 (1)	23.2 (0.1)	0.003 (0.001), 3 specimens
70.3 (1)	23.2 (0.1)	0.003 (0.001), 3 specimens
50.1 (1)	23.2 (0.1)	0.002 (0.002), 3 specimens
33.2 (1)	22.4 (0.1)	0.002 (0.001), 3 specimens

Table A.37 Dry cup measurements of EPS

Specimen Thickness mm	Chamber RH %	Chamber Temperature °C	WVT Rate kg/s·m^2
26.64	50.16 (1)	23.30 (0.1)	5.34E-08 (9.39E-10)
25.67	50.16 (1)	23.30 (0.1)	5.59E-08 (6.44E-10)
25.67	50.16 (1)	23.30 (0.1)	5.52E-08 (7.68E-10)
26.64	70.90 (1)	23.24 (0.1)	8.28E-08 (1.19E-09)
25.67	70.90 (1)	23.24 (0.1)	8.29E-08 (1.13E-09)
25.67	70.90 (1)	23.24 (0.1)	8.30E-08 (1.77E-09)
26.64	90.83 (1)	23.04 (0.1)	1.03E-07 (1.97E-09)
25.67	90.83 (1)	23.04 (0.1)	1.04E-07 (7.98E-10)
25.67	90.83 (1)	23.04 (0.1)	1.02E-07 (1.52E-09)

Table A.38 Wet cup measurements of EPS

Specimen Thickness mm	Chamber RH %	Chamber Temperature °C	WVT Rate kg/s·m^2
26.64	70.40 (1)	23.00 (0.1)	3.26E-08 (6.37E-10)
25.67	70.40 (1)	23.00 (0.1)	3.27E-08 (4.82E-10)
25.67	70.40 (1)	23.00 (0.1)	3.37E-08 (2.40E-10)
26.64	91.18 (1)	22.98 (0.1)	1.09E-08 (1.94E-10)
25.67	91.18 (1)	22.98 (0.1)	1.05E-08 (2.92E-10)
25.67	91.18 (1)	22.98 (0.1)	1.02E-08 (3.58E-10)

Table A.39 Derived water vapor permeability for EPS

RH %	Permeability kg/m·s·Pa	RH %	Permeability kg/m·s·Pa
10	1.03E-12	60	1.08E-12
20	1.04E-12	70	1.09E-12
30	1.05E-12	80	1.10E-12
40	1.06E-12	90	1.11E-12
50	1.07E-12	100	1.12E-12

Extruded polystyrene foam sheathing has very low water absorption rate. Therefore, the partial immersion test of this material is hard to carry out. In addition, the test specimens are impermeable and no measurable airflow obtained for pressure differences up to several kPa.

A.7. Hygrothermal Properties of Asphalt Impregnated Paper

Density: (1033 ± 17) kg/m^3

Thickness: (0.64 ± 0.016) mm

Table A.40 Dry cup measurements of asphalt impregnated paper

Specimen Thickness mm	Chamber RH %	Chamber Temperature °C	WVT Rate kg/s·m2
0.65	50.10	23.31	6.24E-08 (1.20E-09)
0.63	50.10	23.31	7.40E-08 (1.14E-09)
0.62	50.10	23.31	1.44E-07 (1.43E-09)
0.65	70.50	23.26	1.11E-07 (1.57E-09)
0.63	70.50	23.26	1.29E-07 (1.23E-09)
0.62	70.50	23.26	2.40E-07 (2.01E-09)
0.65	90.50	23.13	2.62E-07 (1.17E-09)
0.63	90.50	23.13	2.81E-07 (8.06E-10)
0.62	90.50	23.13	4.25E-07 (1.22E-09)

Table A.41 Wet cup measurements of asphalt impregnated paper

Specimen Thickness mm	Chamber RH %	Chamber Temperature °C	WVT Rate kg/s·m^2
26.64	70.30	23.25	4.47E-07 (3.85E-09)
25.67	70.30	23.25	4.41E-07 (4.79E-09)
25.67	70.30	23.25	4.90E-07 (5.80E-09)
26.64	89.77	23.21	3.36E-07 (5.14E-09)
25.67	89.77	23.21	3.44E-07 (4.94E-09)
25.67	89.77	23.21	3.69E-07 (6.60E-09)

Table A.42 Derived water vapor permeability for asphalt impregnated paper

RH %	Permeability kg/m·s·Pa	RH %	Permeability kg/m·s·Pa
10	1.74E-14	60	1.53E-13
20	3.30E-14	70	2.01E-13
30	5.38E-14	80	2.56E-13
40	8.05E-14	90	3.18E-13
50	1.14E-13	100	3.90E-13

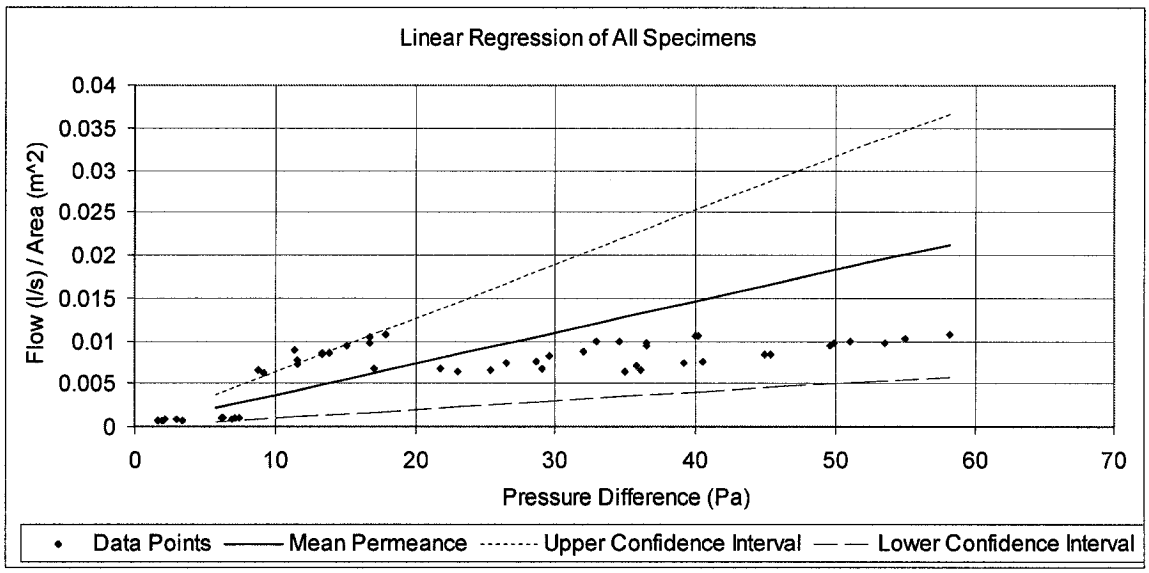

Figure A.6 The dependence of airflow rate on pressure difference for asphalt impregnated paper

At the range of pressure differences from 1 to 60 Pa, the flow rate of asphalt impregnated paper increases with the pressure difference. The air permeability of asphalt impregnated paper under test is (2.7 ± 1.9) E-10 kg/m·Pa·s.

A.8. Hygrothermal Properties of Stucco

Density: (1411.98 ± 65) kg/m^3

Thickness: (19.56 ± 0.78) mm

Table A.43 Thermal conductivity of stucco

Specimen thickness (mm)	Hot Surface Temperature (°C)	Cold Surface Temperature (°C)	Mean Temperature (°C)	Conductivity ($Wm^{-1}K^{-1}$)
19.23	26.44	23.30	24.87	0.336
19.23	4.39	2.14	3.27	0.322
19.03	26.63	23.39	25.01	0.334
19.03	5.60	3.09	4.39	0.322

Table A.44 Results from sorption isotherm measurement of stucco

RH, %	Temperature, °C	Moisture Content, kg/kg
93.1 (1)	23.0 (0.1)	0.059 (0.001), 3 specimens
89.7 (1)	23.0 (0.1)	0.049 (0.001), 3 specimen
70.0 (1)	22.9 (0.1)	0.024 (0.004), 3 specimen
50.3 (1)	22.9 (0.1)	0.013 (0.0003), 3 specimen

Table A.45 Results from desorption isotherm measurement of stucco

RH, %	Temperature, °C	Moisture Content, kg/kg
100, Vacuum Saturation	Lab at 22 (1)	0.21 (0.01), 29 specimens
93.4 (1)	23.0 (0.1)	0.058 (0.001)
88.9 (1)	23.0 (0.1)	0.055 (0.002)
70.2 (1)	23.0 (0.1)	0.033 (0.0004)
50.3 (1)	23.0 (0.1)	0.022 (0.003)

Table A.46 Dry cup measurements of stucco

Specimen Thickness mm	Chamber RH %	Chamber Temperature °C	WVT Rate $kg/s \cdot m^2$
15.75	49.87	23.08	9.68E-07(3.29E-09)
15.28	49.87	23.08	1.04E-06(5.06E-09)
15.63	49.87	23.08	9.30E-07(4.29E-09)
15.75	70.40	23.10	1.42E-06(3.51E-09)
15.28	70.40	23.10	1.51E-06(1.04E-09)
15.63	70.40	23.10	1.36E-06(5.24E-09)
15.75	89.42	22.88	1.95E-06(1.78E-08)
15.28	89.42	22.88	2.11E-06(1.93E-08)
15.63	89.42	22.88	1.90E-06(2.18E-08)

Table A.47 Wet cup measurements of stucco

Specimen Thickness mm	Chamber RH %	Chamber Temperature °C	WVT Rate kg/s·m^2
14.06	70.53	23.04	9.39E-07(6.10E-09)
13.96	70.53	23.04	9.82E-07(4.81E-09)
15.53	70.53	23.04	7.03E-07(2.72E-09)
14.06	87.82	23.12	2.49E-07(4.53E-09)
13.96	87.82	23.12	2.81E-07(5.12E-09)
15.53	87.82	23.12	1.57E-07(2.83E-09)

Table A.48 Derived water vapor permeability for stucco

RH %	Permeability kg/m·s·Pa	RH %	Permeability kg/m·s·Pa
10	1.27E-11	60	1.83E-11
20	1.37E-11	70	1.97E-11
30	1.47E-11	80	2.12E-11
40	1.58E-11	90	2.29E-11
50	1.7E-11	100	2.47E-11

Table A.49 Water absorption of stucco

Square Root of Time $s^{1/2}$	Water Absorption (Average of 4 specimens) Kg/m^2
7.75	0.68(0.17)
13.42	0.88(0.22)
17.32	1.01(0.26)
20.49	1.10(0.31)
23.24	1.18(0.33)
26.83	1.28(0.37)
30.00	1.35(0.39)
34.64	1.45(0.43)
38.73	1.54(0.46)
45.83	1.69(0.51)
51.96	1.80(0.55)
57.45	1.89(0.58)
62.45	1.97(0.60)
67.08	2.05(0.62)

Through the linear regression of the first linear part of the absorption curve, the absorption coefficient of stucco is calculated, and the value is 0.088 ± 0.022 kg/m^{2}s$^{1/2}$.

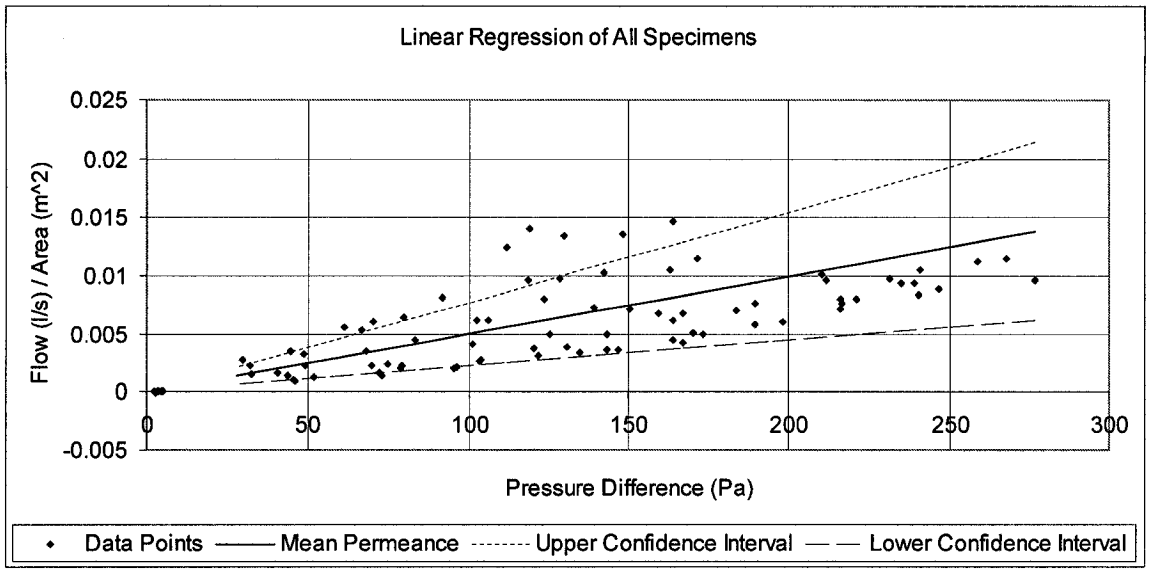

Figure A.7 The dependence of airflow rate on pressure difference for stucco

At the range of pressure differences from 30 to 270 Pa, the flow rate of stucco increases with the pressure difference. The air permeability of stucco under test is (1.2 ± 0.7) E-09 kg/m·Pa·s.

A.9. Hygrothermal Properties of Glass Fiber Batt Insulation

Density: (11.51 ± 0.09) kg/m^3

Table A.50 Thermal conductivity of glass fiber batt insulation

Specimen thickness (mm)	Hot Surface Temperature (°C)	Cold Surface Temperature (°C)	Mean Temperature (°C)	Conductivity ($Wm^{-1}K^{-1}$)
127.04	15.14	-5.40	4.87	0.036
127.04	35.09	12.69	23.89	0.040
127.21	16.47	-5.17	5.65	0.036
127.21	35.19	13.17	24.18	0.040

A.10. Hygrothermal Properties of Polyethylene sheet

Density: (1739 ± 52) kg/m^3

Thickness: (0.153 ± 0.003) mm

Table A.51 Dry cup measurements of polyethylene sheet

Specimen Thickness mm	Chamber RH %	Chamber Temperature °C	WVT Rate kg/s·m^2
0.16	49.80	23.26	4.48E-09(3.17E-11)
0.15	49.80	23.21	4.03E-09(5.55E-11)
0.15	49.80	23.26	4.84E-09(3.76E-11)
0.16	70.38	23.04	6.56E-09(2.36E-10)
0.15	70.38	23.04	6.01E-09(1.43E-10)
0.15	70.38	23.04	6.69E-09(2.50E-10)
0.16	89.87	22.79	8.39E-09(1.32E-10)
0.15	89.87	22.79	7.96E-09(1.52E-10)
0.15	89.87	22.79	8.77E-09(7.32E-11)

Table A.52 Wet cup measurements of polyethylene sheet

Specimen Thickness mm	Chamber RH %	Chamber Temperature °C	WVT Rate kg/s·m^2
0.15	70.51	23.20	2.53E-09(4.54E-11)
0.15	70.51	23.20	3.89E-09(4.14E-11)
0.15	70.51	23.20	1.88E-09(2.16E-11)
0.15	90.05	22.94	3.40E-09(5.14E-10)
0.15	90.05	22.94	4.24E-09(4.24E-09)
0.15	90.05	22.94	3.09E-09(5.39E-10)

Table A.53 Derived water vapor permeability for polyethylene sheet

RH %	Permeability kg/m·s·Pa	RH %	Permeability kg/m·s·Pa
10	4.47E-15	60	4.79E-15
20	4.59E-15	70	4.82E-15
30	4.66E-15	80	4.84E-15
40	4.71E-15	90	4.86E-15
50	4.75E-15	100	4.88E-15